Studies on the Mechanisms and Consequences of Drug-induced Perturbations of Lysosomal Structure and Function

BY

Randall L. Logan

M.S., University of Kansas, 2010

Submitted to the graduate degree program in the Pharmaceutical Chemistry Department and the Graduate Faculty of the University of Kansas in partial fulfillment of the requirements for the degree of Doctor of Philosophy.

_____

Chairperson Jeffrey P. Krise

_____

Teruna J. Siahaan

_____

Thomas Tolbert

_____

David B. Volkin

_____

Thomas Prisinzano

Date Defended: September 18, 2013

The Thesis Committee for Randall L. Logan

certifies that this is the approved version of the following thesis:

Studies on the Mechanisms and Consequences of Drug-induced Perturbations of Lysosomal Structure and Function

_____

Chairperson Jeffrey P. Krise

Date approved: 18 September, 2013

Studies on the mechanisms and consequences of drug-induced perturbations of lysosomal structure and function

Randall Louis Logan

The University of Kansas, 2013

From a clinical perspective, a drug's pharmacokinetic properties (e.g., the volume of distribution, clearance, and half-life) are vitally important as these parameters are used to establish the proper dosing regimen necessary to achieve a desired drug exposure. Failure to properly account for changes to a drug's expected pharmacokinetic properties, whether perpetrated by pharmacological insult (drug-drug interaction) or a disease state, can result in an improper dosing regimen that either fails to achieve therapeutic drug levels or, conversely, can result in drug levels that reach toxic concentrations. Identifying conditions that can alter the expected pharmacokinetic properties of drugs is therefore immensely important. Previous work in our lab has shown that lysosomotropic drugs, i.e., drugs that preferentially accumulate within lysosomes due to an ion trapping-type mechanism, cause a marked expansion in the volume of lysosomes which can result in a drug-drug interaction involving lysosomes. Although this novel drug-drug interaction was well characterized the mechanistic basis explaining how it developed was not established. Within this work we have explored the cellular mechanisms underlying the development of the drug-induced expansion in lysosomal volume and the ensuing drug-drug interaction. Our data shows that the drug-induced expansion in lysosomal volume is achieved through a combination of reduced vesicle-mediated trafficking out of the lysosomes, the induction of autophagy, and the activation of lysosome biogenesis. We have additionally explored a structure activity relationship which implicates a drug's amphiphilicity and lysosomotropic properties as important features that correlate with their propensity to induce an expansion in lysosomal volume. Overall, the

data presented in this work can be used to help explain the sources of variability seen in the pharmacokinetic properties of lysosomotropic drugs.

In parallel to these studies we have also explored potential treatment strategies that can reduce the bloated lysosomal volume seen in cells with dysfunctional lysosomes. Using two cell models that exhibit dysfunctional lysosomes (lysosomotropic drug-treated cells or lysosomal storage diseased cells), we have examined how vitamin E helps to recover lysosomal volume. Our data indicates that vitamin E reduces both ion trapping-dependent (aqueous volume of lysosomes) and ion trapping-independent (lipid binding) drug accumulation mechanisms within cells. To our knowledge, this is the first report detailing that vitamin E reduces the aqueous volume of lysosomes. This finding is important as it helps to more fully explain how vitamin E is eliciting its positive effects within cells. Additionally, we have also examined a structure activity relationship of vitamin E and its ability to reduce lysosomal volume. Our data indicates that the physical structure of vitamin E, rather than its antioxidant properties, is the primary feature of vitamin E that correlates with its ability to reduce the bloated lysosomal volume seen in cells with dysfunctional lysosomes. Overall, this data can be used as a foundation to stage additional studies that could ultimately lead to the development of more potent and better drug-like molecules that could be used to treat lysosomal storage diseases and the toxic effects of lysosomotropic drug-treatments.

Table of Contents

Content **Page**

Chapter 1. Introduction

Statement of the Problem

Lysosomes are dynamic organelles that have a centralized role in maintaining normal catabolic and conversionary processes of lipids, proteins, nucleic acids, and carbohydrates in virtually all human cells. Many vital cellular components are also transited through this organelle leading lysosomes to be one of the main trafficking hubs within cells (Gahl 1989). Dysfunction of normal lysosome activity, whether perpetrated by pharmacological insult or genetic mutation, can have profound effects on cellular physiology which can result in enlarged lysosomes, phospholipidosis, induction of autophagy, and overt cytotoxicity. Many publications have detailed the impact of these effects in that they can create a distribution-based drug-drug interaction (Funk and Krise 2012, Logan, Funk et al. 2012), alter drug activity and toxicity (Ndolo, Forrest et al. 2010, Ndolo, Jacobs et al. 2010), alter the efficiency of virus entry and replication (Levine and Kroemer 2008, Kudchodkar and Levine 2009), and alter the clearance of aggregation prone proteins such as mutated huntingtin, α-synuclein, and ß-amyloid which are associated with Huntington's, Parkinson's, and Alzheimer's disease, respectively (Rubinsztein 2006, Madeo, Eisenberg et al. 2009). A large number of currently approved drugs are lysosomotropic which means that they possess physicochemical properties that make them substrates for lysosomal sequestration by an ion-trapping type mechanism. Many of these drugs can cause lysosomal dysfunction which can ultimately give rise to some of the observed cellular effects previously mentioned. Although a direct cause and effect relationship is currently not well established between drug-induced lysosomal changes (namely phospholipidosis) and cytotoxicity, these drugs nonetheless can trigger the FDA to request additional biochemical and toxicological studies to prove the safety of drug candidates prior to FDA approval. For this reason, drug-induced perturbations of lysosome

structure and function are becoming recognized as an important consideration in the drug development process (Reasor, Hastings et al. 2006, Tengstrand, Miwa et al. 2010). A more complete understanding of the mechanisms underlying these drug-induced changes to lysosomes and their ultimate impact on in vitro and in vivo pharmacokinetics could therefore be highly valuable from a pharmacological perspective. In this work we have sought to characterize the drug-induced changes to lysosomes that arise after treating cells with lysosomotropic drugs. We have specifically analyzed the molecular and cellular mechanisms underlying these effects and have detailed the potential clinical ramifications of these changes.

Lysosomes and the accompanying protein machinery are also recognized as being a "genetic-mutation hotspot" in that a large number of neurodegenerative diseases, collectively referred to as lysosomal storage diseases (LSD), can arise from functional mutations in these lysosome-associated proteins (Table 1.1) (Jeyakumar, Dwek et al. 2005). Interestingly, some lysosomotropic drugs are capable of inducing a cellular phenotype similar to that seen in lysosomal storage diseased cells. These similarities include an expanded lysosomal volume (Karageorgos, Isaac et al. 1997, Kolter and Sandhoff 2010, Xu, Liu et al. 2012), an impaired rate of vesicle-mediated lysosomal egress (Goldman, Funk et al. 2009), and the hyper-accumulation of lipids resulting in the formation of membrane whorls (lipid-laden lysosomes) (Jeyakumar, Dwek et al. 2005). Many LSDs cause progressive neurodegeneration and can ultimately lead to death. To date, there are limited options for treating LSDs. These treatment regimens include substrate limitation/depletion, enzyme replacement therapy, or the use of cyclodextrins (Desnick, Thorpe et al. 1976, Grabowski and Hopkin 2003, Mehta 2008, Liu, Turley et al. 2009). There is, therefore, a demand for additional therapies that might be used to treat these diseases. With this in mind, we have also sought to develop and characterize in vitro treatment strategies that can help to recover lysosome function in these diseased cells. Ultimately we hope that these treatment strategies

will provide the foundation necessary to catalyze the development of novel treatment options for patients harboring a lysosomal storage disease.

Objectives of this work

In this work we have sought to characterize how weakly basic drugs change lysosome form and function in cultured human cells. We have identified several of the physiological processes underlying the mechanistic basis for the expanded lysosomal volume phenotype seen in cells treated with lysosomotropic drugs. We have also provided evidence depicting how these drug-induced changes to lysosomes influence drug accumulation and detailed the impact that these changes might have on whole body pharmacokinetics. In addition, we have evaluated the structure activity relationship of weakly basic drugs and correlated certain physicochemical properties of these drugs with their propensity to induce changes to lysosomes.

In parallel to the work exploring the basis for the drug-induced expansion in lysosomal volume we have also sought to develop treatment strategies for recovering a normal lysosome phenotype. Using the two cellular models that exhibit an expanded steady state lysosomal volume (lysosomotropic drug-treated and lysosomal storage diseased cells), we have evaluated the ability of vitamin E and many amphiphilic phenols to restore lysosome function and thereby reduce the expanded lysosomal volume. We have also laid the foundation for a structure activity relationship for vitamin E and its ability to restore lysosome function.

Introduction

Many drugs that are currently approved for human use possess physiochemical properties that cause them to be lysosomotropic, meaning that they are substrates for lysosomal sequestration. Lysosomal sequestration of weakly basic drugs occurs due to an ion-trapping type mechanism which is governed by three major parameters: the large pH gradient existing between the lumen of the lysosome and the

cytosolic and extracellular space, the basicity of the molecule (pKa), and the membrane permeability of the ionized species of the weak base (alpha value) (de Duve, de Barsy et al. 1974).

Lysosomal sequestration can cause significant changes to the intracellular disposition and total cellular accumulation of a drug. These effects can have significant clinical considerations as they can alter drug activity, influence toxicity, and alter whole body pharmacokinetic parameters (Obach, Lombardo et al. 2008, Ndolo, Forrest et al. 2010, Ndolo, Jacobs et al. 2010, Funk and Krise 2012, Ndolo, Luan et al. 2012). Much of the previous work in our lab has focused on relating how relatively small changes in lysosomal sequestration can lead to dramatic effects on the activity and toxicity of weakly basic drugs. Using in vitro and in vivo assays Ndolo et al. showed that the activity of weakly basic anticancer drugs can be significantly altered by either tuning the pKa of the drug or by modulating the pH of the lysosomal lumen, both of which lead to altered degrees of drug entrapment in the lysosomes.

Lysosomal sequestration can also impart significant changes to a drug's whole body pharmacokinetic parameters specifically the volume of distribution and half-life. Obach and Coworkers have illustrated this relationship by evaluating the pharmacokinetic properties of over 600 currently approved pharmaceutical drugs and showed that weakly basic drugs tend to possess a significantly larger volume of distribution and half-life versus acid, neutral, or zwitterionic drugs (Obach, Lombardo et al. 2008). A classic example of this relationship can be seen by comparing the pharmacokinetic properties of two structurally similar macrolide antibiotics, erythromycin and azithromycin (Figure 1.1). Due to the additional weakly basic functional group azithromycin theoretically has an enhanced lysosomal sequestration capacity versus its monobasic counterpart erythromycin. The enhanced lysosomal sequestration of azithromycin translates into an increased cellular accumulation in peripheral tissues which ultimately leads to a substantial increase in the volume of distribution and half-life of azithromycin (Figure 1.1).

These examples help to illustrate the relationship between a drug's lysosomal sequestration capacity and its activity, toxicity, and pharmacokinetic properties. With this in mind, Funk and Krise have recently detailed an interesting phenomenon whereby lysosomotropic drugs were capable of increasing the lysosomal sequestration capacity of cultured human cells (Figure 1.2), a condition hereby referred to as the expanded lysosomal volume phenotype (expanded LVP) (Funk and Krise 2012). In these studies they found that this phenomenon was achieved at clinically relevant concentrations, i.e., at media concentrations of drug that are similar to those observed in the tissues of organisms treated under normal dosing regimens. For example, the weakly basic drugs amitriptyline, imipramine, and quinacrine accumulate in the brain of mice and rats up to low micromolar concentrations (Glotzbach and Preskorn 1982, Yung, Huang et al. 2004, Shargel, Wu-Pong et al. 2005) which is comparable to the low micromolar concentrations evaluated by Funk and Krise. This implies that the drug-induced increase to the lysosomal sequestration capacity of cells is a phenomenon that can be expected to occur under normal dosing regimens of weakly basic drugs.

Funk and Krise further postulated that the drug-induced increase to the lysosomal sequestration capacity of cells could result in a drug-drug interaction involving lysosomes. In this drug-drug interaction pathway the lysosomotropic drug that induced the expanded LVP was considered the perpetrator drug as it potentiated an increase to the cellular accumulation of secondarily administered lysosomotropic drugs i.e., the victim drug. We propose that these findings potentially have a broad application in explaining some of the variability seen in the pharmacokinetic properties of lysosomotropic drugs. By virtue of their extensive accumulation in the lysosomes of peripheral tissues, lysosomotropic drugs tend to have a very large volume of distribution and half-life that are accompanied with significant inter- and intra-patient variability. For example, the antiarrhythmic drug amiodarone has a reported steady state volume of distribution ranging from 40 L/kg to 84 L/kg and a terminal half-life ranging from 20 days to 47 days (Chow 1996). The inability to accurately account for changes in a drug's pharmacokinetic

properties could ultimately result in a dosing regimen that either fails to reach therapeutic drug levels or, conversely, rises to toxic drug levels.

Motivated by the potential clinical ramifications of this phenomenon, we have sought to define the mechanisms underlying the development of the expanded LVP caused by lysosomotropic drugs. We have identified two physiological processes that likely contribute to the expanded LVP and detailed how these processes can contribute to a drug-drug interaction involving lysosomes. In an effort to advance our understanding of how these lysosomotropic drugs are interacting with lysosomes on a molecular level we have also reported a structure activity relationship detailing the physiochemical properties of lysosomotropic molecules that correlate with their potency in inducing the expanded LVP. Overall, the information presented in this work will help to elucidate the mechanisms underlying the development of the expanded LVP and the ensuing drug-drug interaction involving lysosomes.

Lysosomes and lysosomal storage diseases

Lysosomes have often been described as the stomach of the cell owing to their functional role in performing many of the cell's catabolic activities. Although this simplistic description is fairly accurate it gives the impression that lysosomes are simplistic as well. In reality, lysosomes are a highly dynamic organelle that can adapt and change to different cellular stresses. Many important cellular pathways converge at the lysosome leading lysosomes to be one of the main trafficking hubs within cells. These pathways/processes include the endocytic pathway, the biosynthetic pathway, autophagy, phagocytosis, and antigen-processing and loading in antigen presenting cells (APCs) (Kornfeld and Mellman 1989, Luzio, Poupon et al. 2003, Hsing and Rudensky 2005, Saftig and Klumperman 2009). Although this list is not all encompassing it is intended to illustrate the point that lysosomes are involved in a diverse set of cellular functions. Lysosomes do however perform a common function for all of these cellular pathways,

which is enzymatic degradation and trafficking. It therefore should not be surprising to discover that cells are highly sensitive to gross changes in the catabolic activity of lysosomes.

Lysosomal storage diseases (LSD)s are a set of inheritable diseases that arise as a result of impaired catabolic activity of lysosomes. These diseases collectively present in the human population at 1 in 8,000 live births. There are currently over 40 documented LSDs arising from mutations in one of the 50-60 soluble hydrolases present within lysosomes. A common feature among these diseases is the buildup of undegraded material within the lysosomal system such as sphingolipids, glycosaminoglycans, or cholesterol (Jeyakumar, Dwek et al. 2005). Although these materials are normal endogenous molecules, the lysosomal system is incapable of sustaining its normal function in the presence of such a massive constipation of substrate. An exact mechanistic understanding of how this substrate-hyperaccumulation affects downstream processes is currently unknown. However, common among these diseases is the presentation of brain pathologies. LSDs typically present in the early stages of life with a progressive neurodegeneration that can ultimately lead to death (Futerman and van Meer 2004, Jeyakumar, Dwek et al. 2005). Patients harboring these LSDs are unfortunately limited to a small number of treatment options including substrate limitation/depletion, enzyme replacement therapy, or the use of cyclodextrins (currently not approved by the FDA as a treatment in the USA) (Desnick, Thorpe et al. 1976, Grabowski and Hopkin 2003, Mehta 2008, Liu, Turley et al. 2009). LSDs therefore represent an underserved set of diseases regarding available pharmaceutical interventions.

Ion Trapping-Type Mechanism

The way in which weakly basic molecules become entrapped within lysosomes is due to an ion trapping-type mechanism (also referred to as pH partitioning, lysosomal entrapment, or lysosomal sequestration) (de Duve, de Barsy et al. 1974). This mechanism is largely governed by the physicochemical properties of the weakly basic molecule and the properties of the cellular environment.

Substrates for an ion trapping-type mechanism (also refered to as lysosomotropic molecules) possess two main physicochemical properties. Firstly, they contain a weakly basic amine with an acid dissociation constant (pKa) of approximately 6 to 7 or higher (Trapp, Rosania et al. 2008, Ndolo, Luan et al. 2012). Secondly, substrates for ion trapping also exhibit relatively high membrane permeabilities while existing in their unionized (uncharged) form but are relatively membrane impermeable while in their ionized (charged) form. This differential membrane permeability is referred to as the α-value and is derived from the ratio between the intrinsic partition coefficient of the ionized versus the unionized forms of the molecule (Duvvuri, Gong et al. 2004).

The properties of the cellular environment also play an important role in the mechanism of ion trapping. The pH of three membrane-isolated compartments, i.e., the extracellular space, the cell cytosol, and the lysosomal lumen, are the primary drivers of this mechanism. The pH of the extracellular space and the cell cytosol are relatively neutral with a pH of approximately 7, while the lysosomal lumen is sustained at a much more acidic pH of approximately 4.0 - 4.5 (Ndolo, Jacobs et al. 2010, Ndolo, Luan et al. 2012).

Figure 1.3 illustrates a cartoon representation of the ion trapping mechanism. In the neutral pH of the extracellular and cytosolic space weakly basic molecules exist in equilibrium between their ionized (BH^+) and unionized form (B). Substrates for ion trapping exhibit a high degree of membrane permeability in their unionized form (B) and are considered to freely partition across all lipid bilayers of the cell. When a weakly basic molecule partitions into the lumen of the lysosome the equilibrium balance of the molecule shifts due to the significantly more acidic enviornment. The vast majority of the weakly basic molecule therefore exists in its ionized form (BH^+). Due to the low degree of membrane permeability of the ionized form of these molecules they are thereby trapped within the acidic lysosomal lumen.

The ion trapping mechanism plays a central role in many of the topics explored within this work. Frequently discussed is the impact that the lysosomal pH gradient, i.e., the difference in pH between the

lysosomal lumen versus the cell cytosol and extracellular space, has on the accumulation of weakly basic drugs. Conditions that dissipate the lysosomal pH gradient, i.e., alkalinize the lyososmal pH, can cause a significant decrease in the lysosomal entrapment of weakly basic molecules (Bawolak, Morissette et al. 2010, Logan, Funk et al. 2012, Ndolo, Luan et al. 2012). If the pH of the lysosomal lumen is brought to the same pH as the cell cytosol then, theoretically, no ion trapping would occur. Throughout this work nigericine and monensin are used as a tool to alkalinize the lysosomes. These two molecules are considered to be ionophores as they are capable of carrying H^+ ions across lipid membranes which ultimately results in the dissipation of the lysosomal pH gradient (Nakazato and Hatano 1991, Prabhananda and Ugrankar 1991).

Table 1 | **Lysosomal storage disorders**

Disease category	Disease	Deficiency
Primary lysosomal hydrolase defect	Gaucher disease	Glucosylceramidase
	GM1 gangliosidosis	GM1-β-galactosidase
	Tay–Sachs disease	β-Hexosaminidase A
	Sandhoff disease	β-Hexosaminidase A and B
	Fabry disease	α-Galactosidase A
	Krabbe disease	β-Galactosyl ceramidase
	Niemann–Pick disease types A and B	Sphingomyelinase
	Metachromatic leukodystrophy	Arylsulphatase A
Post-translational processing defect of lysosomal enzymes	Mucosulphatidosis	Multiple sulphatase
Trafficking defect for lysosomal enzymes	Mucolipidosis types II and IIIA	*N*-acetyl glucosamine phosphoryl transferase
Defect in lysosomal enzyme protection	Galactosialidosis	Protective protein cathepsin A (β-galactosidase and neuraminidase)
Defect in soluble non-enzymatic lysosomal proteins	GM2 activator protein deficiency, variant AB	GM2 activator protein
	Sphingolipid activator protein deficiency	Sphingolipid activator protein
	Neuronal ceroid lipofuscinosis (CLN5)	CLN5 (function unknown)
Transmembrane (non-enzymic) protein	Danon disease	Lysosome-associated membrane protein 2
	Niemann–Pick disease type C (NPC)	NPC1 and NPC2
	Salla disease (free sialic acid storage)	Sialin
	Juvenile neuronal ceroid lipofuscinosis (CLN3, Batten disease)	CLN3 (function unknown)

The table shows selected examples of lysosomal storage disorders classified according to molecular defect. Modified, with permission, from REF. 5 © (2004) Oxford University Press.

Table 1.1 The table shows selected examples of lysosomal storage disorders classified according to molecular defect. Modified, with permission, from REK 5 © (2004) Oxford University Press

(Originally pubished in: Nat Rev Neurosci 6(9): 713-725.)

Erythromycin

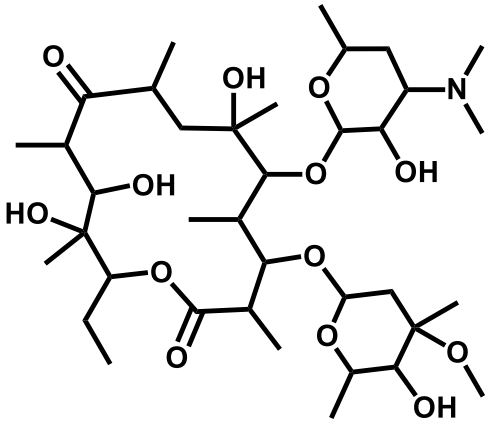

V_d = 2 L/kg

$t_{½}$ = 1-4 hr

Azithromycin

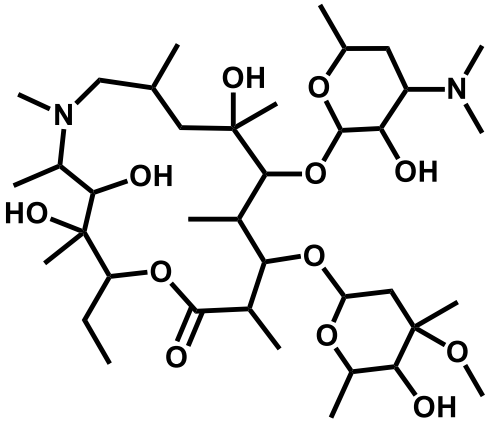

V_d = 100 L/kg

$t_{½}$ = 40-68 hr

Figure 1.1 Two structurally similar macrolide antibiotics erythromycin and azithromycin and their reported volume of distribution (V_d) and half-life ($t_{1/2}$) in humans (package inserts, J*ournal of Pharmaceutical Sciences 67;8 1057-1059 (1978), Antibiotics Chemother. 25, 181-203 (1978), Clinical Therapeutics 18;1 56-72 (1996), Infect Dis Clin N Am 18, 621-649 (2004))*

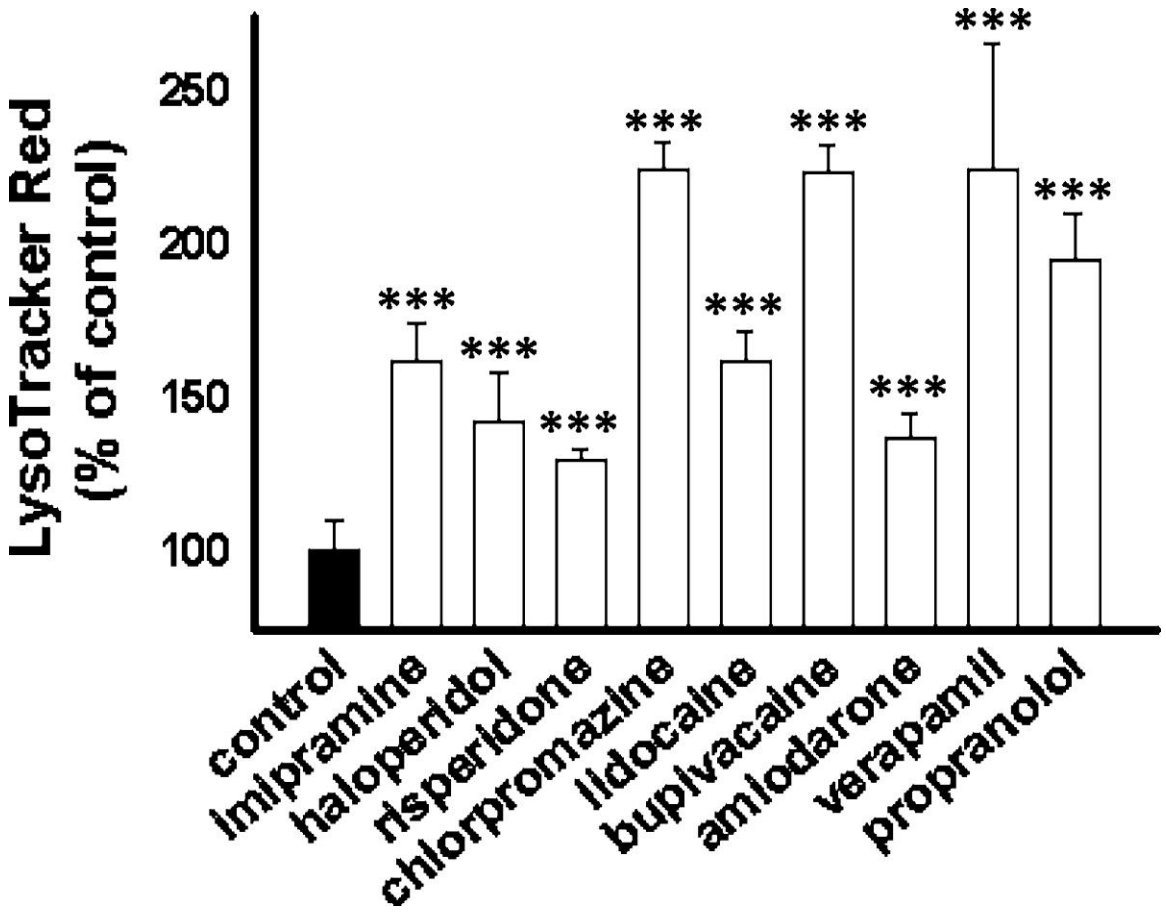

Figure 1.2 LTR accumulation in MDA-1986 cells following a 24 h treatment with vehicle alone or various CADs at a concentration of 10 μM. Cellular accumulation of LTR as a percentage of vehicle-treated control cells is represented as mean ± SD from three independent experimental evaluations (***, $p < 0.001$ by Student's t test).

Published in: Ryan S. Funk; Jeffrey P. Krise; *Mol. Pharmaceutics* 2012, 9, 1384-1395.

DOI: 10.1021/mp200641e

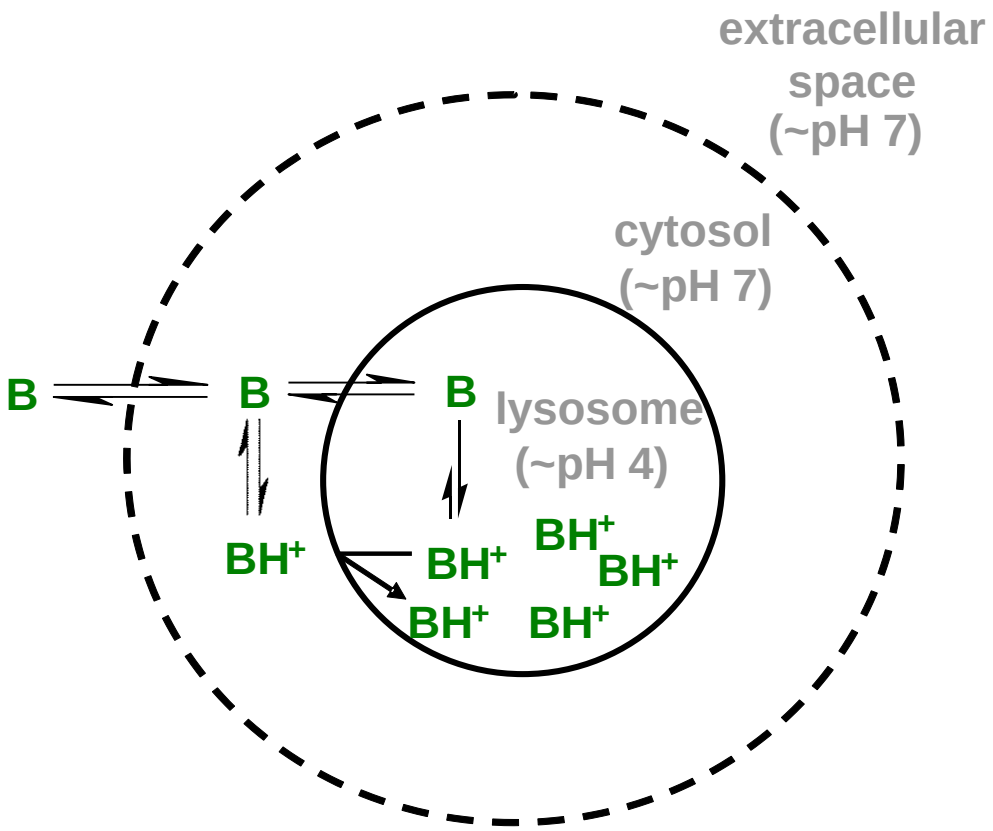

Figure 1.3 Lysosomal sequestration of weakly basic molecules occurs by an ion trapping-type mechanism. The figure represents a single cell. The dotted line signifies the plasma membrane of the cell while the solid line represents the lysosomal membrane. In the neutral pH of the extracellular and cytosolic space weakly basic molecules exist in equilibrium between their ionized (BH^+) and unionized form (B). Substrates for ion trapping exhibit a high degree of membrane permeability in their unionized form (B) and are considered to freely partition across all lipid bilayers of the cell. When a weakly basic molecule partitions into the lumen of the lysosome the equilibrium balance of the molecule shifts due to the significantly more acidic environment (pH ~4). The vast majority of the weakly basic molecule therefore exists in its ionized form (BH^+). Due to the low degree of membrane permeability of the ionized form of these molecules they are thereby trapped within the acidic lysosomal lumen.

References

Anderson, N. and J. Borlak (2006). "Drug-induced phospholipidosis." FEBS Lett 580(23): 5533-5540.

Chow, M. S. (1996). "Intravenous amiodarone: pharmacology, pharmacokinetics, and clinical use." Ann Pharmacother 30(6): 637-643.

de Duve, C., T. de Barsy, B. Poole, A. Trouet, P. Tulkens and F. Van Hoof (1974). "Commentary. Lysosomotropic agents." Biochemical pharmacology 23(18): 2495-2531.

Desnick, R. J., S. R. Thorpe and M. B. Fiddler (1976). "Toward enzyme therapy for lysosomal storage diseases." Physiol Rev 56(1): 57-99.

Funk, R. S. and J. P. Krise (2012). "Cationic amphiphilic drugs cause a marked expansion of apparent lysosomal volume: implications for an intracellular distribution-based drug interaction." Mol Pharm 9(5): 1384-1395.

Futerman, A. H. and G. van Meer (2004). "The cell biology of lysosomal storage disorders." Nat Rev Mol Cell Biol 5(7): 554-565.

Gahl, W. A. (1989). "Lysosomal membrane transport in cellular nutrition." Annu Rev Nutr 9: 39-61.

Glotzbach, R. K. and S. H. Preskorn (1982). "Brain concentrations of tricyclic antidepressants: single-dose kinetics and relationship to plasma concentrations in chronically dosed rats." Psychopharmacology (Berl) 78(1): 25-27.

Goldman, S. D., R. S. Funk, R. A. Rajewski and J. P. Krise (2009). "Mechanisms of amine accumulation in, and egress from, lysosomes." Bioanalysis 1(8): 1445-1459.

Grabowski, G. A. and R. J. Hopkin (2003). "Enzyme therapy for lysosomal storage disease: principles, practice, and prospects." Annu Rev Genomics Hum Genet 4: 403-436.

Honegger, U. E., I. Scuntaro and U. N. Wiesmann (1995). "Vitamin E reduces accumulation of amiodarone and desethylamiodarone and inhibits phospholipidosis in cultured human cells." Biochem Pharmacol 49(12): 1741-1745.

Hsing, L. C. and A. Y. Rudensky (2005). "The lysosomal cysteine proteases in MHC class II antigen presentation." Immunol Rev 207: 229-241.

Jeyakumar, M., R. A. Dwek, T. D. Butters and F. M. Platt (2005). "Storage solutions: treating lysosomal disorders of the brain." Nat Rev Neurosci 6(9): 713-725.

Karageorgos, L. E., E. L. Isaac, D. A. Brooks, E. M. Ravenscroft, R. Davey, J. J. Hopwood and P. J. Meikle (1997). "Lysosomal biogenesis in lysosomal storage disorders." Exp Cell Res 234(1): 85-97.

Kolter, T. and K. Sandhoff (2010). "Lysosomal degradation of membrane lipids." FEBS Lett 584(9): 1700-1712.

Kornfeld, S. and I. Mellman (1989). "The biogenesis of lysosomes." Annu Rev Cell Biol 5: 483-525.

Kudchodkar, S. B. and B. Levine (2009). "Viruses and autophagy." Rev Med Virol 19(6): 359-378.

Levine, B. and G. Kroemer (2008). "Autophagy in the pathogenesis of disease." Cell 132(1): 27-42.

Liu, B., S. D. Turley, D. K. Burns, A. M. Miller, J. J. Repa and J. M. Dietschy (2009). "Reversal of defective lysosomal transport in NPC disease ameliorates liver dysfunction and neurodegeneration in the npc1-/- mouse." Proc Natl Acad Sci U S A 106(7): 2377-2382.

Logan, R., R. S. Funk, E. Axcell and J. P. Krise (2012). "Drug-drug interactions involving lysosomes: mechanisms and potential clinical implications." Expert Opin Drug Metab Toxicol 8(8): 943-958.

Luzio, J. P., V. Poupon, M. R. Lindsay, B. M. Mullock, R. C. Piper and P. R. Pryor (2003). "Membrane dynamics and the biogenesis of lysosomes." Mol Membr Biol 20(2): 141-154.

Madeo, F., T. Eisenberg and G. Kroemer (2009). "Autophagy for the avoidance of neurodegeneration." Genes Dev 23(19): 2253-2259.

Matsuzawa, Y., A. Yamamoto, S. Adachi and M. Nishikawa (1977). "Studies on drug-induced lipidosis. VIII. Correlation between drug accumulation and acidic phospholipids." J Biochem 82(5): 1369-1377.

Mehta, A. (2008). "Gaucher disease: unmet treatment needs." Acta Paediatr Suppl 97(457): 83-87.

Ndolo, R. A., M. L. Forrest and J. P. Krise (2010). "The role of lysosomes in limiting drug toxicity in mice." J Pharmacol Exp Ther 333(1): 120-128.

Ndolo, R. A., D. T. Jacobs, M. L. Forrest and J. P. Krise (2010). "Intracellular Distribution-based Anticancer Drug Targeting: Exploiting a Lysosomal Acidification Defect Associated with Cancer Cells." Mol Cell Pharmacol 2(4): 131-136.

Ndolo, R. A., Y. Luan, S. Duan, M. L. Forrest and J. P. Krise (2012). "Lysosomotropic properties of weakly basic anticancer agents promote cancer cell selectivity in vitro." PLoS One 7(11): e49366.

Obach, R. S., F. Lombardo and N. J. Waters (2008). "Trend analysis of a database of intravenous pharmacokinetic parameters in humans for 670 drug compounds." Drug Metab Dispos 36(7): 1385-1405.

Reasor, M. J., K. L. Hastings and R. G. Ulrich (2006). "Drug-induced phospholipidosis: issues and future directions." Expert Opin Drug Saf 5(4): 567-583.

Rubinsztein, D. C. (2006). "The roles of intracellular protein-degradation pathways in neurodegeneration." Nature 443(7113): 780-786.

Saftig, P. and J. Klumperman (2009). "Lysosome biogenesis and lysosomal membrane proteins: trafficking meets function." Nat Rev Mol Cell Biol 10(9): 623-635.

Shargel, L., S. Wu-Pong and A. B. C. Yu (2005). Applied biopharmaceutics & pharmacokinetics. New York, Appleton & Lange Reviews/McGraw-Hill, Medical Pub. Division.

Shichiri, M., N. Kono, Y. Shimanaka, M. Tanito, D. E. Rotzoll, Y. Yoshida, Y. Hagihara, H. Tamai and H. Arai (2012). "A novel role for alpha-tocopherol transfer protein (alpha-TTP) in protecting against chloroquine toxicity." J Biol Chem 287(4): 2926-2934.

Tengstrand, E. A., G. T. Miwa and F. Y. Hsieh (2010). "Bis(monoacylglycerol)phosphate as a non-invasive biomarker to monitor the onset and time-course of phospholipidosis with drug-induced toxicities." Expert Opin Drug Metab Toxicol 6(5): 555-570.

Wang, X. and P. J. Quinn (1999). "Vitamin E and its function in membranes." Prog Lipid Res 38(4): 309-336.

Xu, M., K. Liu, M. Swaroop, F. D. Porter, R. Sidhu, S. Firnkes, D. S. Ory, J. J. Marugan, J. Xiao, N. Southall, W. J. Pavan, C. Davidson, S. U. Walkley, A. T. Remaley, U. Baxa, W. Sun, J. C. McKew, C. P. Austin and W. Zheng (2012). "delta-Tocopherol reduces lipid accumulation in Niemann-Pick type C1 and Wolman cholesterol storage disorders." J Biol Chem 287(47): 39349-39360.

Yung, L., Y. Huang, P. Lessard, G. Legname, E. T. Lin, M. Baldwin, S. B. Prusiner, C. Ryou and B. J. Guglielmo (2004). "Pharmacokinetics of quinacrine in the treatment of prion disease." BMC Infect Dis 4: 53.

Chapter 2. The role of autophagy and lysosomal trafficking defects on the development of a drug-drug interaction involving lysosomes

Introduction

Many drugs that are currently approved for human use possess physiochemical properties that cause them to be substrates for lysosomal sequestration. Lysosomal sequestration of weakly basic drugs occurs due to an ion-trapping type mechanism which is governed by three major parameters: the large pH gradient existing between the lumen of the lysosome and the cytosol and extracellular space, the basicity of the small molecule (pKa), and the membrane permeability of the ionized species of the weak base (alpha value) (de Duve, de Barsy et al. 1974). In addition to these parameters the total volume of the lysosomal system can also influence the lysosomal sequestration capacity of a cell. Conditions that lead to changes in the steady state volume of the lysosomes can therefore lead to changes in a cell's capacity to accumulate lysosomotropic drugs. This can lead to changes in the degree of drug accumulation in peripheral tissues and ultimately affect a drug's pharmacokinetic properties, specifically the volume of distribution and half-life.

From a clinical perspective understanding and predicting changes to the pharmacokinetic properties of a drug is vitally important as these properties are used to establish the proper dosing regimen prescribed to patients. The inability to properly account for changes in a drug's pharmacokinetic properties could result in dosing regimens that either fail to reach therapeutic drug levels or, conversely, reach drug levels that are too high and become cytotoxic. With this in mind, a greater understanding of conditions or mechanisms by which the pharmacokinetic properties of a drug can change would be highly valuable.

Lysosomotropic drugs are unique in that they typically have an extremely large volume of distribution and half-life but these parameters can also exhibit extremely large variability. For example, the lysosomotropic drug amiodarone has been reported to have a steady state volume of distribution

ranging from 40 L/kg to 84 L/kg and a terminal half-life ranging from 20 days to 47 days (Chow 1996). Keeping in mind that changes in the steady state volume of lysosomes could translate into changes in the volume of distribution and half-life of these lysosomotropic drugs, we have focused on evaluating the potential influence that autophagy might have in altering lysosomal volume. Ultimately, this could be used to explain why lysosomotropic drugs, such as amiodarone, are exhibiting such a large variability in their volume of distribution and half-life.

Funk and Krise previously reported that many lysosomotropic drugs were capable of perpetrating an intracellular distribution based drug-drug interaction which was mediated by an expansion in the steady state volume of the lysosomes (Funk and Krise 2012). Although this phenomenon was well described, the mechanistic basis for this phenomenon was not determined. In this chapter we explore the cellular mechanisms that are involved in causing an increase in the steady state volume of lysosomes seen in cells treated with these lysosomotropic drugs. We have specifically focused on how autophagy, a normal physiological process involved in the clearance of long-lived proteins and dysfunctional organelles (Levine and Kroemer 2008), can influence the steady state volume of lysosomes. We then explored the potential involvement of autophagy as a physiological process that contributes to the expanded lysosomal volume phenotype (expanded LVP) seen in cells treated with these perpetrator drugs. We also detailed the impact that these lysosomotropic drugs have on vesicle mediated trafficking out of the lysosomes. We further explored how the changes to the steady state volume of lysosomes caused by autophagy and the expanded LVP can lead to a drug-drug interaction involving lysosomes.

Materials and Methods

Cell Lines and Reagents

Wild-type (WT) human fibroblasts (catalogue # CRL-2076) were purchased from ATCC (Manassas, VA). All cells were cultured in glutamine-free DMEM supplemented with 10% FBS, 10mM HEPES, 1mM Sodium Pyruvate, and 2mM Glutamax and maintained at 37 degrees C and 5% CO 2. Cells were routinely subcultured to maintain 50% to 90% confluency. Experiments were carried out within 10 passages following removal from cryopreservation. Dulbecco's phosphate buffered saline (D-PBS), Dulbecco's modified Eagle's medium (DMEM), HEPES, sodium pyruvate, glutamax, and LysoTracker Red DND-99 (LTR) were purchased from Invitrogen (Carlsbad, CA). Fetal bovine serum (FBS) was purchased from Atlanta Biologicals (Lawrenceville, GA). Carbamazepine, rapamycin, valproic acid, halofantrine, propranolol, U18666A, lidocaine, imipramine, haloperidol, chloroquine, bupivacaine, quinacrine, Laemmli buffer, and sodium deoxycholate were purchased from Sigma-Aldrich (St. Louis, MO). (S)-naproxen was purchased from Cayman Chemical Company (Ann Arbor, MI). Pierce BCA protein assay kit was ordered from ThermoScientific (Rockford, IL). Anti-LCB3I/II antibody (catalogue # ab51520) was purchased from AbCam (Cambridge, United Kingdom). Anti-beta actin antibody (catalogue #8H10D10) was purchased from Cell Signaling Technology (Danvers, MA). 3[H]-dextran 70,000 MW, 3[H]-halofantrine, and 3[H]-propranolol were purchased from American Radiolabeled Chemicals, Inc. (St. Louis, MO).

LysoTracker Red accumulation assay

WT human fibroblasts were grown in plastic 12-well culture plates (Corning Life Sciences) at a seeding density of approximately 75,000 cells per well. Following a 48-hour pretreatment with various drugs (concentrations for each drug is stated in the figure legend), LysoTracker Red was spiked into the growth media to a concentration of 200nM and the cells were incubated for 1 hour. Cells were then rapidly washed twice with 4 degrees C D-PBS. Cells were lysed with lysis buffer (50 mM tris base, 150 mM NaCl, 1% NP40, pH 7.4). The quantity of LTR was determined by fluorescent signal in relative fluorescence

units (RFU) using a Bio-Tek FL600 microplate fluorescence reader. Protein abundance was measured for each sample using the BCA method. Measured LTR signal (RFU) was then normalized to protein. These normalized values were then compared to the control condition (vehicle treated) and depicted as a percentage of the control.

Drug Accumulation Assays

Following a 48-hour pretreatment with rapamycin (200nM) or vehicle alone, cells were exposed to propranolol or halofantrine for 1 hour. Naproxen accumulation (5µM) was conducted concurrently with the pretreatment of rapamycin (200nM) or vehicle alone for 48 hours. The concentrations chosen for these compounds (200nM propranolol, 200nM halofantrine, 5uM naproxen) were determined as the necessary concentrations to yield adequate signal while also being incapable of inducing a lysosomal volume expansion. Cells were then washed twice with 4 degrees C D-PBS rapidly to prevent diffusion of cell-associated drug. The cells were then lysed using lysis buffer (50 mM tris base, 150 mM NaCl, 1% NP40, pH 7.4). The quantity of tritium-labeled drug (propranolol and halofantrine) was measured in disintegrations per minute (DPM) using a Beckman LS 60001C liquid scintillation counter, and naproxen was measured by LC-MS/MS using the method stated in LC-MS/MS quantification of naproxen . Background signal contributed from non-specific binding to the plate surface was subtracted from each measurement. Protein abundance was measured for each sample using the BCA method. All measured quantities of drug accumulation were then normalized to protein. These normalized values were then compared to the corresponding control condition (vehicle treated) and depicted as a percentage of the control.

LC-MS/MS quantification of naproxen

To measure naproxen cellular accumulation, a drug extraction was performed to recover naproxen from the cell lysate using the following technique. Methyl tert-butyl ether was combined with the cell lysates

in a 5:1 ratio (v/v), respectively. The samples were vortexed for 10 minutes and then centrifuged at 15,000g for 10 minutes. The top 95% of the supernatant was removed and the process was repeated. The supernatant was evaporated and the remaining solid particulates were then reconstituted in mobile phase prior to injection. An integrated Agilent 1100 series liquid chromatography system with an API 2000 (Applied Biosciences) triple quadrupole mass spectrometer was employed to quantitate drug extracted from cell lysates. Liquid chromatography was conducted on an Agilent Zorbax Eclipse XDB-C18 column (2.1 x 150 mm 3.5µm particle size) (Santa Clara, CA). All samples were analyzed with an 8 µL sample injection. Mobile phase A consisted of 10 mM ammonium acetate at pH 8.0. Mobile phase B consisted of ACN. Using 150 µL/min flow rate, the first minute of elution was an isocratic mixture of 82% A followed by a linear gradient to 5% A for 3 minutes. A linear gradient was then executed to 82% A over 0.5 minutes and maintained at 82% A for an additional 3.5 minutes. The first 1.8 minutes of eluted sample was diverted to waste in order to avoid non-volatile material from entering the mass spectrometer. The mass spectrometer was equipped with an atmospheric ionization source and operated in the negative mode. Detection was by multiple reaction monitoring (MRM).

Cell imaging

All cell imaging was performed on a Nikon Eclipse 80i epifluorescence microscope equipped with a 60× (1.40 NA) oil immersion objective. All images were acquired on a Hamamatsu ORCA ER digital camera. Images were analyzed using Metamorph software version 7.0 (Universal Imaging) and ImageJ software (free online atrsbweb.nih.gov) software. WT human fibroblasts were grown on glass coverslips under the stated growth conditions. LTR was spiked into the growth media one hour prior to cell imaging. The cells were then washed once quickly with 37 degrees C D-PBS. The live cells were then rapidly imaged using the appropriate filter sets for LTR fluorescence. Images were captured under identical instrument settings and scaled equally so that a direct comparison of fluorescence intensity and localization could be performed.

Western blot analysis

WT human fibroblasts were grown in 100mm plastic Petri dishes (Corning Life Sciences) at a seeding density of approximately 500,000 cells per dish. Following a 48-hour treatment with various drugs (concentrations stated in figure legends) cells were washed twice with 4 degrees C D-PBS. Cells were then lysed with RIPA buffer (150mM sodium chloride, 1% TX-100, 0.5% sodium deoxycholate, 0.1% SDS, 50mM tris, pH 8.0, and the protease inhibitors APL & PMSF). The protein abundance was then determined by the BCA method. Protein samples were then mixed with Laemmli buffer. All protein samples (25 µg per lane) were subjected to 12% sodium dodecyl sulfate-polyacrylamide gel electrophoresis (SDS-PAGE) for 120 minutes. The proteins were then transferred to a 0.2 µm pore PVDF membrane (Millipore) using 300 V*hours. The PVDF membrane was then exposed to primary antibody (1:4000 LC3B, 1:30,000 beta-actin) for two hours, washed, and then exposed to secondary antibody (1:4000 goat anti-rabbit HRP and goat anti-mouse HRP) for two hours. Detection of HRP-conjugated antibody was achieved by chemiluminescence using Western Lightning-ECL (PerkinElmer) on autoradiograph film.

Dextran release assay

WT human fibroblasts were grown in plastic 6-well culture plates (Corning Life Sciences) at a seeding density of 175,000 cells per well. Following a 48-hour treatment with various drugs or vehicle alone (concentrations stated in figure legends), the extracellular media was replaced with 1 mg/ml 70,000 MW dextran including 0.1 mg/mL tritium-labeled dextran also containing the indicated drug or vehicle alone. The cells were incubated for 6 hours in the presence of the dextran containing media. Cells were then washed three times with 37 degrees C D-PBS. The extracellular media was then replaced with dextran-free media containing the indicated drug or vehicle alone. Following a 24-hour release period, the quantity of tritium-labeled dextran was measured in the extracellular media and in the cell lysates. The cells were washed three times with 37 degrees C D-PBS and then lysed with lysis buffer (50 mM tris

base, 150 mM NaCl, 1% NP40, pH 7.4). The quantity of tritium-labeled dextran was measured in disintegrations per minute (DPM) using a Beckman LS 60001C liquid scintillation counter. Background signal contributed from non-specific binding to the plate surface was subtracted from each measurement. The relative dextran release for each test condition was then compared to the control (vehicle treated) and depicted as a percentage of the control.

Results and Discussion

Lysosomotropic drugs are capable of inducing autophagy

Funk and Krise previously identified a novel drug-drug interaction whereby one lysosomotropic drug could alter the cellular accumulation of a secondarily administered lysosomotropic drug. In this work they discovered that these perpetrator drugs were causing an expanded lysosomal volume phenotype (expanded LVP). They proposed that it was by virtue of this expanded lysosomal volume that the secondarily administered drug was achieving a greater cellular accumulation thereby resulting in a drug-drug interaction. Although several drugs were identified that could elicit this effect (Figure 1.2) the mechanistic basis for this phenomenon was not determined (Funk and Krise 2012). In continuation of this work, we have sought to determine the cellular processes or conditions that might contribute membrane and material to lysosomes and thereby increase the steady state volume of the lysosomal system.

The steady state volume of the lysosomes is achieved when the rate of input of membrane and material into the lysosomal system equals the rate of output of membrane and material from the lysosomal system. There are several cellular processes or pathways that can deliver membrane and material to this system: the endocytic pathway, phatocytosis, the biosynthetic pathway, and the autophagic pathway (Figure 2.1) (Kornfeld and Mellman 1989, Luzio, Poupon et al. 2003). Modulation of one pathway or a combination of them could foreseeably result in changes to the steady state volume of

lysosomes. Using wild type human fibroblasts we first sought to isolate one of these input pathways, autophagy, and determine if the lysosomotropic perpetrator drugs were capable of modulating its normal homeostatic levels. Under normal cell culture conditions the basal level of autophagy is relatively very low in Wild Type (WT) human fibroblasts. We therefore hypothesized that if these perpetrator drugs influenced autophagy we should see a concomitant increase or induction of autophagy in the drug-treated cells.

Prior to evaluating the potential involvement of autophagy in the development of the expanded LVP we first had to rationally choose an appropriate perpetrator drug concentration and exposure time. With this in mind we reasoned that the concentration of drug should be high enough and the duration of exposure should be long enough to allow the formation of the expanded LVP. We would then use a concentration of drug that exhibited no cytotoxic effects but maximized the expanded LVP. Once these conditions were established we would then evaluate the drug's potential to induce autophagy.

Using lysotracker red (LTR), a fluorescent lysosomotropic molecule, we evaluated the dose dependency of 8 different lysosomotropic drugs' abilities to cause an expanded LVP (Figure 2.2). We found that the drugs exhibited varying degrees of cytotoxicity and potency in causing the expanded LVP. This observation proved that a single uniform concentration of drug could not be used in future assessments. Instead, a unique concentration of drug was chosen for each of the 8 lysosomotropic drugs that exhibited no cytotoxicity but maximized the expanded LVP. In general, the concentrations of drug that met this criteria ranged from high nanomolar to low micromolar levels (exact values are listed in Figure 2.2).

Following the optimization of drug concentrations, the autophagy induction potential was then evaluated for these lysosomotropic drugs. One of the standard methods for evaluating autophagy induction involves the use of western blot analysis to monitor the processing of LC3 (microtubule-

associated protein 1 (MAP1) light chain 3). During normal autophagic processing, post-translational modification converts LC3 to the soluble cytosolic form LC3I. LC3I is then lipidated with phosphatidylethanolamine to form LC3II which is bound to the autophagosome membrane. LC3II levels can therefore be used as a protein marker for measuring the abundance of autophagosomes and by extension the levels of autophagy in cells (Tanida, Ueno et al. 2004, Kimura, Noda et al. 2007, Mizushima, Yoshimori et al. 2010). Under conditions that lead to the induction of autophagy, the cell would theoretically initiate the creation of more autophagosomes which would thereby increase the abundance of LC3II relative to the corresponding control. Autophagy induction can therefore be monitored by evaluating changes to the abundance of LC3II.

Using the optimal concentrations of drug, determined from the dose response curves (Figure 2.2), each lysosomotropic drug was then evaluated for its ability to induce autophagy. Interestingly, many of the lysosomotropic drugs caused an increase in the abundance of LC3II which likely indicates that these drugs were inducing autophagy (Figure 2.3). Rapamycin was included in Figure 2.3 as a positive control as it is widely used as a known chemical inducer of autophagy (Sarkar, Floto et al. 2005, Rubinsztein, Gestwicki et al. 2007, Williams, Sarkar et al. 2008, Drake, Kang et al. 2010).

Although this finding alone does not completely explain the entire expanded LVP, it does provide evidence supporting the possibility that autophagy might play a contributing role in the development of the expanded LVP seen in cells treated with these lysosomotropic perpetrator drugs.

Chemical inducers of autophagy are capable of expanding lysosomal volume

After establishing that the lysosomotropic drugs were capable of inducing autophagy we then needed to isolate autophagy and assess its capacity to modulate the steady state volume of lysosomes. Although we would rationally consider autophagy induction to lead to an expansion in lysosomal volume, as it is a cellular process that delivers membrane and material to the lysosomes, we nonetheless found it

prudent to validate that autophagy induction is capable of expanding lysosomal volume. We reasoned that if autophagy induction caused an increase in the steady state volume of lysosomes, then we should see a concomitant increase in the cellular accumulation of LTR within these cells.

In this section we assessed the impact that autophagy induction had on the steady state volume of lysosomes. Using three well characterized chemical inducers of autophagy (rapamycin, carbamazepine, or valproic acid) (Sarkar, Floto et al. 2005, Rubinsztein, Gestwicki et al. 2007, Williams, Sarkar et al. 2008, Drake, Kang et al. 2010), which are not considered to be lysosomotropic, we assessed the impact that elevated levels of autophagy had on the steady state volume of lysosomes. By comparing the cellular uptake of the fluorescent lysosomotropic probe LTR, we were able to measure the relative changes in lysosomal volume caused by autophagy induction. Interestingly, it was found that all three of the chemical inducers of autophagy were capable of expanding the steady state volume of lysosomes as indicated by the increase in the cellular accumulation of LTR compared to the vehicle treated control (Figure 2.4).

Establishing that autophagy induction alone can expand the steady state volume of lysosomes was a key finding. It provided evidence indicating that drug treatments leading to the induction of autophagy can ultimately result in an expansion of lysosomal volume. Pairing this with the recent findings that the lysosomotropic perpetrator drugs were capable of inducing autophagy, we then had additional support for the hypothesis that autophagy induction might be contributing to the development of the expanded LVP.

Chemical inducers of autophagy are capable of perpetrating a drug-drug interaction involving lysosomes

Previous reports have indicated that autophagy can be induced in vitro and in vivo under various conditions that do not involve lysosomotropic drugs, including calorie restriction, genetic manipulations,

inhibition of insulin/insulin-like growth factor signaling, pharmaceutical interventions such as resveratrol (a polyphenol), and RNAi knockdown of genes required for optimal mitochondrial function (Madeo, Tavernarakis et al. 2010, Rubinsztein, Marino et al. 2011). Considering the many routes by which autophagy can be induced, particularly calorie restriction, we envisaged the possibility that humans might be subjected to conditions leading to variable levels of autophagy in their tissues. With this in mind, we found it prudent to evaluate the potential for elevated levels of autophagy to instigate a drug-drug interaction involving lysosomes.

In this section autophagy induction is evaluated for its capacity to perpetrate a drug-drug interaction involving lysosomes. Using rapamycin, a non-lysosomotropic chemical inducer of autophagy (Sarkar, Floto et al. 2005, Rubinsztein, Gestwicki et al. 2007, Williams, Sarkar et al. 2008, Drake, Kang et al. 2010), WT human fibroblasts were subjected to a 2 day autophagy induction period prior to evaluating the cellular uptake of various clinically relevant drugs: propranolol, halofantrine, and naproxen. Propranolol is a secondary amine-containing beta-blocker (structure illustrated in Figure 2.5), while halofantrine is a tertiary amine-containing antimalarial drug (structure illustrated in Figure 2.5). Because of their weakly basic properties both of these drugs are considered to be lysosomotropic. The cellular uptake of propranolol and halofantrine should therefore be sensitive to changes in the volume of the lysosomal system. Included in these assessments is the non-steroidal anti-inflammatory drug naproxen which contains a carboxylic acid and is not considered to be lysosomotropic (structure illustrated in Figure 2.5). Naproxen therefore would not be expected to be sensitive to changes in the volume of the lysosomal system.

Consistent with these expectations, elevated levels of autophagy induced by rapamycin caused a significant increase in the cellular accumulation of both propranolol and halofantrine but not naproxen (Figure 2.5). These results indicate that chemical-inducers of autophagy can act as perpetrators of a

drug-drug interaction involving lysosomes. We reasoned that under conditions that induce autophagy the steady state volume of lysosomes is increased which results in an increased capacity of these cells to accumulate lysosomotropic drugs. Secondarily administered lysosomotropic drugs would therefore be subjected to cells with an enhanced lysosomal sequestration capacity. Ultimately this condition would be expected to increase the cellular accumulation of the secondarily administered lysosomotropic drug (as seen in Figure 2.5).

Lysosomotropic drugs are capable of impairing vesicle-mediated trafficking out of the lysosomes

As discussed previously, the steady state volume of lysosomes is achieved when the rate of input of membrane and material into the lysosomes equals the rate of output of membrane and material from the lysosomes. After implicating autophagy induction as a potential mechanism involved in the development of the expanded LVP seen in cells treated with the lysosomotropic perpetrator drugs, we then sought to explore how these drugs might influence the vesicle-mediated egress efficiency of membrane and material out of the lysosomes. We reasoned that conditions leading to an impairment of lysosomal egress would ultimate result in an increase to the steady state volume of lysosomes.

In this section the impact that 8 lysosomotropic perpetrator drugs had on the efficiency of vesicle-mediated lysosomal egress was assessed using a dextran secretion assay. Briefly, cells were exposed to a tritium labeled, membrane impermeable, dextran polymer that was allowed to accumulate in lysosomes using the pulse chase protocol previously established by Goldman et al. (Goldman, Funk et al. 2009). The release of dextran into the extracellular media was then monitored over a 24 hr time period. Conditions that impair or enhance vesicle-mediated lysosomal egress would be expected to result in a corresponding decrease or increase (respectively) in the extracellular release of the dextran polymer.

Interestingly, we found that the lysosomotropic perpetrator drugs were capable of impairing the efficiency of vesicle-mediated lysosomal egress compared to the vehicle-treated control (Figure 2.6).

Knowing that these perpetrator drugs also induced autophagy, we evaluated the influence that autophagy alone has on vesicle-mediated trafficking out of the lysosomes (Figure 2.7). All three of the chemical inducers of autophagy showed no impairment in lysosomal egress. Instead they showed an enhancement in the lysosomal egress of the dextran polymer, indicating that they were increasing the efficiency of lysosomal egress. Although this finding might seem to confound the results obtained with the lysosomotropic drugs, it is likely that despite the enhancement in lysosomal egress arising from the induction of autophagy, the perpetrator drugs are impairing lysosomal egress to such an extent that the overall egress efficiency is still lower than the vehicle treated control.

Conclusion

Recent work by Funk and Krise has identified a novel drug-drug interaction involving lysosomes whereby one lysosomotropic drug can cause an increase in the accumulation of a secondarily administered lysosomotropic drug (Funk and Krise 2012). In this work they showed that the perpetrator drug caused a significant increase in the steady state volume of lysosomes, a condition referred to as the expanded lysosomal volume phenotype (expanded LVP). This expanded LVP imparted an increase to the lysosomal sequestration capacity of the cells which ultimately resulted in an enhanced cellular accumulation of secondarily administered lysosomotropic drugs.

Although Funk and Krise provided a well detailed description of the drug-drug interaction pathway, a mechanistic basis for the development of the expanded LVP was not provided. The work presented in this chapter is a continuation of their work and reveals the importance that autophagy induction plays in the development of this phenomenon.

The steady state volume of lysosomes results when the rate of input of membrane and material into the lysosomes equals the rate of membrane and material moving out of the lysosomes. Logically, conditions that increase the rate of input or decrease the rate of output, or a combination of the two, could

conceivably result in an increase of lysosomal volume i.e., the formation of an expanded LVP. We show that well known chemical inducers of autophagy are capable of expanding the steady state volume of lysosomes and that the induction of autophagy can lead to a drug-drug interaction similar to that seen with the lysosomotropic perpetrator drugs. We then show that autophagy induction contributes to the development of the expanded LVP seen with the lysosomotropic perpetrator drugs. We also show that these lysosomotropic drugs are capable of impairing the efficiency of vesicle-mediated lysosomal egress.

Overall these results indicate that the expanded LVP perpetrated by lysosomotropic drugs is the result of an increased rate of input of membrane and material into the lysosomal system, via autophagy induction, and an impaired rate of the vesicle-mediated egress of membrane and material out of the lysosomes. We propose that the combination of these two conditions ultimately results in an increase to the steady state volume of lysosomes and the development of the expanded LVP.

We propose that these findings provide a greater understanding of the mechanisms underlying the variability seen in the pharmacokinetic properties of drugs administered to humans. By virtue of their extensive accumulation in the lysosomes of peripheral tissues, lysosomotropic drugs tend to have a very large volume of distribution and half-life. In addition these parameters often exhibit significantly large variability. For example, the antiarrhythmic drug amiodarone has a reported steady state volume of distribution ranging from 40 to 84 L/kg and a terminal half-life ranging from 20 to 47 days (Chow 1996). Although the cause of this variability is likely multifaceted, we propose that changes in the levels of autophagy could account for a significant portion of this variability. Our results indicate that patients experiencing conditions that induce autophagy would have peripheral tissues that possess a significantly greater capacity to accumulate lysosomotropic drugs. Clinically, this would result in a larger volume of distribution and half-life for these drugs. In light of recent reports that have identified many pathways leading to autophagy induction, particularly a calorie restricted diet (Madeo, Tavernarakis et al. 2010,

Rubinsztein, Marino et al. 2011), we feel that autophagy induction might become an increasingly important consideration in predicting the pharmacokinetic behavior of lysosomotropic drugs although future in vivo studies are required to fully characterize this drug-drug interaction mechanism.

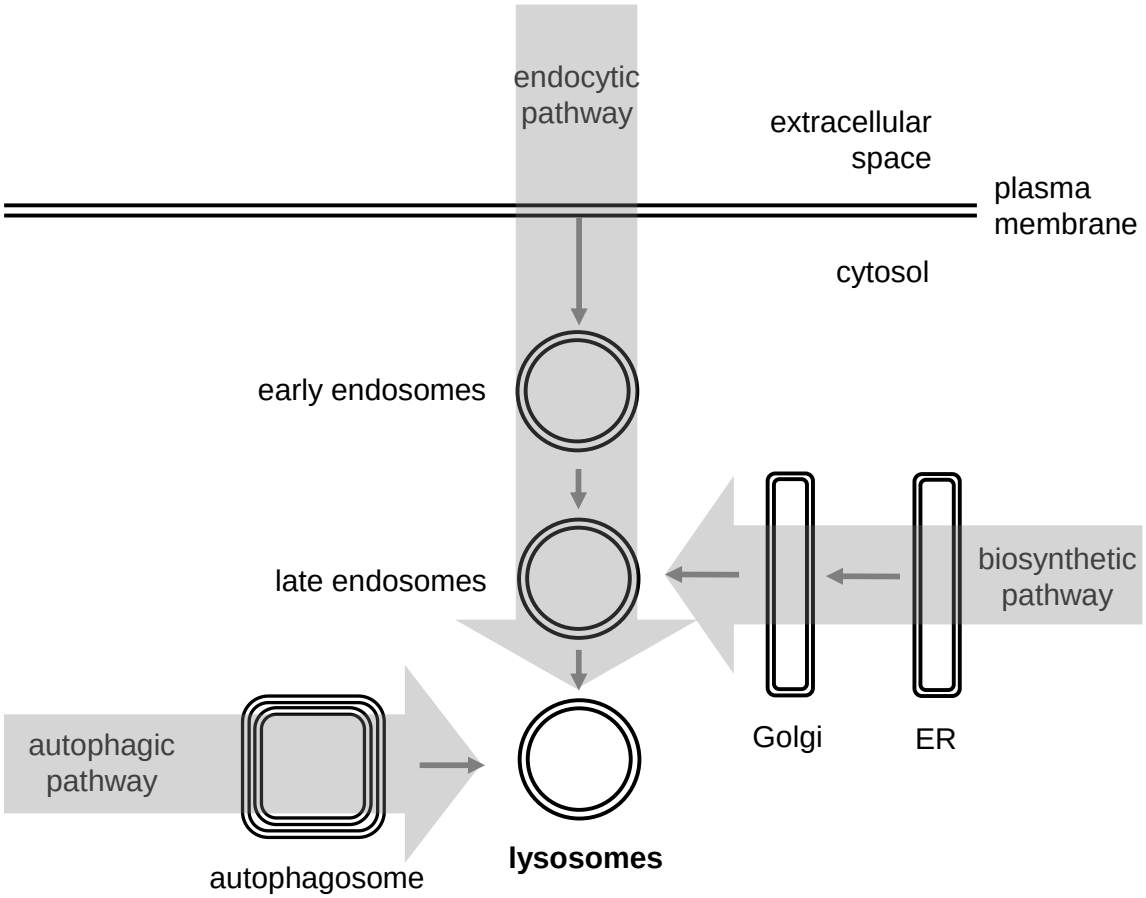

Figure 2.1 Three well established biological process that can deliver membrane and material to the lysosomal system. Each pathway (endocytic, biosynthetic, and autophagic pathway) is highlighted with a grey arrow.

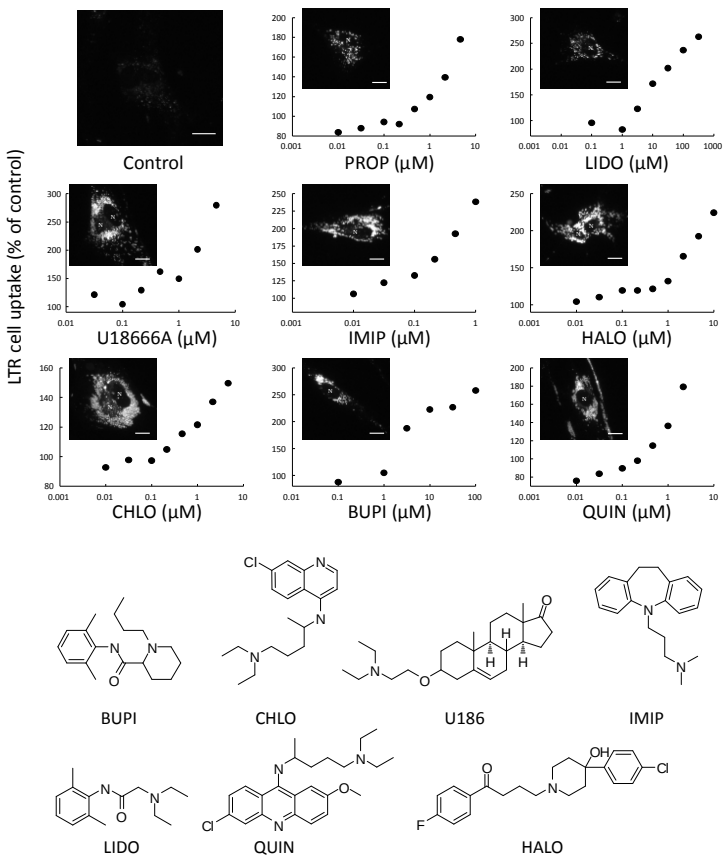

Figure 2.2 Concentration-dependent cellular accumulation of LysoTracker Red (200 nM for 1 hour) in wild-type human fibroblasts with a 48 hour pretreatment of various lysosomotropic drugs measured by (inset) epifluorescence microscopy and whole cell lysates of approximately 500,000 cells. For each inset the cell nuclei is designated with "N" and the scale bar represents 10 micrometers in length. Cellular accumulation of LysoTracker Red was measured in fluorescence units and then normalized to protein. The normalized LTR uptake was then compared to the control condition (vehicle alone) and reported as a percentage of the control. The drug concentrations used for the fluorescent micrographs was determined as the value that yielded the greatest expansion of lysosomal volume while showing no loss in viability or visible signs of toxicity: U18666A (2μM), quinacrine (2μM), propranolol (4μM), haloperidol (10μM), chloroquine (4μM), bupivacaine (100μM), lidocaine (100μM), imipramine (1μM).

(Originally published in: J Pharm Sci. 2013 Aug 22. doi: 10.1002/jps.23706)

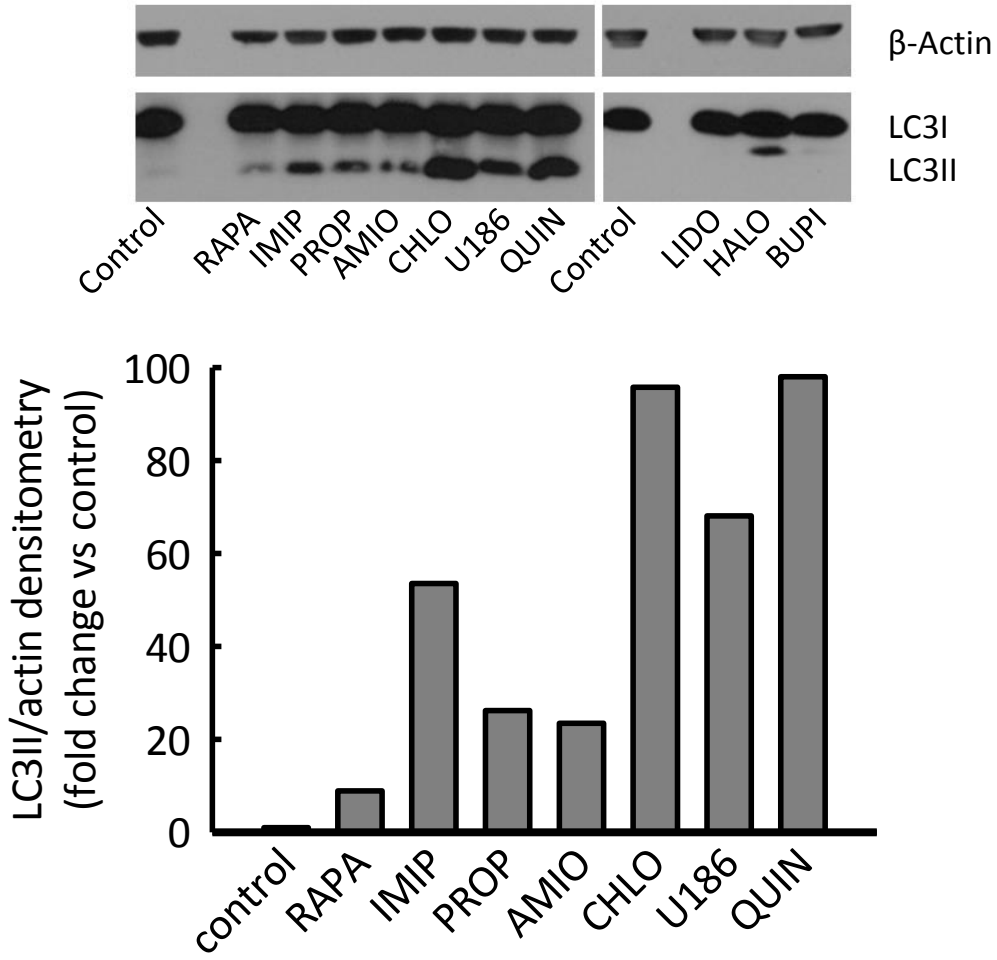

Figure 2.3 Western blot analysis of the protein markers of autophagy LC3BI/II (18kDa, 16kDa respectively) with a 48-hour treatment of various lysosomotropic drugs or vehicle alone. The concentration of lysosomotropic drug used in these assessments (A) & (B) was as follows: U18666A (2μM), quinacrine (2μM), propranolol (4μM), haloperidol (10μM), chloroquine (4μM), bupivacaine (100μM), lidocaine (100μM), imipramine (1μM), amiodarone (5μM).

(Originally published in: J Pharm Sci. 2013 Aug 22. doi: 10.1002/jps.23706)

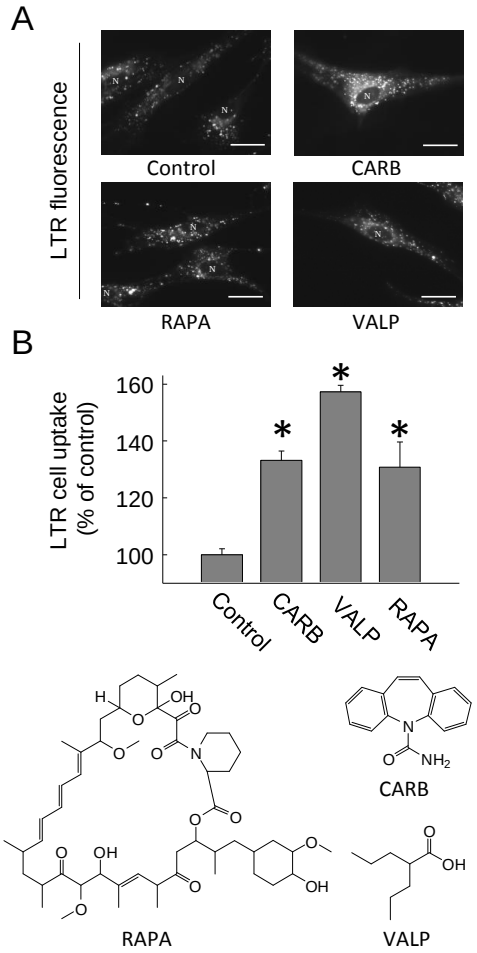

Figure 2.4 Cellular accumulation of LysoTracker Red (200nM for 1 hour) in wild-type human fibroblasts with a 48-hour pretreatment of the autophagy inducers rapamycin (200nM), valproic acid (1.5mM), carbamazepine (50µM), or vehicle alone assessed by (A) epifluorescence microscopy and (B) whole cell lysates of approximately 500,000 cells (n=3). In section (A) each cell nuclei is designated with "N" and scale bars represent 10 micrometers in length. Cellular accumulation of LysoTracker Red in (B) was measured in fluorescence units and then normalized to protein. The normalized LTR uptake was then compared to the control condition (vehicle alone) and reported as a percentage of the control. The values represented in this plot are the mean +/- SD from three independent experimental evaluations (*, p <.02 by Student's t-test).

(Originally published in: J Pharm Sci. 2013 Aug 22. doi: 10.1002/jps.23706)

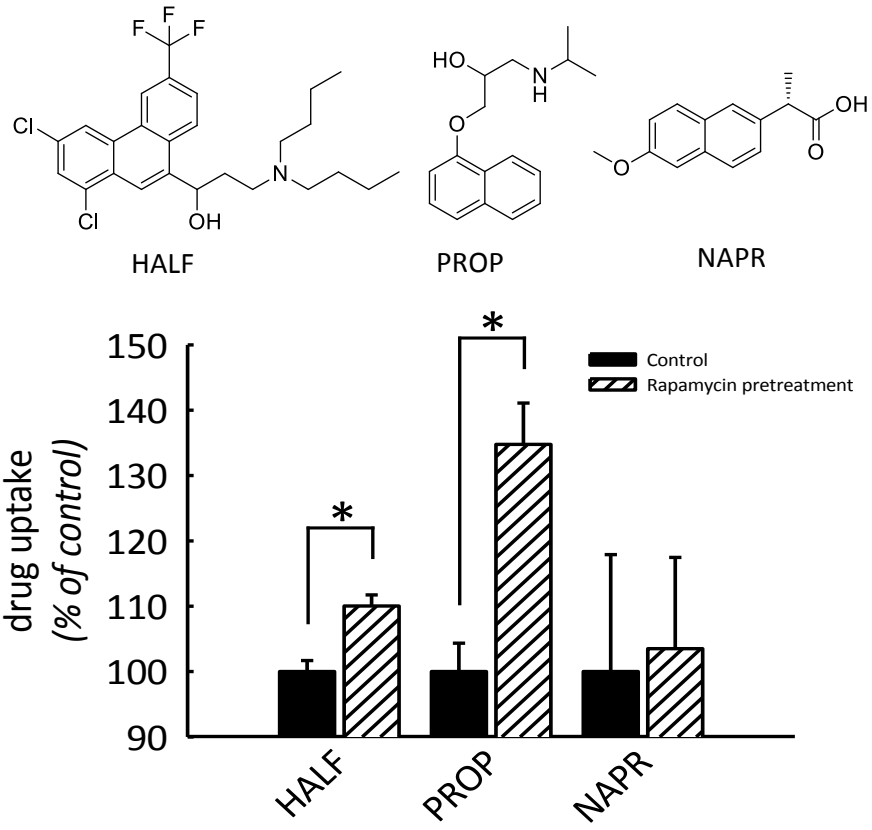

Figure 2.5 Cellular accumulation of the lysosomotropic drugs propranolol (200nM), halofantrine (200nM) or the non-lysosomotropic drug naproxen (5μM) with a 48-hour pretreatment of the autophagy inducer rapamycin (200nM) or vehicle alone. Cellular accumulation of tritium-labeled propranolol and halofantrine was measured in radioactive units (DPM) and normalized to protein. Naproxen cellular accumulation was measured by LC-MS/MS and normalized to protein. The normalized drug uptakes were then compared to the corresponding control sample devoid of rapamycin pretreatment, and the value is reported as a percentage of the control. The values represented in this plot are the mean +/- SD from three independent experimental evaluations (*, $p < .01$ by Student's t-test).

(Originally published in: J Pharm Sci. 2013 Aug 22. doi: 10.1002/jps.23706)

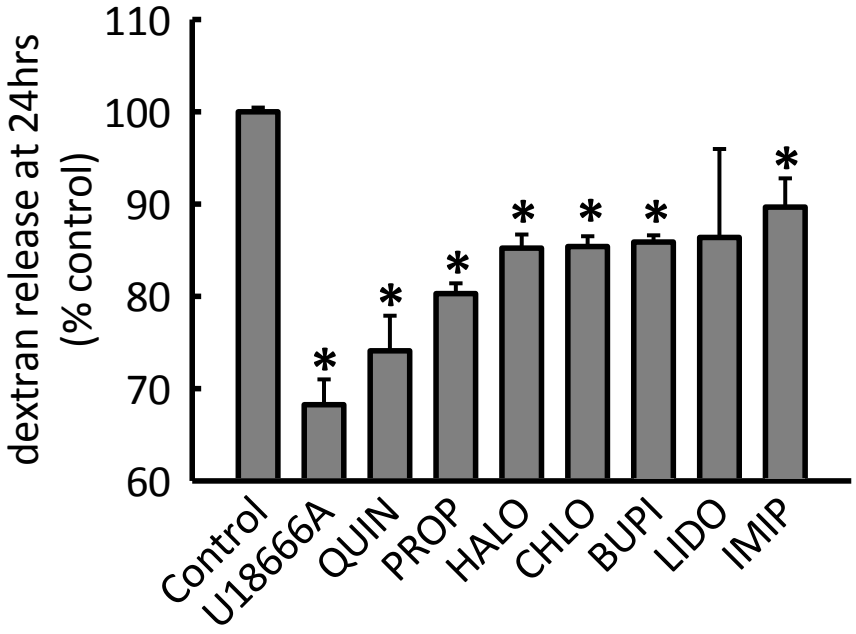

Figure 2.6 Vesicle-mediated lysosomal egress assessed by dextran secretion (24-hour release period) with a 48-hour pretreatment of various lysosomotropic drugs or vehicle alone. Secretion of tritium-labeled dextran was measured in radioactive units (DPM) and normalized to protein. The normalized dextran secretion was then compared to the control condition (vehicle alone) and reported as a percentage of the control. The values represented in this plot are the mean +/- SD from three independent experimental evaluations (*, $p < .05$ by Student's t-test). The drug concentrations used were as follows: U18666A (2μM), quinacrine (2μM), propranolol (4μM), haloperidol (10μM), chloroquine (4μM), bupivacaine (100μM), lidocaine (100μM), imipramine (1μM).

(Originally published in: J Pharm Sci. 2013 Aug 22. doi: 10.1002/jps.23706)

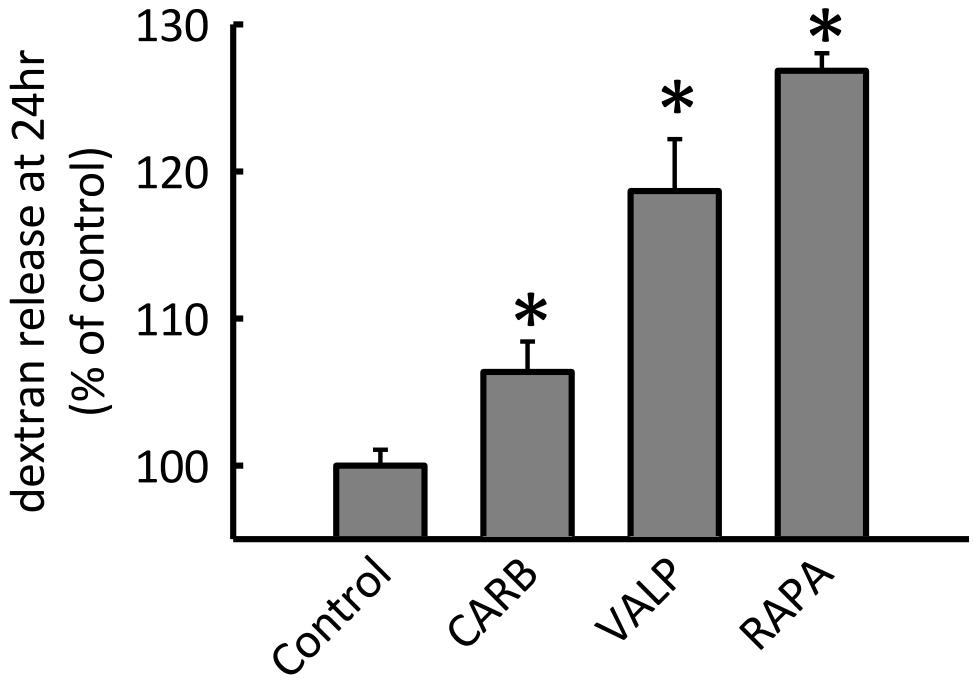

Figure 2.7 Vesicle-mediated lysosomal egress assessed by dextran secretion (24-hour release period) with a 48-hour pretreatment of the autophagy inducers rapamycin, carbamazepine, valproic acid, or vehicle alone. Secretion of tritium-labeled dextran was measured in radioactive units (DPM) and normalized to protein. The normalized dextran secretion was then compared to the control condition (vehicle alone) and reported as a percentage of the control. The values represented in this plot are the mean +/- SD from three independent experimental evaluations (*, $p < .05$ by Student's t-test).

(Originally published in: J Pharm Sci. 2013 Aug 22. doi: 10.1002/jps.23706)

References

Chow, M. S. (1996). "Intravenous amiodarone: pharmacology, pharmacokinetics, and clinical use." Ann Pharmacother 30(6): 637-643.

Drake, K. R., M. Kang and A. K. Kenworthy (2010). "Nucleocytoplasmic distribution and dynamics of the autophagosome marker EGFP-LC3." PLoS One 5(3): e9806.

Funk, R. S. and J. P. Krise (2012). "Cationic amphiphilic drugs cause a marked expansion of apparent lysosomal volume: implications for an intracellular distribution-based drug interaction." Mol Pharm 9(5): 1384-1395.

Goldman, S. D., R. S. Funk, R. A. Rajewski and J. P. Krise (2009). "Mechanisms of amine accumulation in, and egress from, lysosomes." Bioanalysis 1(8): 1445-1459.

Kimura, S., T. Noda and T. Yoshimori (2007). "Dissection of the autophagosome maturation process by a novel reporter protein, tandem fluorescent-tagged LC3." Autophagy 3(5): 452-460.

Kornfeld, S. and I. Mellman (1989). "The biogenesis of lysosomes." Annu Rev Cell Biol 5: 483-525.

Levine, B. and G. Kroemer (2008). "Autophagy in the pathogenesis of disease." Cell 132(1): 27-42.

Luzio, J. P., V. Poupon, M. R. Lindsay, B. M. Mullock, R. C. Piper and P. R. Pryor (2003). "Membrane dynamics and the biogenesis of lysosomes." Mol Membr Biol 20(2): 141-154.

Madeo, F., N. Tavernarakis and G. Kroemer (2010). "Can autophagy promote longevity?" Nat Cell Biol 12(9): 842-846.

Mizushima, N., T. Yoshimori and B. Levine (2010). "Methods in mammalian autophagy research." Cell 140(3): 313-326.

Rubinsztein, D. C., J. E. Gestwicki, L. O. Murphy and D. J. Klionsky (2007). "Potential therapeutic applications of autophagy." Nat Rev Drug Discov 6(4): 304-312.

Rubinsztein, D. C., G. Marino and G. Kroemer (2011). "Autophagy and aging." Cell 146(5): 682-695.

Sarkar, S., R. A. Floto, Z. Berger, S. Imarisio, A. Cordenier, M. Pasco, L. J. Cook and D. C. Rubinsztein (2005). "Lithium induces autophagy by inhibiting inositol monophosphatase." J Cell Biol 170(7): 1101-1111.

Tanida, I., T. Ueno and E. Kominami (2004). "LC3 conjugation system in mammalian autophagy." Int J Biochem Cell Biol 36(12): 2503-2518.

Williams, A., S. Sarkar, P. Cuddon, E. K. Ttofi, S. Saiki, F. H. Siddiqi, L. Jahreiss, A. Fleming, D. Pask, P. Goldsmith, C. J. O'Kane, R. A. Floto and D. C. Rubinsztein (2008). "Novel targets for Huntington's disease in an mTOR-independent autophagy pathway." Nat Chem Biol 4(5): 295-305.

Chapter 3. Time-dependent effects of lysosomotropic drugs on the biogenesis of lysosomes

Introduction

Understanding the sources of variability in the pharmacokinetic properties of administered drugs is vitally important in ensuring that the proper dosing regimen is prescribed to each patient. Failure to adequately account for unexpected pharmacokinetic behavior can conceivably result in drug exposure levels that either fail to achieve the desired activity or rise to toxic levels. With this in mind, lysosomotropic drugs should be rigorously evaluated as they represent a category of drugs that typically have unique pharmacokinetic properties including a large volume of distribution and half-life. Lysosomotropic drugs also exhibit a significant degree of inter- and intra-patient variability in these same pharmacokinetic parameters. For example, the lysosomotropic drugs methadone, chloroquine, halofantrine, and amiodarone all exhibit a very wide range of reported values for their elimination half-lives (Table 3.1) as stated by the manufacturers' package insert and Ducharme et. al. (Ducharme and Farinotti 1996).

In our evaluations of lysosomotropic drugs we have found that their total cellular accumulation is almost entirely accounted for by lysosomal sequestration (Figure 3.1), a finding that corroborates a similar report by Funk and Krise (Funk and Krise 2012). With this in mind, we reasoned that the unique pharmacokinetic properties of these drugs, specifically their large volume of distribution, are primarily the result of lysosomal sequestration in the peripheral tissues. Although the volume of distribution is a pharmacokinetic parameter that is often stated to be a constant (Shargel, Wu-Pong et al. 2005), we have begun to consider the possibility that it is a dynamic parameter that is subject to fluctuation. Based on our knowledge that the cellular accumulation of lysosomotropic drugs is sensitive to changes in the lysosomal sequestration capacity of cells, we reasoned that conditions or cellular processes that lead to

increases or decreases in the lysosomal sequestration capacity of peripheral tissues could result in a significant change to the volume of distribution of lysosomotropic drugs. Due to the proportional relationship between the volume of distribution and half-life, increases to a drug's volume of distribution could foreseeably result in a longer half-life (Greenblatt 1985). Based on this, it seems feasible that this mechanism could, at least in part, be contributing to the variability observed in the volume of distribution and half-life of lysosomotropic drugs.

Inspired by the potential clinical ramifications of this hypothesis we have focused the efforts of the current chapter on evaluating the time- and concentration-dependent changes to lysosomes caused by exposing cells to one of three different lysosomotropic drugs that have a range of relative lipophilicities from low to high (Log P: methylamine -0.63, propranolol 2.32, and halofantrine 7.93). We have sought to characterize the changes occurring to the cellular accumulation of these drugs and provide a mechanistic basis for these observed changes. Ultimately, this information could be used to explain, at least in part, some of the inter- and intra-patient variability seen in the pharmacokinetic parameters of lysosomotropic drugs.

Materials and Methods

Cell Lines and Reagents

Wild-type (WT) human fibroblasts (catalogue # CRL-2076) were purchased from ATCC (Manassas, VA). All cells were cultured in glutamine-free DMEM supplemented with 10% FBS, 10mM HEPES, 1mM Sodium Pyruvate, and 2mM Glutamax and maintained at 37°C and 5% CO_2. Cells were routinely subcultured to maintain 50% to 90% confluency. Experiments were carried out within 10 passages following removal from cryopreservation.

Dulbecco's phosphate buffered saline (D-PBS), Dulbecco's modified Eagle's medium (DMEM), HEPES, sodium pyruvate, glutamax, and Lysotracker Red DND-99 (LTR) were purchased from Invitrogen

(Carlsbad, CA). Fetal bovine serum (FBS) was purchased from Atlanta Biologicals (Lawrenceville, GA). Halofantrine, propranolol, methylamine, laemmli buffer, Triton X-100 (TX-100), and sodium deoxycholate were purchased from Sigma-Aldrich (St. Louis, MO). Pierce BCA protein assay kit was ordered from ThermoScientific (Rockford, IL). Anti-beta actin antibody (catalogue #8H10D10) was purchased from Cell Signaling Technology (Danvers, MA). Anti-TFEB antibody (catalogue #A303-673A) was purchased from Bethyl Laboratories Inc (Montgomery, TX). The anti-LAMP1 monoclonal antibody (H4A3) developed by J. Thomas August and James E.K. Hildreth was obtained from the Developmental Studies Hybridoma Bank developed under the auspices of the NICHD and maintained by the University of Iowa, Department of Biology (Iowa City, IA). ^{3}[H]-halofantrine and ^{3}[H]-propranolol were purchased from American Radiolabeled Chemicals, Inc. (St. Louis, MO). ^{14}[C]-methylamine was purchased from Moravek Biochemicals (Brea, CA).

Drug Accumulation Assays

WT human fibroblasts were grown in plastic 12-well culture plates (Corning Life Sciences) at a seeding density of 10,000 cells per well. All cell samples utilized to determine the time-dependent uptake of drug were grown for 8 days in a 12-well plate in order to control for variability in cellular confluency upon completion. During the 8 day growth period the extracellular media was replaced with drug containing media (^{3}[H]-propranolol at .06µCi/mL, ^{3}[H]-halofantrine at .1µCi/mL or ^{14}[C]-methylamine at .1µCi/mL) at the appropriate time in order to attain the indicated duration and concentration of drug exposure. During this time period the media was refreshed every 48 hrs in order to maintain optimal nutrient conditions for cell growth. To assess the total drug accumulation, the cells were immediately washed twice with 4°C D-PBS once the desired exposure time was achieved. To assess the drug uptake by ion-trapping independent mechanisms, nigericin and monensin was spiked directly into the existing

cell culture media (final concentration of 10µM and 20µM, respectively) 2 hrs prior to reaching the desire drug exposure duration. Once the desire drug exposure time was achieved, the cells were then washed twice with 4°C D-PBS. The washed cells were then lysed using lysis buffer (50 mM tris base, 150 mM NaCl, 1% NP40, pH titrated to 7.4 with HCl) for 30mins at 37°C. The lysate was recovered from each well by aspiration using a standard pipette. The quantity of radio-labeled drug was measured in DPMs using a Beckman LS 60001C liquid scintillation counter. Background signal contributed from non-specific binding of drug to the plate surface was subtracted from each measurement. Dilutions of each radiolabeled drug stock were performed to attain a standard curve relating DPMs to nanomoles of drug. Measured DPMs in the cell samples were then converted to nanomoles of drug. Protein abundance was measured for each sample using the BCA method. The calculated nanomoles of drug present in each sample was then normalized to mg protein.

The ion-trapping dependent cellular accumulation of propranolol or halofantrine was determined mathematically by subtracting the ion-trapping independent cellular accumulation (nigericin/monensin treated samples) from the total cellular accumulation at each indicated time point. In order to facilitate direct comparison of the cellular uptake of drug between the 5nM exposure and the 5µM exposure, the activity of the radiolabeled drug was held constant between the two conditions (.06µCi/mL ^{3}H-propranolol or .1µCi/mL ^{3}H-halofantrine). Unlabeled drug was then added to the radiolabeled-drug-containing-media in order to achieve the total target concentration of drug. A direct comparison of the drug accumulation for the 5nM and 5µM drug exposures could only be achieved with propranolol and halofantrine as the cellular accumulation of methylamine was below the limit of quantification at nanomolar concentrations.

Drug Release Assay

WT human fibroblasts were grown in plastic 12-well culture plates at a seeding density of 20,000 cells per well. The cells were exposed to 5µM propranolol (consisting of 4.995µM unlabeled propranolol and 5nM of ^{3}H-propranolol at a final activity of .06µCi/mL) or 5µM halofantrine (consisting of 4.995µM unlabeled halofantrine and 5nM ^{3}H-halofantrine at a final activity of .1µCi/mL) for 6 days. At the end of this 6 day exposure the extracellular media was replaced with drug-free media which marked time point zero of the drug washout period. The drug-free extracellular media was replaced every 24hrs to maintain sink conditions. At the indicated time points cells were then rapidly washed twice with 4°C D-PBS. The cells were then lysed for 30 min at 37°C using lysis buffer and the lysate was capture by aspiration using a standard pipette. The quantity of tritium-labeled drug (propranolol or halofantrine) was measured in disintegrations per minute (DPM) using a Beckman LS 60001C liquid scintillation counter. Background signal contributed from non-specific binding of drug to the plate surface was subtracted from each measurement. Dilutions of each radiolabeled drug stock were performed to attain a standard curve relating DPMs to nanomoles of drug. Measured DPMs in the cell samples were then converted to nanomoles of drug. Protein abundance was measured for each sample using the BCA method. Measured DPMs were then converted to nanomoles of drug and normalized to protein.

Lysotracker Red Accumulation Assay

WT human fibroblasts were grown in plastic 12-well culture plates at a seeding density of 20,000 cells per well. The cells were exposed to vehicle or 5µM of propranolol or halofantrine for 6 days. The extracellular media was refreshed after 2 days in order to maintain optimal nutrient conditions. At the end of this 6 day exposure the extracellular media was replaced with drug-free media which marked time point zero of the drug washout period. The drug-free extracellular media was replaced every 24hrs to maintain sink conditions. At the indicated time points during the drug washout phase LTR cellular

accumulation was measured as previously described.(Funk and Krise 2012) Briefly, LTR was spiked into the existing media to a concentration of 200nM and the cells were incubated at 37°C for 1 hour. Cells were then rapidly washed twice with 4 °C D-PBS. Cells were lysed with lysis buffer for 30mins at 37°C. The lysate was recovered from each well by aspiration using a standard pipette. The quantity of LTR was determined by fluorescent signal in relative fluorescence units (RFU) using a Bio-Tek FL600 microplate fluorescence reader. Background signal contributed from non-specific binding of LTR to the plate surface was subtracted from each measurement. Protein abundance was measured for each sample using the BCA method. Measured LTR signal (RFU) was then normalized to protein. These normalized values were then compared to the control condition (vehicle treated) and depicted as a percentage of the control.

Western Blot Analysis

WT human fibroblasts were grown in 100mm plastic Petri dishes (Corning Life Sciences) at a seeding density of approximately 200,000 cells per dish. The extracellular media was replaced with 5µM propranolol and the cells were exposed to the drug for the indicated duration (Figure 2.3). The extracellular media was refreshed every 48 hrs in order to maintain optimal nutrient conditions for cell culture. Upon reaching the desired duration of drug exposure, cells were quickly washed three times with 4°C D-PBS. Whole cells were then lysed with RIPA buffer (150mM sodium chloride, 1% TX-100, 0.5% sodium deoxycholate, 0.1% SDS, 50mM tris, pH 8.0, and the protease inhibitors APL & PMSF). The protein abundance was then determined by the BCA method. Protein samples were then mixed with Laemmli buffer (250mM Tris-HCl, 8% Sodium Dodecyl Sulfate (SDS), 40% Glycerol, 8% ß-mercaptoethanol, .02% bromophenol). Protein samples from whole cell lysates or isolated nuclear fractions (see method section *Isolation of cell nuclei*) were subjected to 12% sodium dodecyl sulfate-

polyacrylamide gel electrophoresis (SDS-PAGE) for 120 mins. The proteins were then transferred to a 0.2 µm pore PVDF membrane (Millipore) using 300 V*hrs. The PVDF membrane was then blocked using 5% non-fat milk for 1hr at room temperature. The PVDF membrane was then exposed to primary antibody (1:1000 anti-LAMP1, 1:30,000 anti-beta actin, or 1:3000 anti-TFEB) for two hrs, washed for 5mins X3 in .2% TX-100/D-PBS to remove non-bound primary antibodies, and then exposed to secondary antibody (1:4000 goat anti-rabbit HRP or goat anti-mouse HRP) for two hrs and then washed for 5mins X3 in .2% TX-100/D-PBS. Detection of HRP-conjugated antibody was achieved by chemiluminescence using Western Lightning-ECL (PerkinElmer) on autoradiograph film.

Isolation of Cell Nuclei

Isolation of the nuclear fraction of WT human fibroblasts was carried out as described.(Settembre, Di Malta et al. 2011) Briefly, WT human fibroblasts were grown in 100mm plastic Petri dishes at a seeding density of approximately 200,000 cells per dish. The extracellular media was replaced with 5µM propranolol and the cells were exposed to the drug for the indicated duration (Figure 2.3). The extracellular media was refreshed every 48 hrs in order to maintain optimal nutrient conditions for cell culture. Upon reaching the desired duration of drug exposure, cells were quickly washed three times with 4°C D-PBS. Cells were then lysed using soft-lysis buffer (50mM Tris-HCl, 137.5mM NaCl, .5% TX, 10% glycerol, 5mM EDTA, pH 8, and the protease inhibitors APL & PMSF) for 15mins at 4°C. The petri dishes were then scraped using a cell scraper to liberate all cellular debris. The soluble and insoluble portions of the cell lysate were then centrifuged for 3mins at 3,000g. The supernatant was removed and the resulting nuclear pellet was washed twice with ice-cold D-PBS. The remaining nuclear pellet was then solubilized in RIPA buffer.

Transmission Electron Microscopy

WT human fibroblasts were grown in 175cm^2 culture flasks for 6 days with vehicle alone or 5µM propranolol. Media was refreshed every 48 hrs in order to maintain optimal nutrient conditions. At the end of the 6 day time period the cells were removed and fixed using 0.25% glutaraldehyde for 2 hrs at room temperature. Cells were then washed once and stained with osmium tetroxide 2% w/v in D-PBS for 1 hour at room temperature. The cells were washed one time with D-PBS and stained with tannic acid 1% for one hour at room temperature. The cells were then washed with water and stained with uranyl acetate 4% for 30mins at room temperature. Following one wash step with water the cells were washed in progressively higher concentrations of ethanol until the wash reached 100% ethanol. Following the ethanol washes the cells were stained with propylene oxide. Cells were then embedded in EPON resin. All images were taken on an FEI Tecnai F20 XT Field Emission Transmission Electron Microscope.

Sizing of the lysosomal structures was performed manually using the Image J software (freely available at http://rsbweb.nih.gov/ij/). The data obtained from the manual sizing was then normalized to the surface area of cytosol present within the analyzed cell slice and then reported as counts per mm^2. Lysosomes were divided into three distinct categories, primary, secondary, and lipid laden membrane whorls, using published descriptions of their structural features as a guide.(Fawcett 1981) Briefly, small dense granules with homogenous contents were considered to be primary lysosomes. Due to the excessive number of primary lysosomes present within each cell slice, the data present in Figure 3.5 B for primary lysosomes is representative of one cell slice (n=1) for each condition. Larger bodies with heterogeneous content including undigested material were considered to be secondary lysosomes. Larger densely stained bodies with multiple concentric membrane-like whorls were considered to be

lipid-laden membrane whorls. Data presented in Figure 3.5 B for secondary lysosomes and membrane whorls are representative of ten cell slices (n=10) for each condition.

Results and Discussion

Lysosomotropic drugs increase their own cellular accumulation and exhibit biphasic cellular accumulation.

In vitro studies that evaluate the dynamics of drug uptake and release have proven to be a valuable tool in developing an understanding of the mechanisms underlying the variability observed in the activity and pharmacokinetic properties of drugs administered to humans (Sirotnak, Moccio et al. 1981, Leonessa, Jacobson et al. 1994, Demant and Friche 1998). In chapters 1 and 2 we have detailed the phenomenon whereby lysosomotropic drugs caused an expansion in the lysosomal sequestration capacity of cells, a condition referred to as the expanded lysosomal volume phenotype (expanded LVP). Although we provided a mechanistic foundation for the development of the expanded LVP, we did not evaluate the time-dependent aspect of this phenomenon. In the current section we have evaluated the dynamics of drug uptake of methylamine, propranolol, or halofantrine. We have sought to answer the simple question, are these lysosomotropic drugs capable of increasing their own cellular accumulation as a result of the expanded LVP?

To answer this first question, we initially investigated the cellular uptake of low nanomolar levels of a tritium-labeled drug (propranolol or halofantrine) following a 6 day exposure to the drug. After establishing the cellular accumulation of the tritium-labeled drug we then repeated the experiment including a low micromolar concentration of native un-labeled drug. We found that cells exposed to a low micromolar concentration of these drugs accumulated significantly more of the tritium-labeled probe versus the low nanomolar concentration (Figure 3.2 A). Because the concentration of tritium-

labeled probe was identical under these two conditions the radioactive abundance within the cells should be directly comparable. The native unlabeled drug does not possess a radiolabeled element so it should therefore not contribute any additional signal in our assay regardless of its concentration. These results support the notion that lysosomotropic drugs are capable of increasing their own cellular accumulation in a dose-dependent manner. Due to the low abundance of methylamine cellular accumulation we were not able to determine if methylamine was capable of increasing its own cellular accumulation in a dose-dependent fashion as the low nanomolar concentration yielded a signal that was below our limit of quantification.

After establishing this dose-dependent phenomenon we then sought to characterize the kinetic uptake profile for these two concentrations (i.e., the low nanomolar and low micromolar concentrations) over an 8 day period. From these evaluations we hoped to glean information regarding when this dose-dependent phenomenon was occurring. Interestingly, we found that the kinetic uptake profile at the 5µM concentration exhibited a bi-phasic characteristic for both propranolol and halofantrine (Figure 3.2 B). Similar to other published work, an initial steady state was reached after a short period of time with propranolol achieving the initial steady state after a few hours and halofantrine after one day (Figure 3.2 B). Importantly, the kinetic uptake profile at the 5nM concentration failed to exhibit a biphasic characteristic for both propranolol and halofantrine (Figure 3.2 C). The difference in the kinetic uptake profiles between the low micromolar versus the low nanomolar concentrations was consistent with the dose-dependent phenomenon that we observed in Figure 3.2 A. Another interesting observation was that the much more hydrophilic molecule, methylamine, did not exhibit a biphasic kinetic uptake profile at the 5µM concentration (Figure 3.2 C). As mentioned previously, the 5nM kinetic uptake profile for methylamine could not be assessed due to analytical limitations.

Propranolol and halofantrine increase the lysosomal ion-trapping capacity of cells in a time-dependent fashion.

The total cellular accumulation of lysosomotropic drugs is achieved from the additive effects of two separate mechanisms, ion trapping-dependent and ion trapping-independent mechanisms. The ion trapping-independent mechanisms includes drug-binding to components such as intracellular proteins, lipid membranes, and DNA. Changes in the cellular uptake of lysosomotropic drugs could conceivably occur due to changes in one or both of these mechanisms. In this section we have sought to characterize the contribution that ion trapping-dependent and ion trapping-independent mechanisms play in the cellular uptake of propranolol and halofantrine.

To delineate the contribution that each of these cellular uptake mechanisms were exhibiting we employed the use of nigericin and monensin. These small molecule drugs are capable of carrying hydrogen ions across lipid bilayers thereby dissipating the pH gradients existing within the cell, i.e., alkalinizing the lysosomal pH. To determine the contribution of each cellular uptake mechanism we first measured the total cellular uptake of propranolol or halofantrine under normal conditions. This value represented the drug uptake due to both ion trapping-dependent and ion trapping-independent mechanisms. In parallel to this assessment we also measured the cellular accumulation of propranolol or halofantrine in the presence of nigericin and monensin. Disrupting the pH gradients within the cells would result in the release of any drug that was accumulating due to ion trapping. The cellular uptake in nigericin/monensin treated cells would therefore represent only the ion trapping-independent mechanisms. By subtracting the ion trapping-independent value from the total uptake value we could arrive at the cellular uptake due to ion trapping-dependent mechanisms. Using this approach we were able to characterize how the ion trapping-dependent mechanisms changed over the course of an 8 day drug treatment (Figure 3.3). Figure 3.3 illustrates that the ion trapping based accumulation of these drugs increases significantly for both 5μM propranolol and 5μM halofantrine.

Hydrophobic amines increase nuclear localization of TFEB, increase the expression of LAMP1, and increase the abundance of smaller secondary lysosomes and lipid-laden lysosomes.

Following the observation that both propranolol and halofantrine caused a significant and progressive increase in the ion trapping-dependent component of their total cellular uptake (Figure 3.3), we next sought to explore the cellular mechanisms that might be involved in this phenomenon. Based on the theory of ion trapping, we reasoned that there were two conceivable changes that can occur within the cells to explain our observations. The pH gradients that exist between the lysosomal lumen and the cell cytosol and extracellular space are vital for the ion trapping mechanism. Increases to this pH gradient, i.e., hyper-acidification of the lysosomal lumen, could result in an enhanced ion trapping-dependent accumulation of lysosomotropic drugs (de Duve, de Barsy et al. 1974). To explore this possibility we employed the use of a pH sensitive fluorophore (oregon-green) conjugated to a membrane impermeable dextran polymer. After localizing this polymer to the lysosomes we then assessed the pH within the lysosomal lumen. We found that cells exposed to 5µM propranolol for 4 days failed to cause a significant decrease in the pH of the lysosomes (Figure 3.4).

After ruling out the possibility of lysosome hyper-acidification we then explored alternative mechanisms to explain our observations. In the theory of ion trapping the volume of lysosomes can also influence the total cellular accumulation of lysosomotropic drugs (de Duve, de Barsy et al. 1974). We envisaged several possible ways in which the volume of the lysosomes could be increasing. First, the total number of lysosomes could increase inside the cell thereby resulting in an overall increase in the lysosomal volume. Second, the diameter of the lysosomes could also increase which would result in a corresponding increase in the lysosomal volume. Last, there could conceivably be a combination of these two possibilities. To determine which of these possibilities were at play we performed a quantitative analysis of the diameter and overall abundance of lysosomes in cells treated for 6 days with or without exposure to 5µM propranolol using electron microscopy (Figure 3.5 A, B). In this analysis, we

categorized lysosomes as either primary, secondary, or those containing multiple concentric membrane whorls (lipid-laden) according to previously published work (Fawcett 1981). We then manually sized these lysosomes and reported the abundance and size distribution per surface area of cell cytosol. Interestingly, we found that propranolol caused a significant increase in the number of primary lysosomes seemingly without affecting the size distribution (Figure 3.5 B). Propranolol also caused an increase in the abundance of 500nm to 1500nm sized secondary lysosomes (Figure 3.5 B). Finally, the frequency of lysosomes containing multiple concentric membrane whorls also significantly increased (Figure 3.5 B). Overall, propranolol caused a significant increase in the abundance of all three categories of lysosomes. These results are consistent with the observed increase in both the total cellular accumulation of propranolol (Figure 3.2), and ion trapping-dependent accumulation of propranolol (Figure 3.3).

To corroborate the results obtained from the ultrastructure analysis of lysosomes we also measured the total cellular abundance of LAMP-1 (lysosome-associated membrane protein 1) with the rationale that if increases to the abundance of lysosomes were indeed taking place then a corresponding increase in LAMP-1 should also become evident. We found that 5μM propranolol caused a progressive time-dependent increase in LAMP-1 starting after 1 day of propranolol exposure (Figure 3.5 C). We also found a similar result in cells treated with 5μM halofantrine (Figure 3.6). These results are consistent with the observations made in Figure 3.5 B.

Having established that lysosomotropic drugs are capable of causing an increase in the number of lysosomes we next sought to determine the cellular mechanisms that might be underlying these observed effects. Sardiello and coworkers have recently identified transcription factor EB (TFEB) as a master regulator of lysosome biogenesis which positively regulates genes included in the Coordinated Lysosomal Expression and Regulation (CLEAR) network (Sardiello, Palmieri et al. 2009). With this in

mind, we tested the potential involvement of TFEB in the development of the drug-induced lysosome proliferation observed in Figures 3.5 B, 3.5 C, 3.6. Under normal cellular conditions TFEB is primarily localized to the cell cytosol. Under conditions leading to the activation of TFEB, i.e., conditions that enhance lysosomes biogenesis, TFEB translocates from the cell cytosol to the nucleus where it initiates to expression of lysosomes-associated genes (Sardiello, Palmieri et al. 2009, Settembre, Di Malta et al. 2011). In our analysis of propranolol treated cells, we found that the nuclear abundance of TFEB increased progressively in a time-dependent fashion starting after one day of exposure (Figure 3.5 C). This TFEB activation roughly coincided with the increase in LAMP-1 expression and enhanced cellular uptake of propranolol and halofantrine.

The release of drugs from cells occurs faster than the reversal of the expanded lysosomal volume phenotype.

After establishing the dynamic cellular uptake of propranolol and halofantrine, TFEB activation, and the ensuing expanded LVP, we next sought to determine the reversibility of this phenotype. In this section we measured the kinetic release of propranolol or halofantrine from cells under sink conditions (drug-washout) and compared that with the recovery rate to a normal lysosomal volume phenotype (recovery rate). In order to evaluate the persistence of the expanded LVP, we measured the cellular uptake of the fluorescent lysosomotropic probe lysotracker red (LTR) as a surrogate marker for lysosomal volume. The rate at which the LTR uptake values decline to 100% of control represents the “recovery rate”.

Interestingly, we found that the drug-washout rate for propranolol could exceed the recovery rate (Figure 3.7 A). This suggests that the expanded LVP is likely secondary to the accumulation of drug, i.e., propranolol is initiating some downstream event that ultimately results in the expanded LVP. In contrast to propranolol, halofantrine exhibited a close parallel between the rate of drug-washout and the recovery rate (Figure 3.7 B). The difference between propranolol and halofantrine could likely be

the result of widely different lipophilicities between the two drugs. Halofantrine is significantly more lipophilic which could foreseeably result in reduced rates of drug-washout.

Conclusion

Lysosomtropic drugs tend to have unique pharmacokinetic properties including a very large volume of distribution and a long half-life (Shepard and Falkner 1990, Gong, Zhao et al. 2007, Zheng, Zhang et al. 2011). These drugs also tend to exhibit a significant degree of intra- and inter-patient variability in these same pharmacokinetic parameters. Understanding the sources of variability in the pharmacokinetic properties of administer drugs is immensely important in ensuring that the proper dosing regimen is prescribed to each patient. Failure to adequately account for conditions or diseases that cause unintended changes to the pharmacokinetic behavior of drugs can potentially lead to lack of efficacy (inadequate drug exposure) or even toxicity (drug exposures that are too high), particularly for drugs with narrow therapeutic windows.

With this in mind, we have investigated possible mechanisms that can contribute to the large degree of variability seen in the pharmacokinetic properties of lysosomotropic drugs. For example, methadone, chloroquine, halofantrine, and amiodarone all exhibit a very wide range of reported values for their elimination half-lives (Table 3.1) as stated by the manufacturers' package insert and Ducharme et. al. (Ducharme and Farinotti 1996). The elimination half-life is a dependent variable that is inversely proportional to clearance and proportional related to the volume of distribution (Greenblatt 1985). Traditionally, changes in the elimination half-life of drugs have been attributed to alterations in drug clearance while the volume of distribution was considered to be a constant parameter (Shargel, Wu-Pong et al. 2005). In the current chapter we have explored the possibility that the volume of distribution of lysosomotropic drugs is a dynamic pharmacokinetic parameter that can exhibit significant fluctuations.

We and others have shown that the extensive entrapment of lysosomotropic drugs in the lysosomes accounts for almost all of the cellular accumulation of these drugs (Figure 3.1) (Funk and Krise 2012, Logan, Kong et al. 2013). This is a fascinating observation as the lysosomes only account for approximately 1% of the total cellular volume. With this in mind, relatively minor changes to the lysosomal sequestration capacity of cells could potentially result in large changes in the degree of peripheral tissue accumulation ultimately influencing the volume of distribution for these drugs. Conditions or diseases that result in changes to the lysosomal sequestration capacity of cells could therefore provide the basis for the variability in the elimination half-life of these drugs.

We and others have reported a drug-drug interaction involving lysosomes whereby the cellular accumulation of one drug could influence the cellular accumulation of a secondarily administered drug (Daniel and Wojcikowski 1997, Daniel and Wojcikowski 1999, Funk and Krise 2012). In light of this work, we have focused the effort of the current chapter on characterizing the time-dependent effects that the perpetrator drug exhibits on the lysosomes. We also sought to define the cellular processes that contribute to these observed changes. In addition, we sought to determine if these lysosomotropic drugs were capable of increasing their own cellular accumulation.

We have examined the time-dependent cellular accumulation of 3 lysosomotropic molecules that possess a large range of lipophilic character from a low Log P to a high Log P (methylamine -0.63, propranolol 2.32, and halofantrine 7.93) (Figure 3.2). In this assessment we observed that propranolol and halofantrine exhibited a biphasic cellular accumulation in that they both reached an initial steady state after a relatively short period of time, a finding that is similar to other reports detailing the drug uptake of methotrexate and the weakly basic anticancer drugs vinblastine and daunorubicin (Sirotnak, Moccio et al. 1981, Leonessa, Jacobson et al. 1994, Demant and Friche 1998).

After approximately two days of drug exposure the cells then exhibited a secondary accumulation phase which ultimately resulted in a 3-fold increase in drug levels compared to the initial 1 day steady-state (Figure 3.2 B). Interestingly, this biphasic cellular accumulation was not observed with methylamine. Although methylamine is considered to be lysosomotropic, it has a significantly lower lipophilicity relative to the other two drugs. We reasoned that methylamine's failure to exhibit this same biphasic cellular accumulation was due to its relatively low lipophilicity and the ensuing total cellular uptake that was significantly lower than propranolol and halofantrine (.15nmol/mg protein, 2.5nmol/mg protein, 26nmol/mg protein, respectively) (Figure 3.2 B). Consistent with this reasoning, we showed that cells incubated with low nanomolar concentrations of propranolol or halofantrine failed to exhibit the biphasic cellular accumulation (Figure 3.2 C).

To our knowledge this is the first study reporting a biphasic cellular accumulation phenomenon in cultured cells treated with lysosomotropic drugs. However, other groups have also observed that the cellular accumulation of lysosomotropic drugs (e.g., amiodarone, chloroquine, propranolol, and chlorpromazine) can steadily increase over an 8 day time period (Honegger, Scuntaro et al. 1995, Scuntaro, Kientsch et al. 1996). Honegger and coworkers found that the steadily increasing accumulation of these lysosomotropic drugs was accompanied by an increase in the intracellular accumulation of phospholipids (i.e., phosopholipidosis). They reasoned that the increase in intracellular phospholipids (phospholipidosis) provided additional lipid-binding sites for these cationic drugs and it was by virtue of these additional binding sites that the lysosomotropic drugs exhibited a time-dependent increase in their cellular accumulation (Honegger, Scuntaro et al. 1995, Scuntaro, Kientsch et al. 1996).

Although we found this to be an intriguing and well-reasoned hypothesis, we sought to more fully evaluate the mechanisms associated with the observed increases in the cellular accumulation of

propranolol and halofantrine. By employing the use of 2 ionophores, nigericin and monensin, we separately measured the contribution that ion trapping-dependent and ion trapping-independent mechanisms played in the total cellular accumulation of these drugs.

Our results indicated that the ion trapping-independent mechanisms (i.e., binding to intracellular proteins, lipid membranes, and DNA) exhibited a steadily increasing contribution to the total cellular accumulation of propranolol and halofantrine over the 8 day time period (Figure 3.8), a finding that corroborates the work by Honegger and colleagues. However, we also found that the ion trapping-dependent mechanisms also increased over this 8 day time period (Figure 3.3). This is a significant finding because it implies that phospholipidosis alone cannot account for all of the time-dependent increases seen in the cellular accumulation of these drugs. We reasoned that the volume of the lysosomes must also be increasing in a time-dependent manner and that this mechanism is also contributing to time-dependent increase in drug uptake.

After establishing that an expansion in lysosomal volume was contributing to the time-dependent increases in the cellular accumulation of propranolol and halofantrine, we next sought to determine the basis for this phenomenon. Others have reported observations where lysosomotropic drugs were capable of increasing lysosomal volume by causing massive osmotic swelling to the lysosomes, a process called vacuolization (Yang, Strasser et al. 1965, Finnin, Reed et al. 1969, Ohkuma and Poole 1981, Morissette, Lodge et al. 2008). In these evaluations the expansion in lysosomal volume was so massive that the lysosomes became visible by light microscopy. Although this finding is interesting, it is likely a phenomenon that is only achievable in an in vitro scenario as the drug concentrations required to achieve these results are in the millimolar range. We found it unlikely that lysosome vacuolization was contributing to the observed increase in lysosome volume seen in Figure 3.3 because we failed to see

any visible lysosome vacuolization by light microscopy, and we evaluated drug concentrations that were approximately 3 orders of magnitude lower than the aforementioned vacuolization experiments.

After ruling out lysosomal vacuolization, we then attempted to uncover the basis for this lysosomal volume expansion by examining the ultrastructure of lysosomes in cells treated for 6 days with or without 5µM propranolol. We had envisaged two distinct mechanisms that could lead to an increased lysosomal volume. First, the lysosomes could be coalescing (homotypic fusion) or fusing with other vesicles (heterotypic fusion) which could ultimately result in an increase in lysosomal volume. Secondly, the cell could be generating more lysosomes via the biosynthetic route. Finally, there could be a combination of these two mechanisms. Our results indicated that propranolol treatment caused an increase in the number of primary lysosomes and an increase in the number of smaller diameter secondary lysosomes. There was also an observed increase in the number of lysosomes containing concentric membrane whorls (lipid-laden) lysosomes, which is consistent with previous reports detailing drug-induced phospholipidosis (Xia, Ying et al. 2000, Anderson and Borlak 2006)

These results provide an interesting window into the mechanisms underlying the development of the expanded lysosomal volume seen with propranolol treatment. The lysosome is a dynamic organelle that receives membrane and material from many cellular pathways such as phagocytosis, endocytosis, autophagy, and the biosynthetic pathway (Kornfeld and Mellman 1989, Luzio, Poupon et al. 2003, Saftig and Klumperman 2009). An increase in the normal homeostatic levels of any of these pathways could conceivably result in an increase to the steady state volume of lysosomes. On the other side of the mass-balance equation are pathways that can carry membrane and material away from the lysosomes. Although significantly less is known about these mechanisms, they too must represent an important pathway that can be controlled by the cell. Interestingly, Luzio and coworkers have identified a lysosomal egress pathway that involves a heterotypic fusion event between lysosomes and late

endosomes resulting in the formation of a “hybrid organelle” (Luzio, Poupon et al. 2003, Luzio, Pryor et al. 2005). They hypothesized that this hybrid organelle then stimulates the formation of small transport carrier vesicles that help extract membrane and material from the hybrid organelle, ultimately resulting in the reformation of the primary lysosome (Bright, Reaves et al. 1997). With this in mind, we reasoned that conditions interfering with late endosome-lysosome fusion would result in a greater number of primary lysosomes. Consistent with this hypothesis, we found that the number of primary lysosomes increased dramatically with a prolonged treatment of propranolol (Figure 3.5 B). Previous reports have also observed impaired late endosome-lysosome fusion with the treatment of lysosomotropic drugs using different analytical techniques (Kaufmann and Krise 2008).

In addition to impaired fusion competency between the late endosomes and lysosomes, we also conceived the possibility that these lysosomotropic drugs might be capable of impairing membrane fission events, i.e., vesicle-mediated trafficking away from lysosomes. We reasoned that impaired vesicle-mediated trafficking away from lysosomes would manifest as perturbation in the normal size distribution of secondary lysosomes (hybrid lysosomes) as these bodies would be unable to revert back to primary lysosomes. The histogram presented in Figure 3.5 B shows that the size distribution of secondary lysosomes has dramatically shifted, resulting in an increased abundance of 500nm to 1500nm diameter secondary lysosomes. In corroboration of this idea, the results of the dextran secretion assay also supported the notion that lysosomotropic drugs can impair the vesicle-mediated egress efficiency out of the lysosomal system (Figure 2.6).

The steady state lysosomal volume can also be influenced by pathways that bring membrane and material into the lysosomal system (i.e., endocytosis, autophagy, phagocytosis, and the biosynthetic pathway). As we showed in Chapter 2, induction of autophagy can result in an increased steady state volume of lysosomes (Figure 2.4). In this section we have sought to explore another input pathway, the

biosynthetic route (Figure 2.1). An increase in the normal homeostatic level of this pathway could conceivably result in a greater number of lysosomes and by extension a greater steady state volume of lysosomes. After observing that propranolol and halofantrine both exhibited a biphasic cellular accumulation we hypothesized that at some point prior to the secondary accumulation phase cells are up-regulating lysosome biogenesis. Fortunately, Sardiello and coworkers have recently identified transcription factor EB (TFEB) as a master regulator of lysosome biogenesis and as a driver of autophagy (Sardiello, Palmieri et al. 2009, Settembre, Di Malta et al. 2011).

With this recent discovery in mind, we evaluated the potential involvement of TFEB in the development of the expanded lysosomal volume phenotype. In its inactive form TFEB is normally localized within the cell cytosol, but during activation TFEB translocates to the cell nucleus. We found that cells treated with a low micromolar concentration of propranolol exhibited a time-dependent activation of TFEB (Figure 3.5 C). As expected, TFEB activation occurred after 1 day, just prior to the secondary accumulation phase beginning at approximately 2 days of propranolol exposure (Figure 3.2 B).

To corroborate these findings implicating TFEB activation we also evaluated the time-dependent changes to the cellular abundance of LAMP-1 (lysosome associated membrane protein-1) which can be used as a surrogate marker for lysosome abundance (Fukuda 1991, Furuta, Yang et al. 1999). If lysosome biogenesis was indeed being unregulated, we would expect to see a concomitant increase in the abundance of LAMP-1. As Figures 3.5 C and 3.6 illustrates, the abundance of LAMP-1 increases in a time-dependent manner. Importantly, the increase in LAMP-1 abundance occurs at relatively the same time as TFEB activation (1 day of exposure). Collectively, these results support the hypothesis that TFEB activation is contributing to the drug-induced expansion in lysosomal volume seen in cells treated with lysosomotropic drugs.

The information presented thus far has detailed the dynamic cellular uptake of both halofantrine and propranolol and the ensuing changes that occurred to the lysosomes as a result of these exposures. In addition to these characterizations we have also measured the rate at which these lysosomal changes revert back to normal, i.e., the rate at which the lysosomal volume returns back to 100% of control. In order to test this we incubated cells with a low micromolar concentration of propranolol or halofantrine for 4 days which was enough time to allow the formation of the expanded LVP. The extracellular media was then replaced with drug-free media, a time point which marked the beginning of the drug-washout period. During this drug-washout period both the lysosomal volume and intracellular drug concentrations were measured over time (Figure 3.7).

The results of these experiments allowed two important conclusions to be made. First, the drug-induced expansion in lysosomal volume appears to be fully reversible. But, depending on the lysosomotropic drug, the recovery-rate can be dramatically different. For example, the lysosomal volume in the propranolol treated condition is fully recovered after only a few hours of drug-washout (Figure 3.7 A), while the halofantrine treated cells required several days to recover back to control levels (Figure 3.7 B). It is important to note that this difference in recovery-rate correlates with the rate of drug-release from the cells. This finding is to be expected as we have previously determined that the expanded LVP is dose-dependent (Figure 3.2 B compared to 3.2 C). Secondly, the data presented in Figure 3.7 A illustrates that the release of drug can occur faster than the recover-rate. This is an interesting finding that suggests that the expanded LVP is not the direct result of drug accumulation, as seen with the osmotic swelling of lysosomes in the vacuolization process. Instead, this implies that propranolol is influencing some downstream process, such as membrane fusion or membrane fission that is required for vesicle-mediated transport. Unlike propranolol, the cellular release of halofantrine did not precede the recovery of lysosomal volume likely because the kinetics of drug-release was the rate-limiting process (Figure 3.7 B).

The data presented in this chapter provides valuable insight into the underlying mechanisms involved in how lysosomotropic drugs can alter lysosomes and increase their own cellular accumulation. Although these findings are compelling and interesting, they must be followed with comprehensive in vivo studies to determine the full impact of this phenomenon in a clinical setting.

Drug name	Elimination half life
methadone	8-59 hours
chloroquine	20-60 day
halofantrine	6-10 days
amiodarone	15-100 days

Table 3.1 A table depicting the reported values for the elimination half-lives of four different lysosomotropic drugs. Values are obtained from the package inserts provided by the drug manufacturers.

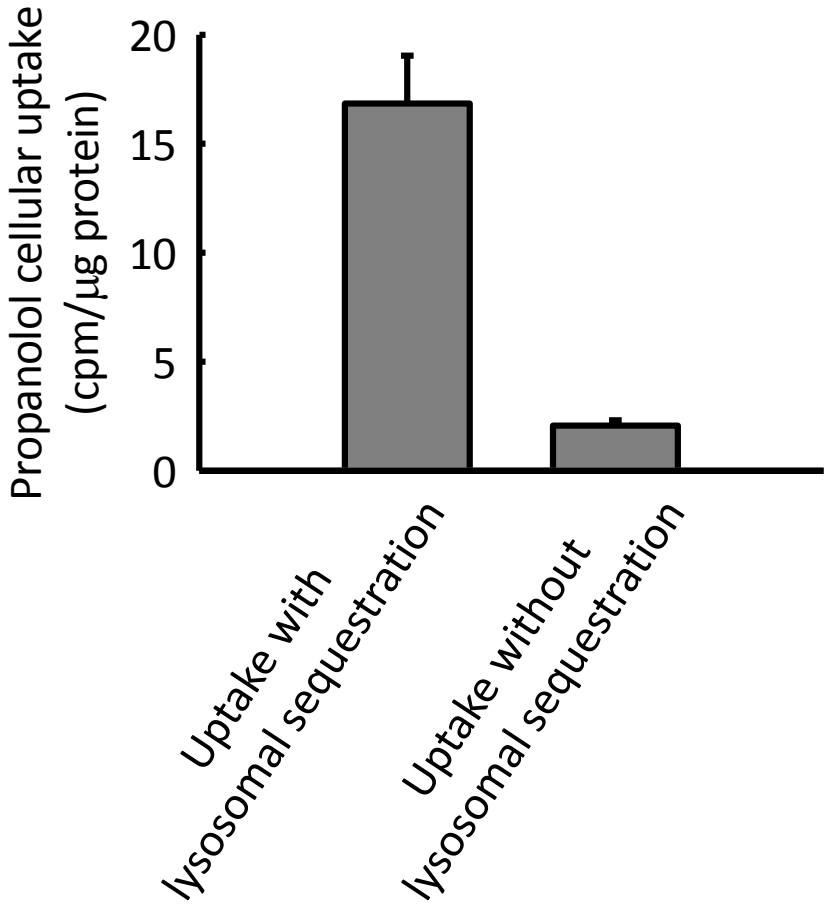

Figure 3.1 Lysosomal sequestration of propranolol accounts for a vast majority of propranolol cellular accumulation. WT human fibroblasts were treated with 5µM tritium labeled propranolol (.06µCi/mL) for 2 days. Following the end of the 2 day treatment the lysosomal pH gradient was either dissipated with 10µM nigericin and 20µM monensin (Uptake without lysosomal sequestration) or left intact (Uptake with lysosomal sequestration). The total cellular accumulation of the tritium labeled probe was then depicted as counts per minute (cpm) normalized to the cellular protein (µg protein).

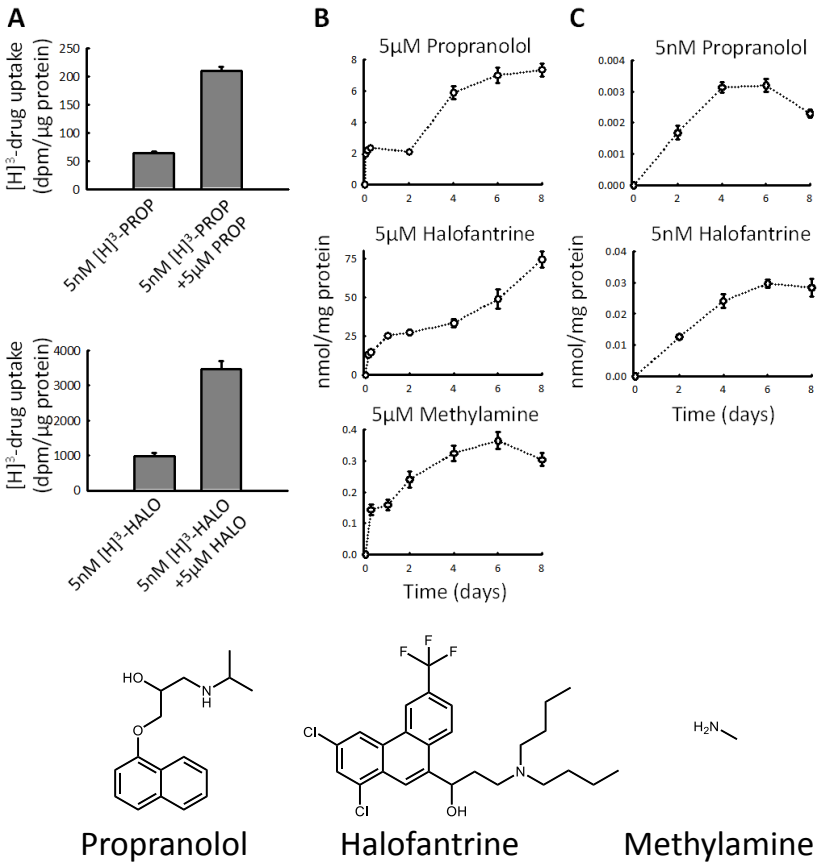

Figure 3.2 Concentration and time dependent cellular accumulation of weakly basic compounds in WT human fibroblasts. (A) Relative cellular accumulation of propranolol or halofantrine after an 8 day exposure to the presence of 5nM tritium labeled drug (final activity of .06µCi/mL or .1µCi/mL, respectively) or 5nM tritium labeled drug plus 5µM unlabeled drug (final activity of .06µCi/mL or .1µCi/mL, respectively) in the cell culture media showing that these drugs are capable of increasing their own cellular accumulation in a dose dependent manner. (B) Time dependent cellular accumulation of 5µM propranolol, 5µM halofantrine, or 5µM methylamine measured using radio-labeled compounds (final activity of .06µCi/mL, .1µCi/mL or .1µCi/mL, respectively). (C) Time dependent cellular accumulation of 5nM propranolol or halofantrine measured using radio-labeled drugs (final activity of .06µCi/mL or .1µCi/mL, respectively).

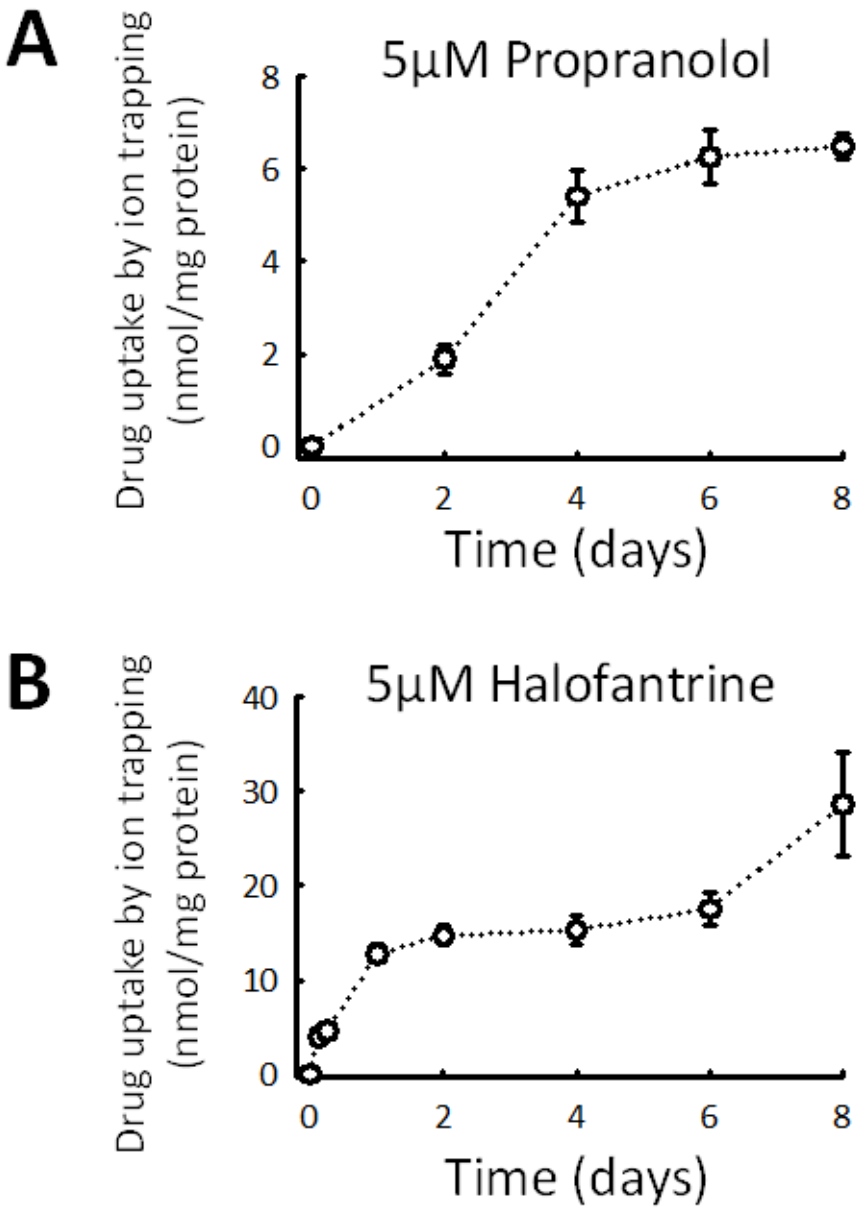

Figure 3.3 Time dependent changes in the ion trapping-based cellular accumulation of (A) propranolol or (B) halofantrine in WT human fibroblasts during an 8 day time period with the extracellular drug concentration held constant at 5µM.

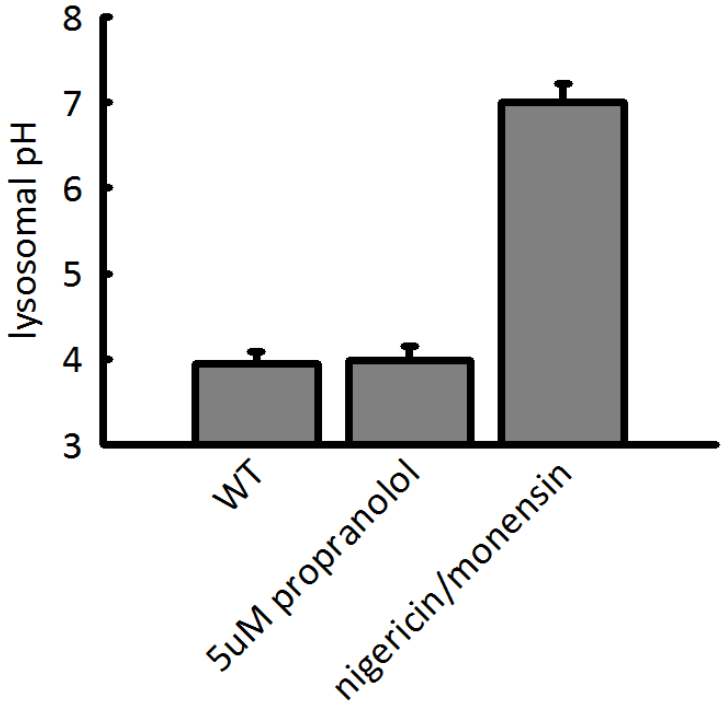

	Lysosomal pH
Control	3.94 +/- .15
5µM Propranolol	3.98 +/- .17
Nigericin/Monensin	7.0 +/-.22

Figure 3.4 Lysosomal pH measurements of WT human fibroblasts exposed to 4 days of vehicle (control), 5µM propranolol, or lysosomal pH disruption (nigericin/monensin). Lysosomal pH was determined through the use of oregon-green dextran as described in the materials and methods section.

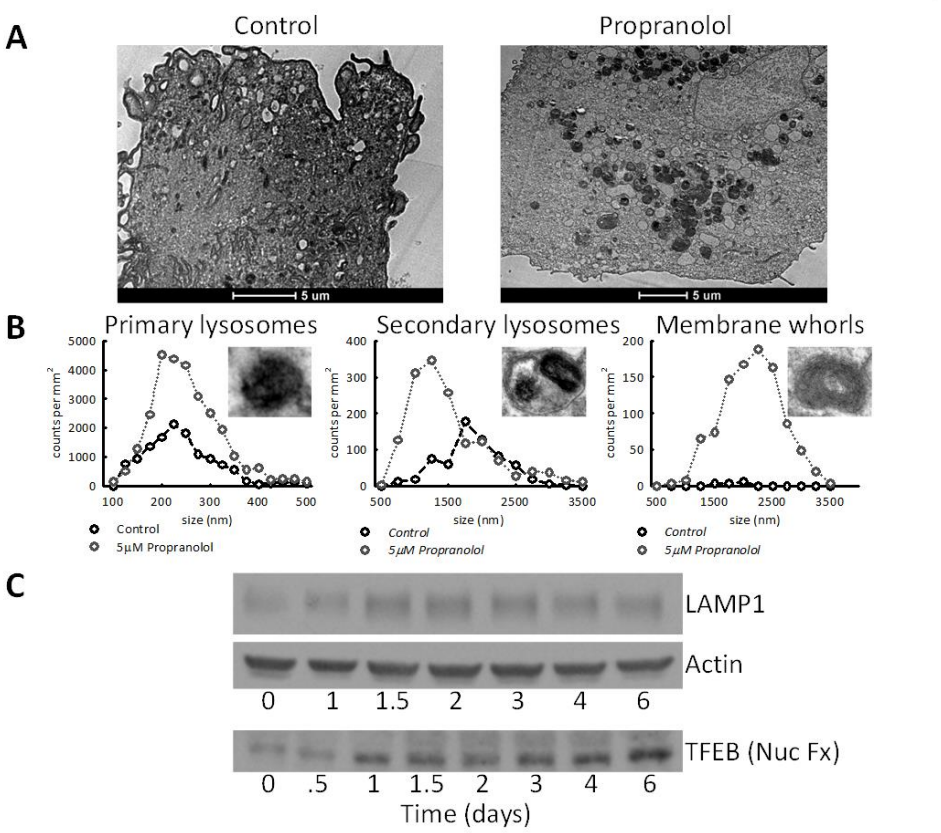

Figure 3.5 Prolonged propranolol treatment (5µM) induces changes to the ultrastructure of WT human fibroblast and the expression and localization of cellular proteins. (A) Transmission electron micrographs of cells treated for 6 days with vehicle (control) or 5µM propranolol showing that propranolol treatment increases the number of visible lipid-laden membrane whorls (intracellular dark circular bodies). (B) Quantitative analysis of the size distribution of primary lysosomes, secondary lysosomes, and membrane whorls in cells treated for 6 days with vehicle (control) or 5µM propranolol. Insets depict a representative example of the associated structure. Total counts are normalized to the surface area of cell cytosol analyzed within the cell slice. (C) Westernblot analysis depicting the time dependent increase in LAMP1 expression and the time dependent activation (cytosol-to-nuclear translocation) of transcription factor EB (TFEB) following exposure to 5µM propranolol.

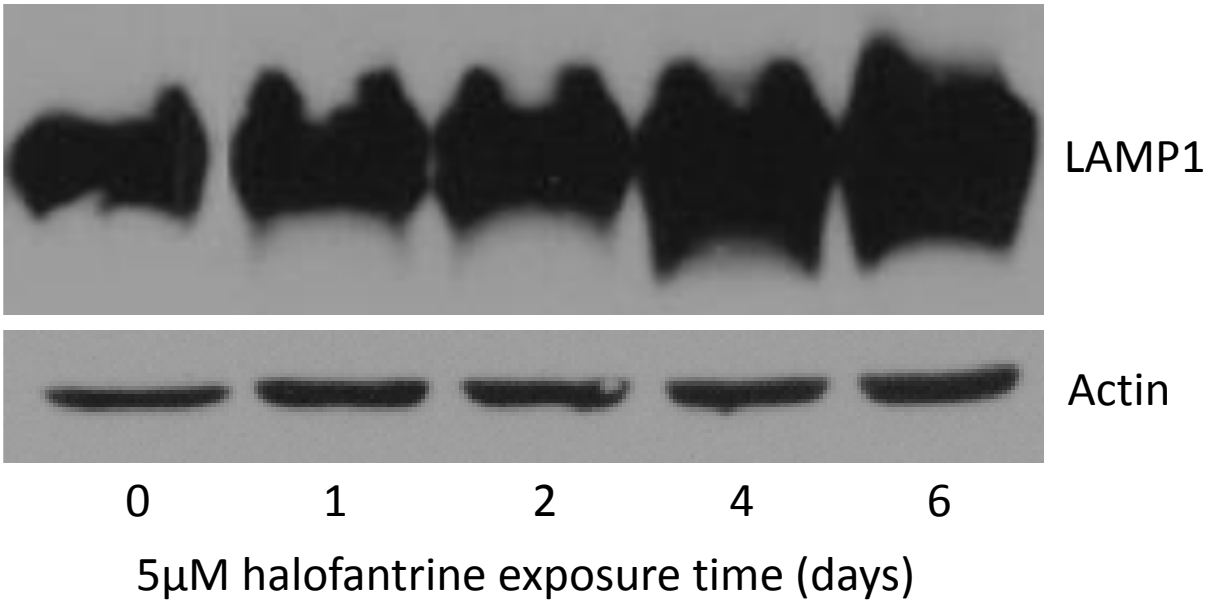

Figure 3.6 Western blot analysis depicting the time-dependent increase of LAMP1 abundance in WT human fibroblasts. Each lane contains approximately 25µg of whole-cell protein from cells exposed to 5µM halofantrine for the indicated exposure time.

Figure 3.7

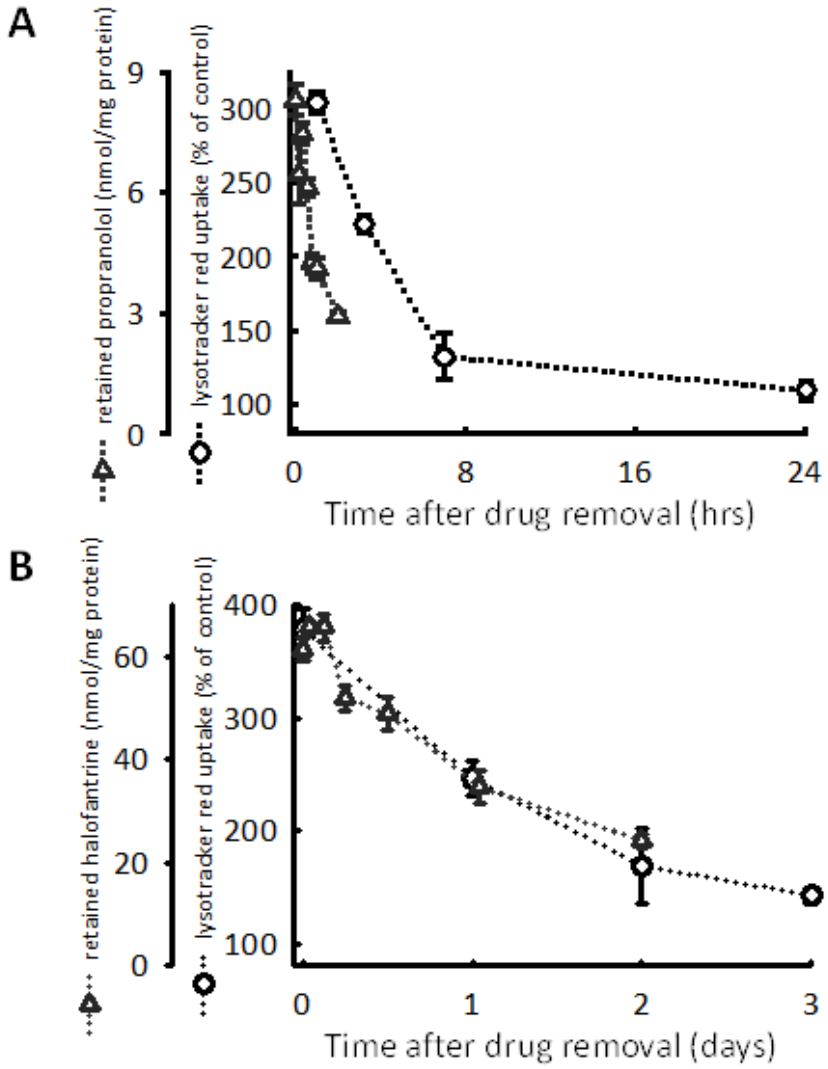

Comparative analysis of the time dependent cellular release of drug from WT human fibroblasts to the rate of reversal of the expanded lysosomal volume phenotype. Cells were pretreated with (A) 5μM propranolol or (B) 5μM halofantrine for 6 days. Following the pretreatment the extracellular media was replaced with drug free media and the rate of drug release and the cellular uptake of lysotracker red was analyzed at specified time points.

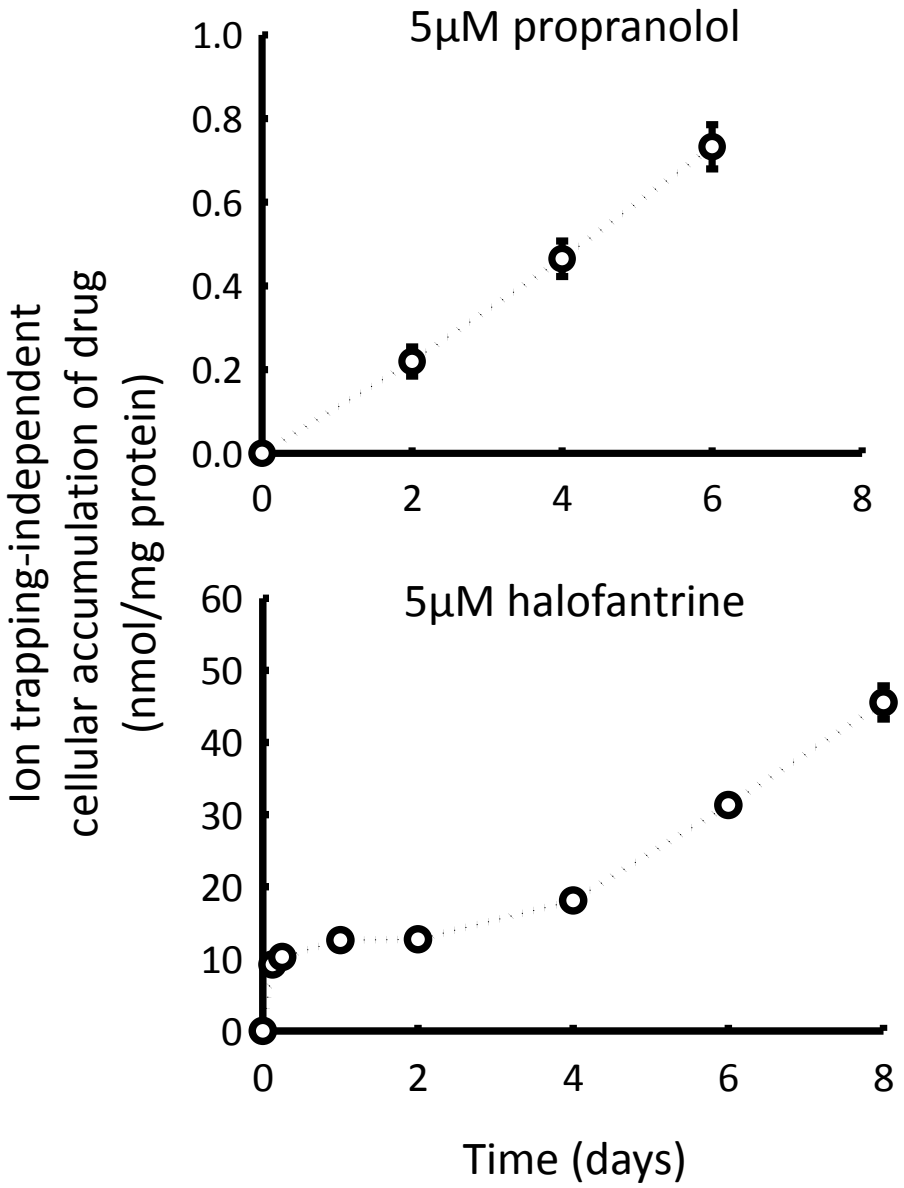

Figure 3.8 Time dependent changes in the ion trapping-independent cellular accumulation mechanisms of (A) propranolol or (B) halofantrine in WT human fibroblasts during an 8 day time period with the extracellular drug concentration held constant at 5µM.

References

Anderson, N. and J. Borlak (2006). "Drug-induced phospholipidosis." FEBS Lett 580(23): 5533-5540.

Bright, N. A., B. J. Reaves, B. M. Mullock and J. P. Luzio (1997). "Dense core lysosomes can fuse with late endosomes and are re-formed from the resultant hybrid organelles." J Cell Sci 110 (Pt 17): 2027-2040.

Daniel, W. A. and J. Wojcikowski (1997). "Interactions between promazine and antidepressants at the level of cellular distribution." Pharmacology & toxicology 81(6): 259-264.

Daniel, W. A. and J. Wojcikowski (1999). "The role of lysosomes in the cellular distribution of thioridazine and potential drug interactions." Toxicology and applied pharmacology 158(2): 115-124.

de Duve, C., T. de Barsy, B. Poole, A. Trouet, P. Tulkens and F. Van Hoof (1974). "Commentary. Lysosomotropic agents." Biochemical pharmacology 23(18): 2495-2531.

Demant, E. J. and E. Friche (1998). "Kinetics of anthracycline accumulation in multidrug-resistant tumor cells: relationship to drug lipophilicity and serum albumin binding." Biochemical pharmacology 56(9): 1209-1217.

Ducharme, J. and R. Farinotti (1996). "Clinical pharmacokinetics and metabolism of chloroquine. Focus on recent advancements." Clin Pharmacokinet 31(4): 257-274.

Fawcett, D. W. (1981). The cell. Philadelphia, W. B. Saunders Co.

Finnin, B. C., B. L. Reed and N. E. Ruffin (1969). "The effects of osmotic pressure on procaine-induced vacuolation in cell culture." J Pharm Pharmacol 21(2): 114-117.

Fukuda, M. (1991). "Lysosomal membrane glycoproteins. Structure, biosynthesis, and intracellular trafficking." J Biol Chem 266(32): 21327-21330.

Funk, R. S. and J. P. Krise (2012). "Cationic amphiphilic drugs cause a marked expansion of apparent lysosomal volume: implications for an intracellular distribution-based drug interaction." Mol Pharm 9(5): 1384-1395.

Funk, R. S. and J. P. Krise (2012). "Cationic Amphiphilic Drugs Cause a Marked Expansion of Apparent Lysosomal Volume: Implications for an Intracellular Distribution-Based Drug Interaction." Molecular pharmaceutics.

Furuta, K., X. L. Yang, J. S. Chen, S. R. Hamilton and J. T. August (1999). "Differential expression of the lysosome-associated membrane proteins in normal human tissues." Arch Biochem Biophys 365(1): 75-82.

Gong, Y., Z. Zhao, D. J. McConn, B. Beaudet, M. Tallman, J. D. Speake, D. M. Ignar and J. P. Krise (2007). "Lysosomes contribute to anomalous pharmacokinetic behavior of melanocortin-4 receptor agonists." Pharm Res 24(6): 1138-1144.

Greenblatt, D. J. (1985). "Elimination half-life of drugs: value and limitations." Annual review of medicine 36: 421-427.

Honegger, U. E., I. Scuntaro and U. N. Wiesmann (1995). "Vitamin E reduces accumulation of amiodarone and desethylamiodarone and inhibits phospholipidosis in cultured human cells." Biochem Pharmacol 49(12): 1741-1745.

Kaufmann, A. M. and J. P. Krise (2008). "Niemann-Pick C1 functions in regulating lysosomal amine content." The Journal of biological chemistry 283(36): 24584-24593.

Kornfeld, S. and I. Mellman (1989). "The biogenesis of lysosomes." Annu Rev Cell Biol 5: 483-525.

Leonessa, F., M. Jacobson, B. Boyle, J. Lippman, M. McGarvey and R. Clarke (1994). "Effect of tamoxifen on the multidrug-resistant phenotype in human breast cancer cells: isobologram, drug accumulation, and M(r) 170,000 glycoprotein (gp170) binding studies." Cancer research 54(2): 441-447.

Luzio, J. P., V. Poupon, M. R. Lindsay, B. M. Mullock, R. C. Piper and P. R. Pryor (2003). "Membrane dynamics and the biogenesis of lysosomes." Mol Membr Biol 20(2): 141-154.

Luzio, J. P., V. Poupon, M. R. Lindsay, B. M. Mullock, R. C. Piper and P. R. Pryor (2003). "Membrane dynamics and the biogenesis of lysosomes." Molecular membrane biology 20(2): 141-154.

Luzio, J. P., P. R. Pryor, S. R. Gray, M. J. Gratian, R. C. Piper and N. A. Bright (2005). "Membrane traffic to and from lysosomes." Biochemical Society symposium(72): 77-86.

Morissette, G., R. Lodge and F. Marceau (2008). "Intense pseudotransport of a cationic drug mediated by vacuolar ATPase: procainamide-induced autophagic cell vacuolization." Toxicol Appl Pharmacol 228(3): 364-377.

Ohkuma, S. and B. Poole (1981). "Cytoplasmic vacuolation of mouse peritoneal macrophages and the uptake into lysosomes of weakly basic substances." J Cell Biol 90(3): 656-664.

Saftig, P. and J. Klumperman (2009). "Lysosome biogenesis and lysosomal membrane proteins: trafficking meets function." Nat Rev Mol Cell Biol 10(9): 623-635.

Sardiello, M., M. Palmieri, A. di Ronza, D. L. Medina, M. Valenza, V. A. Gennarino, C. Di Malta, F. Donaudy, V. Embrione, R. S. Polishchuk, S. Banfi, G. Parenti, E. Cattaneo and A. Ballabio (2009). "A gene network regulating lysosomal biogenesis and function." Science 325(5939): 473-477.

Scuntaro, I., U. Kientsch, U. N. Wiesmann and U. E. Honegger (1996). "Inhibition by vitamin E of drug accumulation and of phospholipidosis induced by desipramine and other cationic amphiphilic drugs in human cultured cells." Br J Pharmacol 119(5): 829-834.

Settembre, C., C. Di Malta, V. A. Polito, M. Garcia Arencibia, F. Vetrini, S. Erdin, S. U. Erdin, T. Huynh, D. Medina, P. Colella, M. Sardiello, D. C. Rubinsztein and A. Ballabio (2011). "TFEB links autophagy to lysosomal biogenesis." Science 332(6036): 1429-1433.

Shargel, L., S. Wu-Pong and A. B. C. Yu (2005). Applied biopharmaceutics & pharmacokinetics. New York, Appleton & Lange Reviews/McGraw-Hill, Medical Pub. Division.

Shepard, R. M. and F. C. Falkner (1990). "Pharmacokinetics of azithromycin in rats and dogs." The Journal of antimicrobial chemotherapy 25 Suppl A: 49-60.

Sirotnak, F. M., D. M. Moccio, L. E. Kelleher and L. J. Goutas (1981). "Relative frequency and kinetic properties of transport-defective phenotypes among methotrexate-resistant L1210 clonal cell lines derived in vivo." Cancer research 41(11 Pt 1): 4447-4452.

Xia, Z., G. Ying, A. L. Hansson, H. Karlsson, Y. Xie, A. Bergstrand, J. W. DePierre and L. Nassberger (2000). "Antidepressant-induced lipidosis with special reference to tricyclic compounds." Prog Neurobiol 60(6): 501-512.

Yang, W. C., F. F. Strasser and C. M. Pomerat (1965). "Mechanism of Drug-Induced Vacuolization in Tissue Culture." Exp Cell Res 38: 495-506.

Zheng, N., X. Zhang and G. R. Rosania (2011). "Effect of phospholipidosis on the cellular pharmacokinetics of chloroquine." J Pharmacol Exp Ther 336(3): 661-671.

Chapter 4. Structure activity relationship of lysosomotropic molecules their ability to induce an expanded lysosomal volume phenotype

Introduction

In the previous chapters we have detailed the ways in which lysosomotropic drugs can cause an expanded lysosomal volume phenotype (expanded LVP) and discussed the potential clinical ramifications of this phenomenon. In this chapter we have sought to explore how specific physicochemical properties of lysosomotropic molecules relate to their potency in eliciting this expanded LVP.

In the drug discovery process pharmaceutical scientists frequently assess a drug candidate's potential to cause toxicity or perpetrate a drug-drug interaction. From a health and safety stand-point this can reduce the chance that unsafe drugs are brought to market. From an economic standpoint these assessments can ultimately save companies vast amounts of research and development resources by either redirecting efforts to a more viable drug candidate or by developing countermeasures to overcome the identified safety issues.

The initial evaluations of a drug candidate's potential to cause toxicity can be performed in silico using structure activity relationships that have been established for unsafe drug-drug target interactions. For example, drug candidates are routinely screened for their potential to interact with the human ether-a-go-go channel (hERG-channel), a potassium ion channel that is critical for proper cardiac function (Vandenberg, Perry et al. 2012, Rayan, Falah et al. 2013). Through the use of in vitro screening techniques and protein crystal structure analysis a structure activity relationship has been developed

that can help predict possible drug-hERG-channel interactions (Tang, Kang et al. 2001, Vandenberg, Perry et al. 2012). Critical to the development of this structure activity relationship was a well-defined biological response, in this case the inhibition of hERG-channel activity, and a clinical imperative that necessitated the elucidation of the structure activity relationship, e.g., hERG-channel interactions can lead to cardiac arrhythmias and sudden cardiac arrest (Rampe and Brown 2013). Although the clinical ramifications of the expanded LVP are likely not as catastrophic as those seen with hERG-channel interactions, we nonetheless feel that the expanded LVP (and the ensuing drug-drug interaction involving lysosomes) represents a significant off-target drug effect that could benefit from a well-defined structure activity relationship.

Many lysosomotropic drugs share a common structure feature in that they possess a region that is relatively hydrophobic and also have a cationic function group (weak base). These drugs are generally referred to as cationic amphiphilic drugs or CADs. Over the last six decades many of these drugs have been observed to cause an interesting biochemical and morphological anomaly referred to as phospholipidosis (PL) (Halliwell 1997, Lowe, Glen et al. 2010). This condition is characterized by the hyper-accumulation of lipids and the appearance of lamellar inclusion bodies that are visible by electron microscopy (Yamamoto, Adachi et al. 1971, Anderson and Borlak 2006, Tomizawa, Sugano et al. 2006). In chapter 3 we detailed the relationship between the expanded LVP and phospholipidosis (PL). We found that the ion trapping-independent mechanisms of drug uptake in cultured cells, i.e., lipid binding (Figure 3.8), exhibited a time-dependent increase which contributed to the enhanced cellular accumulation of lysosomotropic drugs. Not surprising, many of the lysosomotropic drugs that we have identified as inducers of an expanded LVP (Figure 1.2, Figure 2.2) have also been shown to cause PL (e.g., chlorpromazine, imipramine, chloroquine, lidocaine, propranolol etc.) (Lowe, Glen et al. 2010). Previous reports have also implicated PL as a condition that can instigate a drug-drug interaction similar to what we have reported in chapters 2 and 3. For example, Reasor and coworkers have shown that

alveolar macrophages isolated from rats pretreated with the phospholipidosis-inducing drug chlorphentermine can accumulate significantly more amiodarone than alveolar macrophages isolated from rats not pre-treated with chlorphentermine (Reasor 1991). In addition, the phospholipidosis-inducing drug chloroquine has also been shown to increase the cellular accumulation of secondarily administered lysotracker green, a lysosomotropic fluorescent probe similar to lysotracker red (Zheng, Zhang et al. 2011). The exact contribution that PL plays in the total development of this drug-drug interaction is not currently known. However, based on the work in chapters 2 and 3, we would reason that PL likely plays an important but not exclusive role in the development of the expanded LVP and the ensuing drug-drug interaction involving lysosomes.

Irrespective of the exact contribution that PL plays in the development of the expanded LVP, we feel that a drug's potential to cause PL and the expanded LVP represents an important consideration in the drug development process. Consistent with this notion, the FDA considers drug-induced phospholipidosis to be a dubious off-target drug effect. Regardless of the poorly established link between drug-induced PL and clinically significant adverse effects the FDA will frequently require additional toxicological studies to assuage safety concerns. The FDA will also request long-term studies that show the reversibility of the observed drug-induced phenotype (Reasor, Hastings et al. 2006, Chatman, Morton et al. 2009). These additional studies can be both resource and time intensive. Pharmaceutical scientists would therefore benefit from a system that could predict these off-target drug effects. With this in mind, the focus of this chapter was to identify key structural features of lysosomotropic drugs that correlate with their potency in eliciting an expanded LVP which can also be expected to include phospholipidosis.

Materials and Methods

Cell Lines and Reagents

Wild-type (WT) human fibroblasts (catalogue # CRL-2076) were purchased from ATCC (Manassas, VA). All cells were cultured in glutamine-free DMEM supplemented with 10% FBS, 10mM HEPES, 1mM Sodium Pyruvate, and 2mM Glutamax and maintained at 37 degrees C and 5% CO_2. Cells were routinely subcultured to maintain 50% to 90% confluency. Experiments were carried out within 10 passages following removal from cryopreservation. Dulbecco's phosphate buffered saline (D-PBS), Dulbecco's modified Eagle's medium (DMEM), HEPES, sodium pyruvate, glutamax, and LysoTracker Red DND-99 (LTR) were purchased from Invitrogen (Carlsbad, CA). Fetal bovine serum (FBS) was purchased from Atlanta Biologicals (Lawrenceville, GA). Halofantrine, propranolol, U18666A, lidocaine, imipramine, chloroquine, ammonium chloride, ibuprofen, cyclofenil, and all benzylamine derivatives were purchased from Sigma-Aldrich (St. Louis, MO). (S)-naproxen was purchased from Cayman Chemical Company (Ann Arbor, MI). Pierce BCA protein assay kit was ordered from ThermoScientific (Rockford, IL). ^{3}[H]-halofantrine and ^{3}[H]-propranolol were purchased from American Radiolabeled Chemicals, Inc. (St. Louis, MO). ^{14}[C]-methylamine was purchased from Moravek Biochemicals (Brea, CA). NBD-PC was purchased from Avanti Polar Lipids (Alabaster, Alabama).

LysoTracker Red accumulation assay

WT human fibroblasts were grown in plastic 12-well culture plates (Corning Life Sciences) at a seeding density of approximately 75,000 cells per well. Following a 48-hour pretreatment with various drugs (concentrations of each drug is stated in the figure legend), LysoTracker Red was spiked into the growth media to a concentration of 200nM and the cells were incubated for 1 hour. Cells were then rapidly washed twice with 4 degrees C D-PBS. Cells were lysed with lysis buffer (50 mM tris base, 150 mM NaCl, 1% NP40, pH 7.4). The quantity of LTR was determined by fluorescent signal in relative fluorescence

units (RFU) using a Bio-Tek FL600 microplate fluorescence reader. Protein abundance was measured for each sample using the BCA method. Measured LTR signal (RFU) was then normalized to protein. These normalized values were then compared to the control condition (vehicle treated) and depicted as a percentage of the control.

Cell imaging (NBD-PC cellular accumulation)

All cell imaging was performed on a Nikon Eclipse 80i epifluorescence microscope equipped with a 20X phase contrast objective (Ph2). All images were acquired on a Hamamatsu ORCA ER digital camera. Images were analyzed using Metamorph software version 7.0 (Universal Imaging) and ImageJ software (free online atrsbweb.nih.gov) software. WT human fibroblasts were grown on glass coverslips under the stated growth conditions for 2days. 24hrs prior to the cell imaging 40µM NBD-PC was spiked into the existing extracellular growth media of each sample. At the end of the 24hr exposure to NBD-PC the coverslips were washed 3 times with ice-cold PBS and then mounted onto glass slides and imaged using the appropriate filter sets to match the spectral properties of NBD-PC. All images were taken using identical lamp power and exposure times making the NBD-PC signal intensity directly comparable across all images.

Red Blood Cell Hemolysis Assay

Whole blood was obtained from a fasting 23 year old male volunteer via venipuncture. The Red blood cells (RBC)s were then isolated using the procedure detailed by Reinhart and Chien (Reinhart and Chien 1986). Briefly, approximately 15mL of whole blood was drawn into a 25mL syringe. The blood was then spiked with 20 units/mL heparin to prevent clotting. The whole blood was centrifuged at 1,000g for 15minutes which separated the whole blood into three fractions, RBCs, white blood cells, and plasma. After remove the top layers of plasma and white blood cells, the RBCs were washed three times by resuspended them in ice cold PBS using a 1:3 ratio, respectively. The RBC/PBS mixture was then

centrifuged at 1,000g for 15minutes. After the final wash, the RBCs were resuspended in ice cold PBS to an approximate hematocrit value of 10%. 1.6mL aliquots of these washed RBCs were then placed into 2mL centrifuge tubes. The aliquots were then pre-warmed to 37°C for 10 minutes. Various drugs or vehicle alone were then spiked into the 1.6mL aliquots and incubated for 3 hours at 37°C. Following the 3hr incubation, the samples were centrifuged at 1,000g for 10minutes. 200µL of the supernatant was then carefully withdrawn and placed into a 96well plate. Using a UV-plate reader the absorbance at 545nm was then assessed which correlates to the abundance of hemoglobin.

Determination of the percentage of RBCs that were hemolyzed was achieved by evaluating a RBC aliquot that was fully lysed, i.e., 100% of the RBCs were lysed. Briefly, aliquots of RBCs were spiked with Triton X-100 to fully lyse all the cells present in the sample. Following the same procedure used for the drug-containing samples, the absorbance of the supernatant was then measured at 545nm. After accounting for background and the linear range of the instrument, an apparent value was obtained that represented 100% RBC hemolysis. All Abs 545nm values were than normalized to this apparent value to obtain a percentage of RBC hemolysis.

Drug Accumulation Assays

WT human fibroblasts were seeded into plastic 12-well culture plates at a seeding density of 90,000 cells per well overnight. The extracellular media was then replaced with drug-containing media as stated in the figure legend. In addition to the stated drug exposures all samples contained identical concentrations of tritium-labeled propranolol (5nM ^{3}[H]-propranolol at .06µCi/mL). Following a 2day exposure to these stated conditions, the cellular accumulation of tritium-labeled propranolol was then assessed. Briefly, at the end of the two day drug-treatment the extracellular media was removed by aspiration and the cells were washed two times with ice-cold PBS. The cells were then lysed in 250µL

lysis buffer for 30mins at 37°C. The abundance of tritium labeled propranolol was then measured measured in decays per minute (DPM)s using a Beckman LS 60001C liquid scintillation counter. Background signal contributed from non-specific binding of drug to the plate surface was subtracted from each measurement. Protein abundance was measured for each sample using the BCA method. The measured DPMs present in each sample was then normalized to µg of cellular protein.

Results and Discussion

Lysosomotropic properties greatly enhance a molecules ability to induce an expanded LVP

After establishing the cellular mechanisms that contributed to the expanded LVP seen in cells treated with lysosomotropic drugs (chapters 2 and 3), we next sought to determine which physicochemical properties of these molecules correlated with their ability to induce this phenotype. A typical approach to developing a structure activity relationship could include screening a chemical library containing thousands of molecules; however, due to the high expense of this strategy we decided to utilize a more targeted approach. To this end, we first sought to evaluate how lysosomotropic properties could influence a molecule's potency in eliciting this effect. Although potency could refer to many biological processes we will hereby refer to potency in regard to a drug's ability to induce an expanded LVP unless stated otherwise.

In order to evaluate changes in the steady state volume of lysosomes we measured the influence that various drug exposures had on the cellular uptake of the fluorescent lysosomotropic probe lysotracker red (LTR) and then compared those values to the vehicle treated control. Conditions that increased the cellular accumulation of LTR beyond 100% of control would be identified as an inducer of the expanded LVP. Using this approach we evaluated the test compounds' relative potencies by comparing the concentrations of compound necessary to elicit an expanded LVP.

U18666A is a well characterized lysosomotropic molecule that is known to perturb the lysosomal system (Amritraj, Peake et al. 2009, Poh, Shui et al. 2012). In chapter 2 we detailed how U18666A could increase the steady state volume of lysosomes (Figure 2.2) and decrease vesicle-mediated trafficking out of the lysosomes (Figure 2.6). Previous reports have also implicated progesterone as a molecule that could cause similar trafficking defects to those caused by U18666A (Butler, Blanchette-Mackie et al. 1992, te Vruchte, Lloyd-Evans et al. 2004). After establishing that both progesterone and U18666A could produce similar perturbations in the lysosomal system we then sought to evaluate their relative potencies in eliciting an expanded LVP.

Although both progesterone and U18666A were both capable of causing an expanded LVP, U18666A was dramatically more potent (Figure 4.1). Due to the structural similarities between their hydrophobic regions, we reasoned that the >10 fold increase in U18666A potency was likely attributed to its lysosomotropic properties. We further sought to validate this assumption by comparing a different set of structurally similar molecules that differed only in their lysosomotropic properties. The anesthetic drug lidocaine is well established as a lysosomotropic drug (Vandenbroucke-Grauls, Thijssen et al. 1984); however, its quaternary amine analog (lidocaine N-ethyl) would not be considered to be lysosomotropic due to its lack of an ionizable amine. Consistent with our results comparing U18666A and progesterone, we found that lidocaine exhibited a >10 fold increase in its potency compared to its non-lysosomotropic quaternary amine analog (Figure 4.2). Together, these results indicate that lysosomotropic properties can greatly enhance a molecule's potency in eliciting an expanded LVP, and by extension a drug-drug interaction involving lysosomes.

Although these examples are useful in establishing the influence that lysosomotropic properties have on a molecule's potency, they have very little clinical relevance. To our knowledge U18666A and the quaternary amine analog of lidocaine are not used as drugs in humans. In an effort to provide a more

clinically relevant example we next sought to evaluate a wide range of drugs that did or did not possess lysosomotropic properties. We chose a set of 7 different drugs, 4 that possessed lysosomotropic properties (e.g., chlorpromazine, imipramine, propranolol, and lidocaine) and 3 that did not possess lysosomotropic properties (e.g., naproxen, ibuprofen, and cycofenil) (Figure 4.3). We found that all of the lysosomotropic drugs (labeled with dotted lines) were capable of causing an expanded LVP; however, all of the non-lysosomotropic drugs (labeled with solid lines) failed to cause an expanded LVP (Figure 4.3). These results further strength the notion that lysosomotropic properties enhance a molecule's ability to induce an expanded LVP.

Lipophilicity alone does not correlate with a lysosomotropic molecule's potency capacity to induce an expanded LVP

After establishing that lysosomotropic properties greatly enhanced a molecules potency we next sought to determine how the lipophilicity of these molecules might also influence their potency. We initially screen several different lysosomotropic molecules with a calculated Log P ranging from -0.6 to 2.5. Interestingly, we found that none of tested lysosomotropic molecules were capable of inducing an expanded LVP (Figure 4.4). Surprised by these results, we further evaluated 4 FDA approved lysosomotropic drugs (erythromycin, azithromycin, propranolol, and lidocaine) that all possessed a calculated Log P of approximately 2.5 (Figure 4.5). We reasoned that if the lipophilicity of these molecules was the primary physicochemical property that determined potency then all 4 of these drugs should have failed to produce an expanded LVP similar to that seen with triisopropylamine (Figure 4.4) that also possess a Log P of 2.5. Instead, all 4 of the drugs in Figure 4.5 induced an expanded LVP. These results indicated that the lipophilicity of lysosomotropic molecules alone did not determine their capacity to induce an expanded LVP.

In order to more deeply explore the relationship between a drug's lipophilicity and its potency we also screened a large array of 17 different lysosomotropic drugs possessing a calculated Log P from 2.3 to 7.9. By performing a dose response curve for each drug, measuring LTR uptake versus drug concentrations, we were able to compare the relative potencies of each drug. We found that the 17 different drugs varied widely in their potencies. To achieve a more uniform comparison of each drug's potency, we extrapolated the concentration of each drug necessary to achieve a LTR uptake at 150% of control ($EC_{150\%}$). To illustrate the relationship between potency and lipophilicity we then plotted those $EC_{150\%}$ values against the corresponding drug's calculated Log P (Figure 4.6). Overall, we found that lipophilicity roughly correlated with a drug's capacity to induce an expanded LVP; however, the weak correlation (r^2= .497) indicated other physicochemical properties were likely involved in determining the overall potency of each drug.

The aliphatic linkage between the hydrophilic and hydrophobic region of lysosomotropic molecules is proportional its potency in inducing an expanded LVP

In an effort to pinpoint additional structural properties that might influence potency we reviewed the chemical structures present in Figure 4.5 and compared those to Figure 4.4. We had reasoned that the structural differences present between these two sets of molecules would shed light on what key physicochemical properties might be influencing potency, i.e., one set of molecules caused an expanded LVP and one did not. Based on our previous analysis we had already eliminated Log P as the primary factor that determined potency. Upon visual inspection it was clear that the amphiphilic nature of the two sets of molecules were strikingly different. Although methylamine and t-butylamine are amphiphilic, they lack a large separation between their hydrophilic and hydrophobic regions as opposed to propranolol and lidocaine that possess a relatively large separation between their hydrophobic region (aromatic rings) and their hydrophilic region (ionizable amine). In order to explore this more thoroughly we sought to evaluate the potency of several benzylamine analogs that possessed a varying degree of

aliphatic linkage between the hydrophobic benzyl group and the hydrophilic primary amine (Figure 4.7). Interesting, we found that the aliphatic linkage greatly influenced the potency of these molecules. These results showed that as the length of the carbon linkage increased so too did the molecules ability to induce an expanded LVP indicating that the amphiphilic character of these molecules likely played an important role in determining their potencies.

The aromatic bulk of a lysosomotropic molecule correlates with its potency in inducing an expanded LVP

The result of the previous section was indicated that the amphiphilicity of these molecules is a key structural feature that influences potency. With this in mind, we considered other characteristics of amphiphilicity, specifically the surface area of a molecule's hydrophobic region. Although the hydrophilic surface area of these molecules could conceivably be changed as well, these alterations would likely result in dramatically different electronic properties of the ionizable amine. Ultimately these changes could modulate the pKa of the ionizable amine and influence the degree of ion trapping. In an effort to avoid tuning the pKa of the amine we instead focused our efforts on changing the surface area of the hydrophobic region.

Similar to the approach used to assess aliphatic chain length, we again assessed analogs of benzylamine that possessed progressively greater degrees of aromatic bulk (Figure 4.8). These results showed that the aromatic bulk of these molecules dramatically influenced their potency. Each additional aromatic ring caused an approximate 10 fold increase in the molecules relative potency to compared to benzylamine.

The aliphatic chain length and aromatic bulk of a lysosomotropic molecule exhibit an additive influence on its potency to inducing an expanded LVP

After establishing that the aliphatic chain length and the surface area of the hydrophobic region greatly influenced the potency of lysosomotropic molecules we next sought to evaluate how these two structural properties might influence potency in combination. This was an important question to answer as the 17 different lysosomotropic drugs analyzed in the previous section (Figure 4.6) all exhibited varying combinations of these two structural features. To address this question, we analyzed structural analogs of benzylamine that varied in both chain length and the number of aromatic rings (Figure 4.9). These results show that increasing the aliphatic chain length from 1 carbon to 3 carbons imparts an increase to the molecule's potency, as was seen in Figure 4.7. However, if an additional aromatic ring is included on this same molecule its potency is significantly enhanced. Overall, these results show that the total surface area of the hydrophobic region and the aliphatic linkage between this region and the hydrophobic region influence the potency of lysosomotropic molecules in an additive fashion.

A lysosomotropic drug's potency in eliciting an expanded LVP correlates with its capacity to intercalate into cellular membranes

After observing that 17 different lysosomotropic drugs were capable of causing an expanded LVP, we began to reason that their ability to induce this effect was likely the result of some nonspecific drug interaction/effect. Previous work has shown that many of these 17 drugs (chlorpromazine, imipramine, propranolol etc.) were capable of intercalating into biological membranes (Zachowski and Durand 1988, Reinhart and Rohner 1990, Maruoka, Murata et al. 2007). Others have shown that drugs intercalating into biological membranes can lead to changes in membrane fluidity, integral membrane protein activity, and alterations in vesicle-mediated trafficking, all of which are consistent with our observations detailed in the previous chapters (Spinedi, Pacini et al. 1989, Maruoka, Murata et al. 2007, Suwalsky,

Villena et al. 2008). With this in mind, we reasoned that these drugs could be causing the formation of an expanded LVP by intercalating into the lysosomal membranes.

In order to test this hypothesis we narrowed our analysis down to 5 different lysosomotropic molecules that showed a varying degree of potency from low (methylamine) to high (chlorpromazine) (Figure 4.10). We then sought to measure their capacity to intercalate into a biological membrane. If our hypothesis was correct we had expected to see that the same rank-order in potency for both their ability to cause an expanded LVP and their ability to intercalate into membranes.

Over the past few decades red blood cells (RBCs) have been extensively used to measure membrane intercalation of a wide array of different drugs. Due to the robust body of published work, accessibility, and ease of isolation we employed a RBC hemolysis assay to measure a molecules capacity to intercalate into membranes. The basis for the RBC hemolysis assay is that the RBC plasma membrane becomes increasing destabilized as more drug molecules become intercalated into it. Initially the drug intercalation leads to morphological changes in the membranes of RBCs producing spikey membrane-protrusions and conical shaped membrane-invaginations that are visible by light microscopy. After reaching some unknown threshold of destabilization, the RBC plasma membrane becomes perforated resulting in the spillage of the RBC contents into the extracellular environment. The extracellular environment can then be assayed for RBC content, e.g., hemoglobin which has a high absorbance at 545nm (Isomaa, Hagerstrand et al. 1986, Reinhart and Chien 1986, Fujiwara, Hirashima et al. 2001).

Using this approach we measured the percentage of RBC hemolysis over a wide range of test molecule concentrations from low micromolar to high millimolar (Figure 4.11). These results indicated that chlorpromazine possessed the greatest capacity to cause RBC hemolysis while ammonium chloride showed an inability to cause RBC hemolysis up to a 1M concentration. Interestingly, both Figure 4.11 and Figure 4.10 showed the same order of potencies: chlorpromazine> imipramine> propranolol>

lidocaine> ammonium chloride. These results indicate that membrane intercalation is likely one of the primary mechanisms underlying the development of the expanded LVP.

Low concentrations of lysosomotropic drugs can work in a concerted fashion to cause an expanded LVP

The results of the previous section lead us to believe that drugs causing an expanded LVP were not involved in a specific drug-protein or drug-receptor interaction that mediated some down-stream physiological response, but rather, these drugs were acting in a non-specific manner by simply intercalating into the lysosomal membrane and possibly disrupting normal lysosome function. In support of this notion, previous reports have detailed how drug intercalation into biological membranes can alter membrane charge and fluidity and perturb a range of physiological functions such as vesicle-mediated trafficking and enzyme activity (Spinedi, Pacini et al. 1989, Kolzer, Werth et al. 2004, Maruoka, Murata et al. 2007, Suwalsky, Villena et al. 2008).

To investigate this hypothesis in more detail we next evaluated the capacity of these drugs to work in a concerted fashion to bring about an expanded LVP. We reasoned that if these drugs were causing this phenotype in a non-specific manner, simply by intercalating into membranes, then combinations of these drugs should be additive in their ability to perturb lysosome function and by extension increase lysosomal volume. To this end, we first visually inspected the dose responses for 7 different lysosomotropic drugs (drug concentration versus LTR uptake) and identified the highest concentration of drug that was unable to produce an expanded LVP. For example, in Figure 4.10 propranolol begins to induce an expanded LVP phenotype at a concentration of approximately 500nM and higher. Concentrations below 500nM should therefore not produce an expanded LVP. We repeated this process and identified a threshold concentration for 7 different lysosomotropic drugs. These values ranged from low nanomolar to high nanomolar depending on the potency of the lysosomotropic drug.

To test our hypothesis we treated cells with only one drug at a concentration that was just below its threshold for inducing an expanded LVP. In parallel to these individual exposures we also treated cells with a combination of all 7 drugs at those same concentrations (Figure 4.12 A). Consistent with our expectations we found that the drugs were unable to cause an expanded LVP at concentrations below the previously identified threshold; however, when all 7 drugs were combined together we observed that the drugs did induce an expanded LVP. This result supported our hypothesis that these drugs might be interacting with membranes in a non-specific manner.

Although LTR is a well-established lysosomotropic probe, it is technically not considered a drug. In order to provide a more clinically relevant example of this phenomenon we repeated this experiment but instead of measuring LTR cellular uptake we measured the uptake of tritium labeled propranolol (Figure 4.12 B). This experiment was meant to mimic an in vivo scenario where an individual might be exposed to very low concentrations of multiple lysosomotropic amphiphiles (either endogenous amphiphiles or xenobiotic amphiphiles) thereby resulting in a drug-drug interaction involving lysosomes where the perpetrator drugs was actually an array of drugs rather than a single drug. The results of this experiment showed that multiple drugs could work in concert to produce a drug-drug interaction involving lysosomes that results in the enhanced cellular accumulation of a victim drug (propranolol).

Low concentrations of lysosomotropic drugs can work in an additive manner to cause lipid trafficking defects

In previous chapters we showed that impaired vesicle-mediated trafficking was observed in cells treated with lysosomotropic drugs (Figure 2.6); however, these assessments were performed using drug concentrations that were above the threshold for causing an expanded LVP. For example, cells exposed to concentrations of propranolol above 500nM for 2 days will result in the formation of an expanded LVP. The dextran release data illustrated in Figure 2.6 was obtained from cells exposed to 4µM

propranolol for 2 days which is well above the “threshold concentration”. In this section we have sought to determine if multiple lysosomotropic drugs, at concentrations below their respective threshold concentrations, could work in concert as was illustrated in Figure 4.12 to cause a lipid trafficking defect. We reasoned that the lipid transport efficiency of cells should be unimpaired when exposed to lysosomotropic drugs that are below their respective threshold concentration but when cells are exposed to a combination of all these drugs they will exhibit a lipid trafficking defect.

To evaluate this question we employed the use of nitrobenzoxadiazole-phosphotidylcholine (NBD-PC) a fluorescently labeled phospholipid. NBD-PC is frequently used to assess the efficiency of phospholipid transport within cells (Kasahara, Tomita et al. 2006). The rational for this assay is that the total cellular accumulation of NBD-PC will be determined by the rate of NBD-PC uptake versus the rate of NBD-PC release from the cells. If cells are exposed to condition that reduce the efficiency of lipid transport then the cells would be expected to accumulate a greater amount of NBD-PC. The total NBD-PC fluorescence can therefore be used as a surrogate marker for the efficiency of lipid transport, i.e., greater amounts of NBD-PC fluorescence indicates reduced lipid transport efficiency.

Using the same protocol detailed for the experiments in Figure 4.12, we repeated the experiment but instead of measuring LTR uptake or tritium labeled propranolol we measured the cellular accumulation of NBD-PC by fluorescence microscopy (Figure 4.13). In support of our hypothesis, we found that cells exposed to lysosomotropic drugs at concentrations below their respective “threshold” accumulated similar amounts of NBD-PC as compared to control, i.e., the intracellular green fluorescence was similar in intensity between the cells treated with vehicle (control) and cells treated with a single drug. However; when cells were exposed to a combination of all 7 drugs at those same concentrations, the cells exhibited a substantially greater NBD-PC fluorescence.

Conclusion

In cultured human cells we have found that lysosomotropic drugs are capable of causing a significant expansion in the steady state volume of lysosomes. In the previous chapters we detailed how this expansion in lysosomal volume can lead to a drug-drug interaction resulting in the enhanced cellular accumulation of secondarily administered lysosomotropic drugs. We have further detailed the potential clinical ramifications of this phenomenon by predicting how these changes might influence whole-body pharmacokinetic proprieties, specifically the volume of distribution and half-life. With this in mind we consider the drug-induced expansion of lysosomal volume to be a significant off-target drug effect that could benefit from a well-characterized structure activity relationship.

Although a structure activity relationship is currently not established for lysosomotropic drugs and their ability to induce an expanded LVP, others have made attempts to predict a similar drug-induced phenomenon termed phospholipidosis (PL). In chapter 3 we detailed the relationship between the expanded LVP and PL. We found that many of the lysosomotropic drugs that caused an expansion in lysosomal volume have also been shown to induce PL (Lowe, Glen et al. 2010). Based on our data however, we would conclude that PL accounts for only a portion of these cells' enhanced capacity to accumulate lysosomotropic drugs. We feel that the "expanded LVP" is a much broader phenotypic descriptor that includes both changes to phospholipid bindings sites (i.e., phosopholipidosis) and changes to the aqueous volume of lysosomes. We would therefore reason that measuring changes to the steady state volume of lysosomes, using LTR uptake or a similar approach, is a much more inclusive screening criteria rather than analyzing tissue samples for hallmark signs of PL which can pose great variability and inconsistent results. The hallmark sign of PL, i.e., multi-lamellar bodies/membrane whorls/myeloid bodies, can be present in some tissues while absent in others (Reasor, Hastings et al. 2006, Tengstrand, Miwa et al. 2010). Signs of drug-induced phospholipidosis can also exhibit a high degree of variability within a single species and between different species (Halliwell 1997, Chatman,

Morton et al. 2009). For example, the FDA's *Phospholipidosis Working Group* has shown that certain drugs can cause signs of PL in certain animal models but not in humans and vice-versa.

In an effort to establish a structure activity relationship for the development of the expanded LVP we first reviewed the physicochemical properties of drugs that were previously implicated in the development of drug-induced PL. Although drug-induced PL is difficult to predict and likely only accounts for a portion of a cell's total enhanced drug-accumulation capacity we felt that these two conditions would likely share a very similar structure activity relationship. Over the last decade many models have been developed to predict drug-induced PL. Ploemen and coworkders have developed the most simple model that predicts phospholipidosis inducing compounds as those that have a pKa greater than 8 and a Log P greater than 1 while also satisfying the following criteria $(\text{calculated Log P})^2 + (\text{calculated pKa})^2 > 90$. Many additional models have been developed that incorporate machine learning and complex statistical methodologies but the overall success of these more complex models in predicting PL is only marginally better than the model developed by Ploemen and coworker (Lowe, Glen et al. 2010). We therefore focused our attention on the parameters of the simple model which included pKa and Log P. We reasoned that the pKa would likely be important due to its influence on a drugs potential to be entrapped into lysosomes by ion trapping (Ndolo, Forrest et al. 2010, Ndolo, Jacobs et al. 2010). The Log P would likely influence parameters such as cell permeability and the degree of membrane intercalation.

Due to the high cost of developing and running a high throughput assay that can screen thousands of molecules, we employed a more targeted approach and rationally chose specific physicochemical properties that might influence a molecules potency in cause an expanded LVP (referred to hereafter as just potency). We then designed a battery of molecules that would allow us to interrogate how those specific physicochemical properties related to a molecule's potency.

We initially evaluated the influence that lysosomotropic properties had on potency by analyzing two sets of structurally similar molecules (lidocaine vs. lidocaine N-ethyl and U18666A vs. progesterone). We had previously shown that the lysosomotropic drug lidocaine was capable of causing an expanded LVP (Figure 2.2). In order to test how its lysosomotropic properties contributed to its potency we tested its quaternary amine analog (lidocaine N-ethyl) which is not considered to be lysosomotropic due to its lack of an ionizable amine (Figure 4.2). The results of this experiment showed that the lysosomotropic properties of lidocaine imparted a >10fold increase to its potency.

In chapter 2 we had also established that the lysosomotropic molecule U18666A was capable of eliciting an expanded LVP (Figure 2.2). In order to test the contribution that lysosomotropic properties were imparting on U18666A we performed a comparative analysis of U18666A versus progesterone (Figure 4.1). These two molecules possess structurally similar hydrophobic regions; however, progesterone is considered to be non-lysosomotropic due to its lack of an ionizable amine. Similar to the results obtained with lidocaine, we found that the lysosomotropic properties of U18666A also imparted a >10fold increase to its potency.

After establishing the strong influence that lysosomotropic properties had on molecules' potency, we next sought to determine other physicochemical properties that might also modulate their ability to induce an expanded LVP. Based on the model developed by Poloeman and coworkers we reasoned that lipophilicity might also play an important role in determining the potency of lysosomotropic molecules.

A review of data presented in Figure 4.2 showing that lidocaine was capable of inducing an expanded LVP lead us to hypothesis that lysosomotropic molecules with a Log P of approximately 2.4 should be capable of expanding lysosomal volume; however, we did not know if molecules must possess a minimum lipophilic character in order to induce an expanded LVP. To answer this question we evaluated a set of lysosomotropic molecules possess a calculated Log P ranging from -0.6 to 2.5 (Figure

4.4). Interestingly, we found that all of these molecules failed to cause an expanded LVP. Surprised by these results, we further investigated 4 FDA approved drugs that all possessed a Log P of approximately 2.4 (Figure 4.5). We found that all 4 of these drugs were capable of causing an expanded LVP. These results indicated that lipophilicity alone did not determine the potency of these lysosomotropic molecules.

To further confirm these results and more thoroughly evaluate the influence that lipophilicity plays in determining potency we expanded our analysis to include a wide array of 17 different lysosomotropic drugs that possessed a calculated Log P ranging from 2.32 to 7.93 (Figure 4.6). In order to achieve a uniform analysis of potency across these 17 different lysosomotropic drugs we performed a dose response for each drug measuring LTR uptake versus drug concentration. From these dose responses we extrapolated the concentration of drug necessary to achieve a LTR uptake of 150% of control ($EC_{150\%}$). The array of data illustrated in Figure 4.6 showed a very poor correlation between lipophilicity and potency (r^2=.497) which confirmed our initial assessment.

These results lead us to investigate other structural features that might influence their potency. By reviewing the structures in Figure 4.4 and comparing those to Figure 4.5 we began to recognize that molecules capable of causing an expanded LVP tended to have strong amphiphilic characteristics. For example, lidocaine and propranolol possess a hydrophobic ring structure and a weakly basic amine that are separated by a linker of several atoms whereas the molecules incapable of causing an expanded LVP possessed only one carbon between their hydrophobic and hydrophilic regions. The difference in potency observed between lidocaine and propranolol is also interesting to note. Propranolol exhibited a >10 fold increase in its potency (EC150%) versus lidocaine. We reasoned that propranolol was more potent because of its larger hydrophobic moiety (two aromatic rings versus lidocaine's single aromatic

ring) even though their calculated Log Ps were strikingly similar. With this in mind we next sought to specifically evaluate the influence that amphiphilicity had on the potency of lysosomotropic molecules.

In order to test how amphiphilicity influenced potency we employed the use of benzylamine and several of its structural analogs. We first explored the influence that the aliphatic linkage between the hydrophobic moiety and hydrophilic amine had on potency (Figure 4.7). We found that as the linkage between the benzyl group and the amine increased, so too did the molecules potency. We also examined how the size of the hydrophobic moiety could influence potency (Figure 4.8). Consistent with the potency difference between propranolol to lidocaine, increasing the aromatic bulk of the benzylamine analogs caused a concomitant increase in their potency. Intrigued by these results, we then sought to determine if these two structural features of amphiphilicity, i.e., aliphatic chain length and aromatic bulk, could work in an additive manner to increase a molecules overall potency (Figure 4.9). Interestingly, we found that these two features were additive in their ability to influence these potency. This led us to conclude that the amphiphilic character of lysosomotropic molecules must be evaluated in order to predict its potential to cause an expanded LVP.

After learning that the amphiphilic characteristics of these lysosomotropic molecules played an important role in determine their potency, we next began to speculate on why this feature was so important. Although it was possible that these molecules were acting in a specific drug-protein or drug-receptor interaction, we did not consider this possibility to be likely. Due to the high specificity of protein-ligand interactions we found it implausible that a wide array of structurally diverse drugs could all be interacting with the same protein which ultimately lead to the development of the expanded LVP. We therefore considered the possibility that these drugs were interacting with the lysosomal membrane. In support of this notion, previous reports have detailed how drug intercalation into biological membranes can perturb a range of physiological functions such as vesicle-mediated trafficking

and enzyme activity (Spinedi, Pacini et al. 1989, Kolzer, Werth et al. 2004, Maruoka, Murata et al. 2007, Suwalsky, Villena et al. 2008); however, none of these reports correlated this interaction with the development of the expanded LVP. To further investigate the potential relationship between a molecule's membrane intercalation potential and its potency in causing an expanded LVP we performed a comparative analysis relating each molecules' potency (Figure 4.10) with its capacity to intercalate into a biological membrane (Figure 4.11). The results of these experiments showed that the relative membrane intercalation potential of lysosomotropic molecules closely parallels their potency in causing an expanded LVP.

To more fully develop the membrane-intercalation hypothesis we evaluated the ability of lysosomotropic drugs' to work in a concerted fashion to bring about an expanded LVP. We reasoned that if these drugs acted in a non-specific manner by intercalating into the lysosomal membrane then combinations of these drugs at low concentrations should be capable of eliciting the same effect as a single drug at a higher concentration. In support of this hypothesis we found that these drugs elicited this additive effect in both their ability to increase lysosomal volume (Figure 4.12 A) and their ability to induce a drug-drug interaction involving lysosomes (Figure 4.12 B). In addition, these drugs could also work in a concerted fashion to cause lipid trafficking defects (Figure 4.13). These studies help to illustrate a proof-of-principle for how a drug-drug interaction could occur in vivo whereby the peripheral tissues of an individual exposed to several different amphiphilic molecules (either endogenous amphiphiles or xenobiotic amphiphiles) would exhibit an expanded LVP.

The studies in this chapter have provided a foundation for a structure activity relationship that relates key physicochemical properties of lysosomotropic molecules with their ability to cause an expanded LVP, and by extension a drug-drug interaction involving lysosomes. These studies have also provided the mechanistic basis for why different lysosomotropic molecules exhibit varying degrees of potency.

Overall the information presented in this section can potentially be used to instruct individuals on what key physicochemical properties of drugs might lead to a drug-drug interaction involving lysosomes.

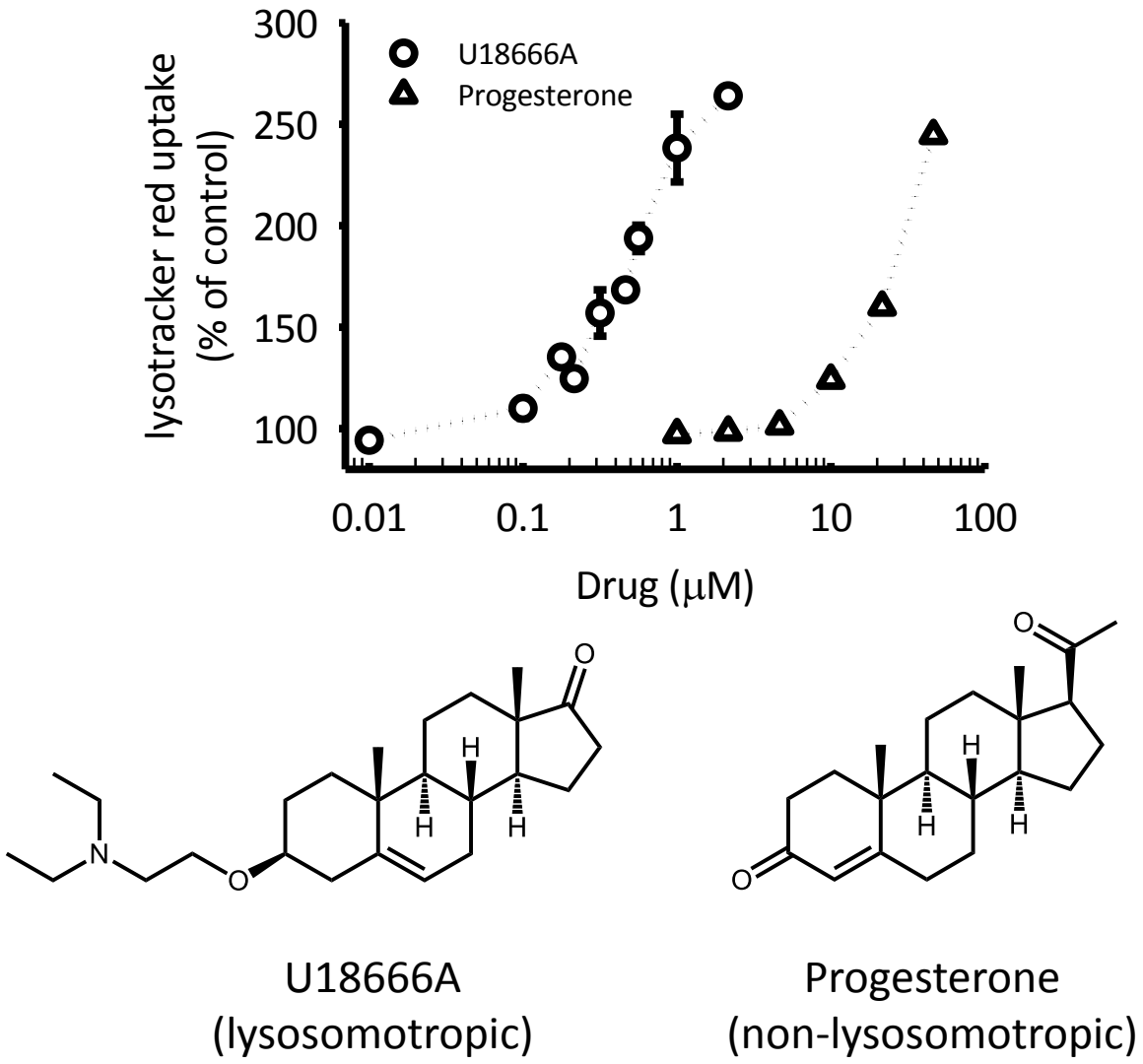

Figure 4.1 Concentration-dependent cellular accumulation of LTR (200 nM for 1 hour) in wild-type human fibroblasts with a 48-hour pretreatment of various lysosomotropic molecules. The reported values represent the average of approximately 500,000 cells. Cellular accumulation of LTR was measured in fluorescence units and then normalized to cellular protein. The normalized LTR uptake was then compared to the control condition (vehicle alone) and reported as a percentage of the control.

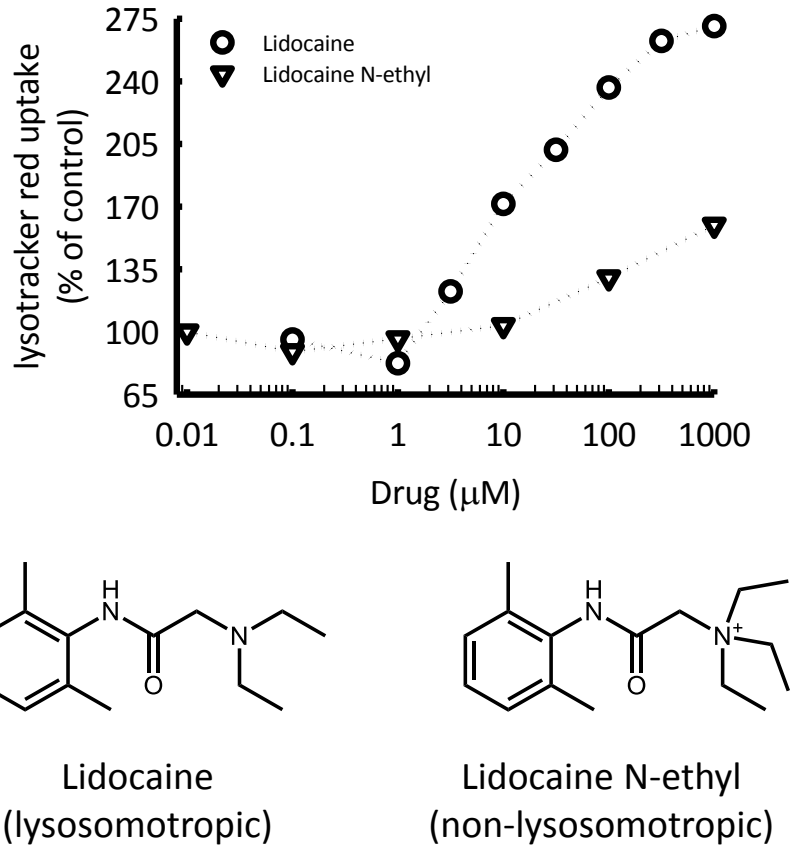

Figure 4.2 Concentration-dependent cellular accumulation of LTR (200 nM for 1 hour) in wild-type human fibroblasts with a 48-hour pretreatment of various lysosomotropic molecules. The reported values represent the average of approximately 500,000 cells. Cellular accumulation of LTR was measured in relative fluorescence units (RFU) and then normalized to cellular protein. The normalized LTR uptake was then compared to the control condition (vehicle alone) and reported as a percentage of the control.

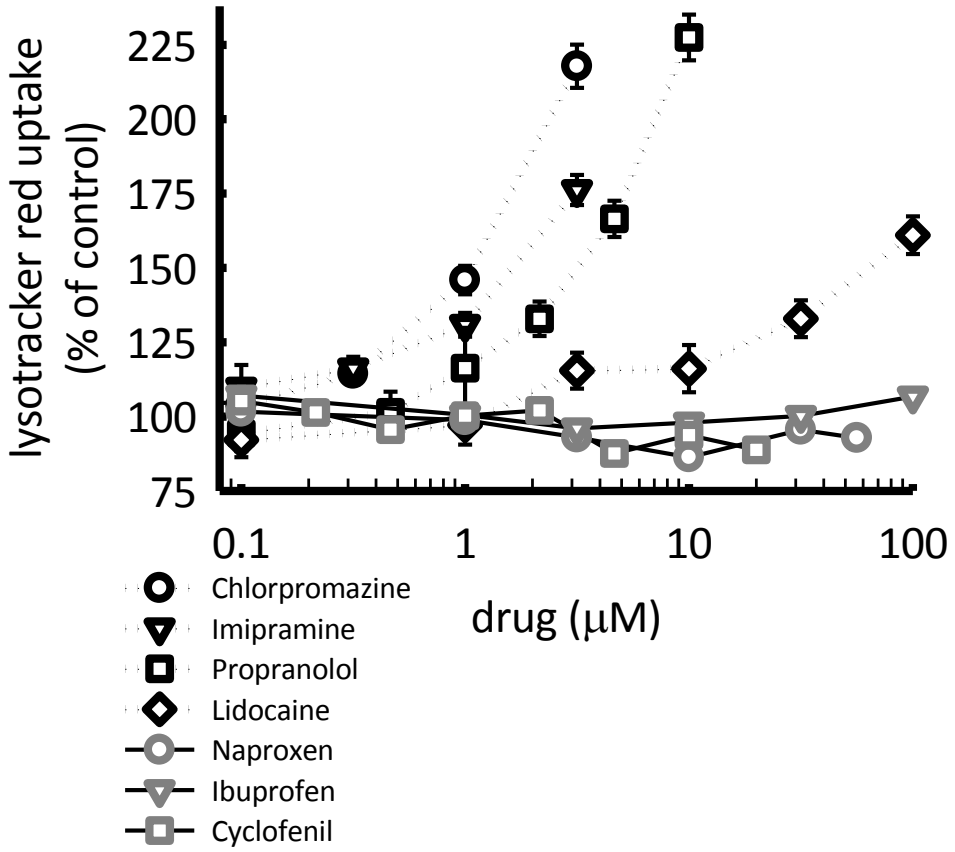

Figure 4.3 Concentration-dependent cellular accumulation of LTR (200 nM for 1 hour) in wild-type human fibroblasts with a 48-hour pretreatment of various drugs. The black symbols with dotted lines all represent lysosomotropic drugs while the grey symbols with solid lines represent non-lysosomotropic drugs. The reported values represent the average of approximately 500,000 cells. Cellular accumulation of LTR was measured in fluorescence units and then normalized to cellular protein. The normalized LTR uptake was then compared to the control condition (vehicle alone) and reported as a percentage of the control.

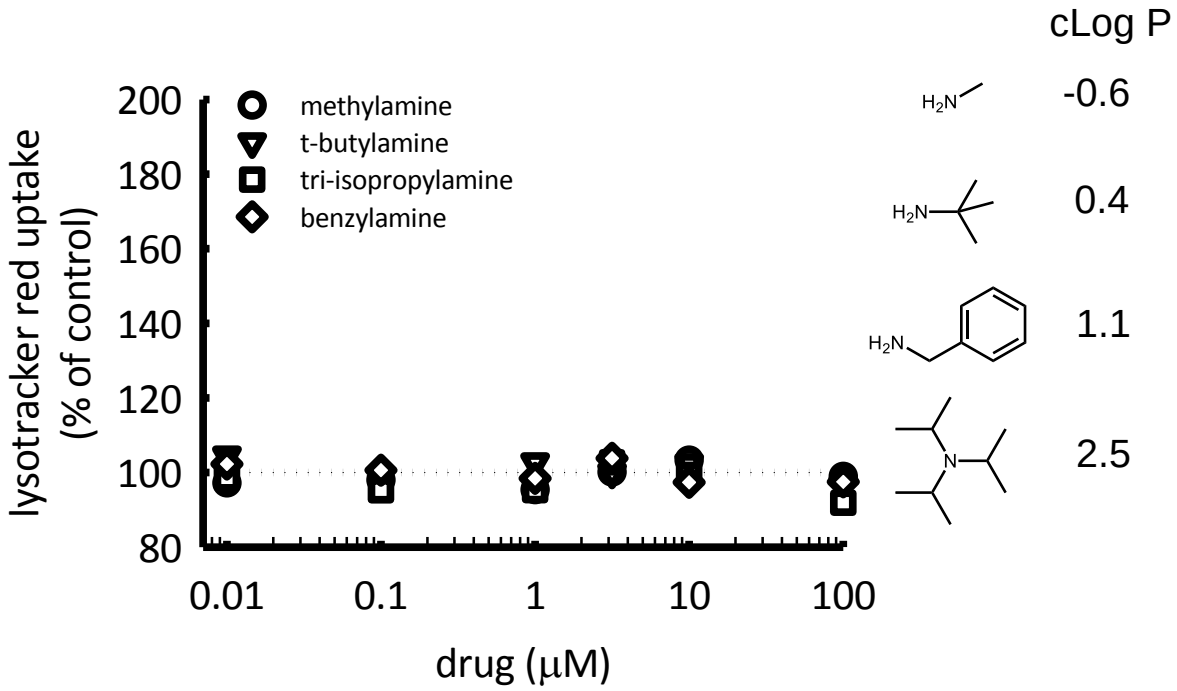

Figure 4.4 Concentration-dependent cellular accumulation of LTR (200 nM for 1 hour) in wild-type human fibroblasts with a 48-hour pretreatment of various lysosomotropic molecules. The reported values represent the average of approximately 500,000 cells. Cellular accumulation of LTR was measured in fluorescence units and then normalized to cellular protein. The normalized LTR uptake was then compared to the control condition (vehicle alone) and reported as a percentage of the control.

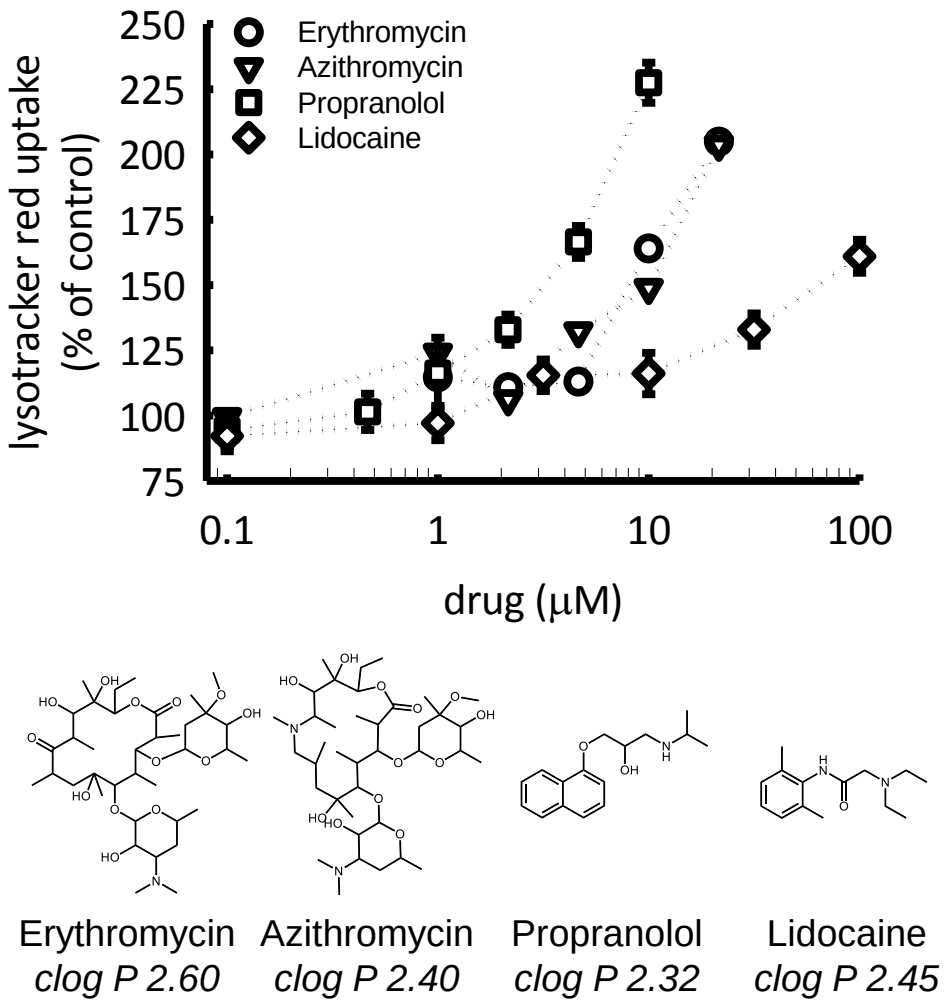

Figure 4.5 Concentration-dependent cellular accumulation of LTR (200 nM for 1 hour) in wild-type human fibroblasts with a 48-hour pretreatment of various lysosomotropic molecules. The reported values represent the average of approximately 500,000 cells. Cellular accumulation of LTR was measured in fluorescence units and then normalized to cellular protein. The normalized LTR uptake was then compared to the control condition (vehicle alone) and reported as a percentage of the control.

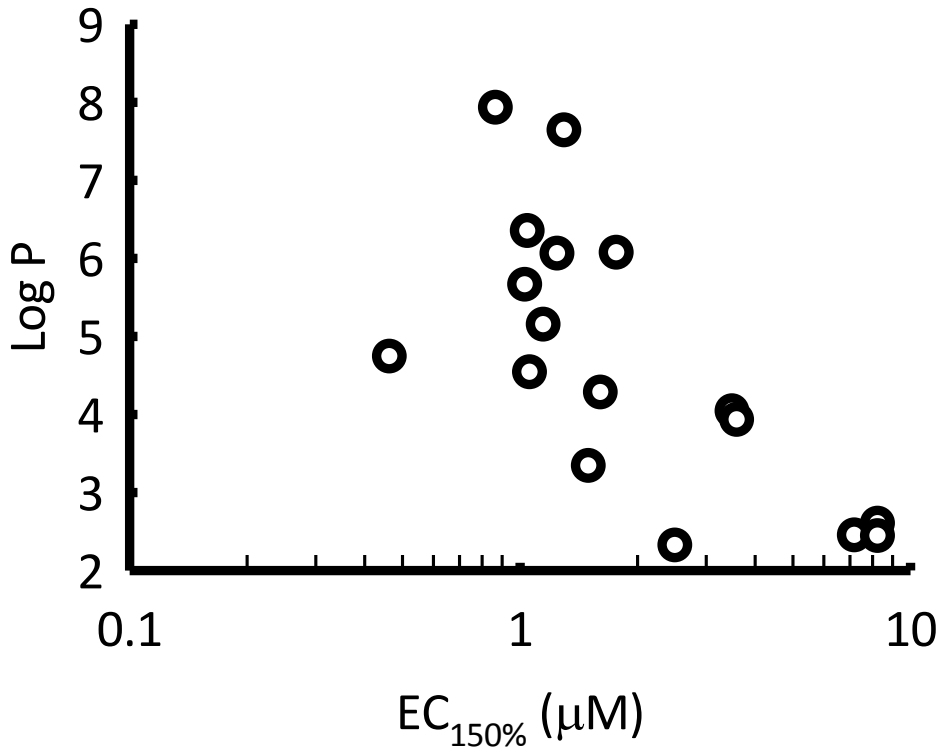

Figure 4.6 Correlation plot showing the relationship between of 17 different lysosomotropic drugs' potency to induce an expanded LVP ($EC_{150\%}$) and their respective lipophilicity (Log P). The ($EC_{150\%}$) was determined by performing a dose-response for each lysosomotropic drug, measuring LTR uptake versus drug concentration, and then extrapolating the concentration of drug necessary to achieve a LTR uptake of 150% of control. The Log P was calculated using MarvinSketch (software freely available at chemaxon.com). The following lysosomotropic drugs were assessed: U18666A, halofantrine, endoxifen, tamoxifen, chlorpromazine, quinacrine, raloxifene, amiodarone, haloperidol, imipramine, Y-134, propranolol, bupivacaine, chloroquine, lidocaine, erythromycin, and azithromycin.

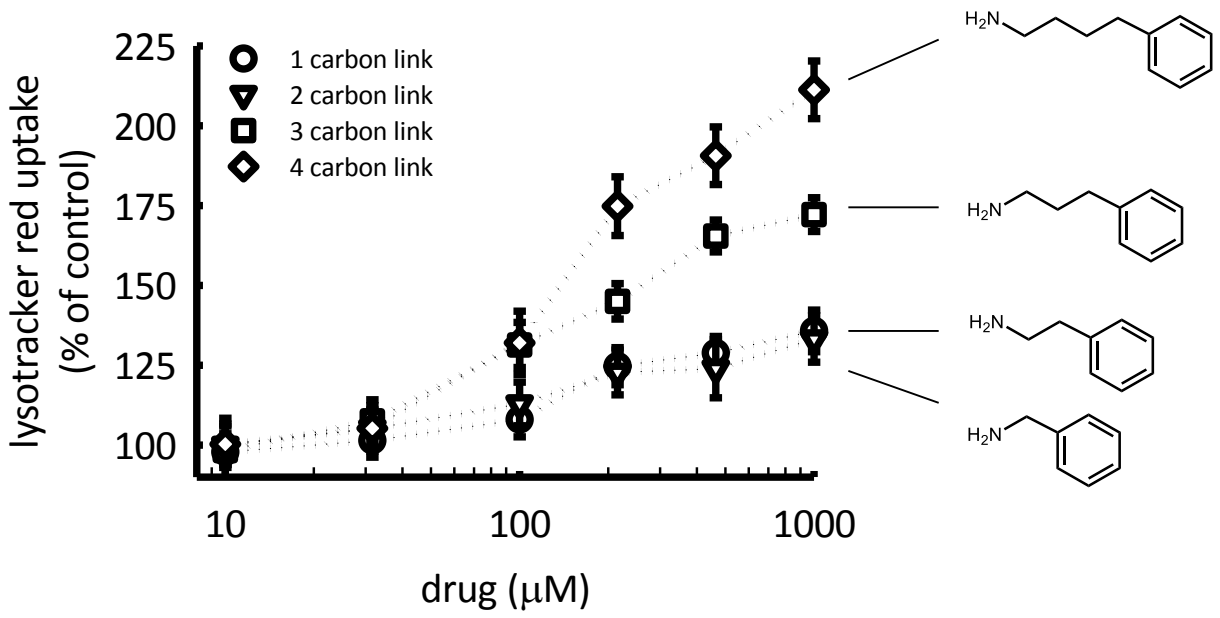

Figure 4.7 Concentration-dependent cellular accumulation of LTR (200 nM for 1 hour) in wild-type human fibroblasts with a 48-hour pretreatment of various lysosomotropic molecules. The reported values represent the average of approximately 500,000 cells. Cellular accumulation of LTR was measured in fluorescence units and then normalized to cellular protein. The normalized LTR uptake was then compared to the control condition (vehicle alone) and reported as a percentage of the control.

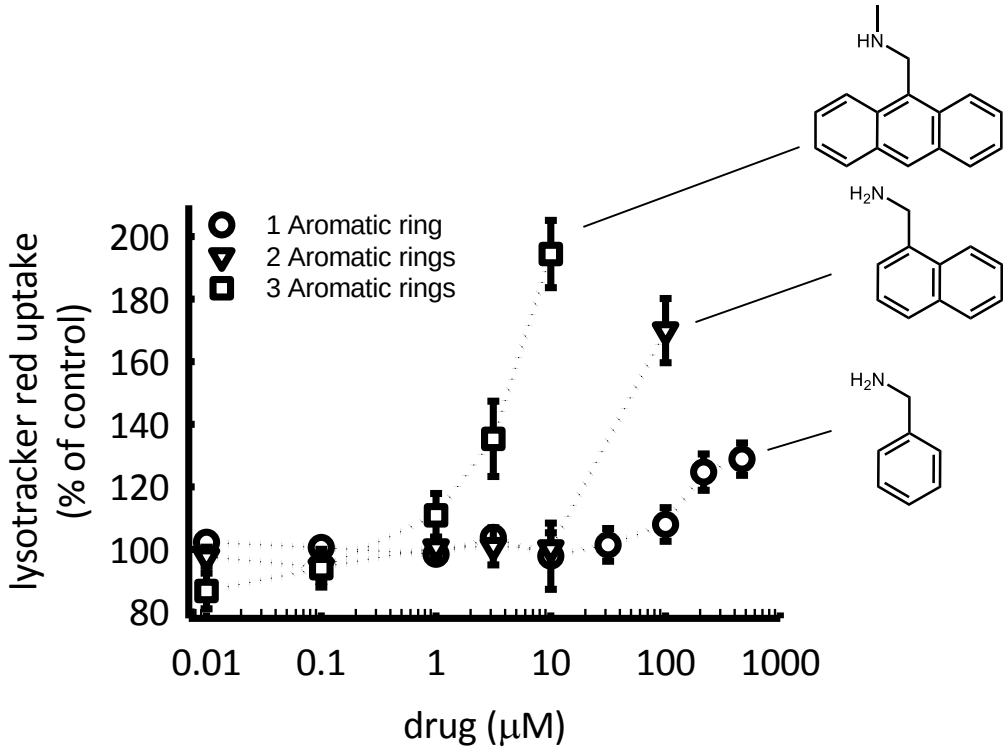

Figure 4.8 Concentration-dependent cellular accumulation of LTR (200 nM for 1 hour) in wild-type human fibroblasts with a 48-hour pretreatment of various lysosomotropic molecules. The reported values represent the average of approximately 500,000 cells. Cellular accumulation of LTR was measured in fluorescence units and then normalized to cellular protein. The normalized LTR uptake was then compared to the control condition (vehicle alone) and reported as a percentage of the control.

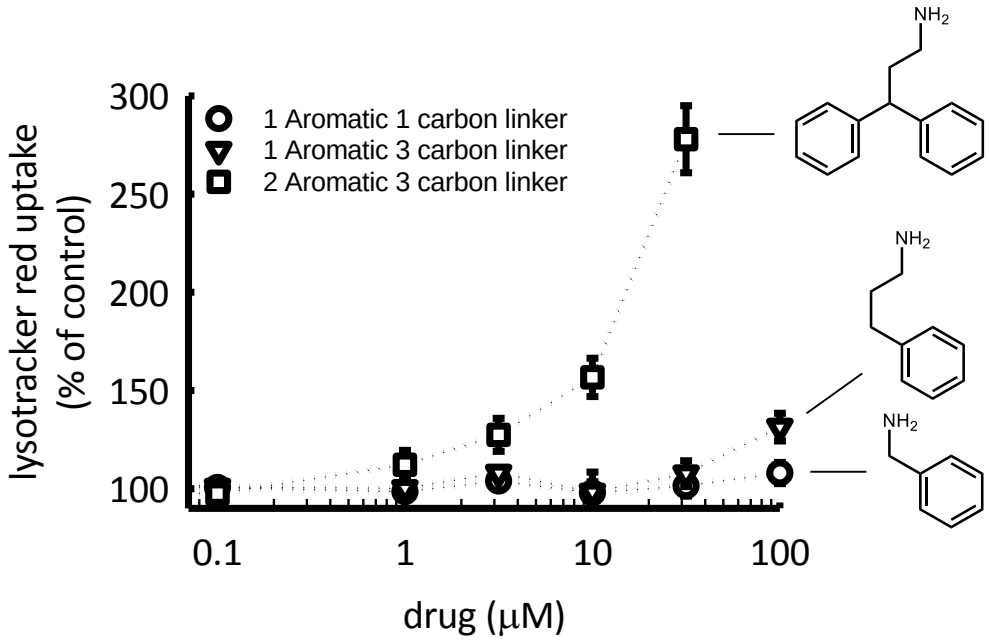

Figure 4.9 Concentration-dependent cellular accumulation of LTR (200 nM for 1 hour) in wild-type human fibroblasts with a 48-hour pretreatment of various lysosomotropic molecules. The reported values represent the average of approximately 500,000 cells. Cellular accumulation of LTR was measured in fluorescence units and then normalized to cellular protein. The normalized LTR uptake was then compared to the control condition (vehicle alone) and reported as a percentage of the control.

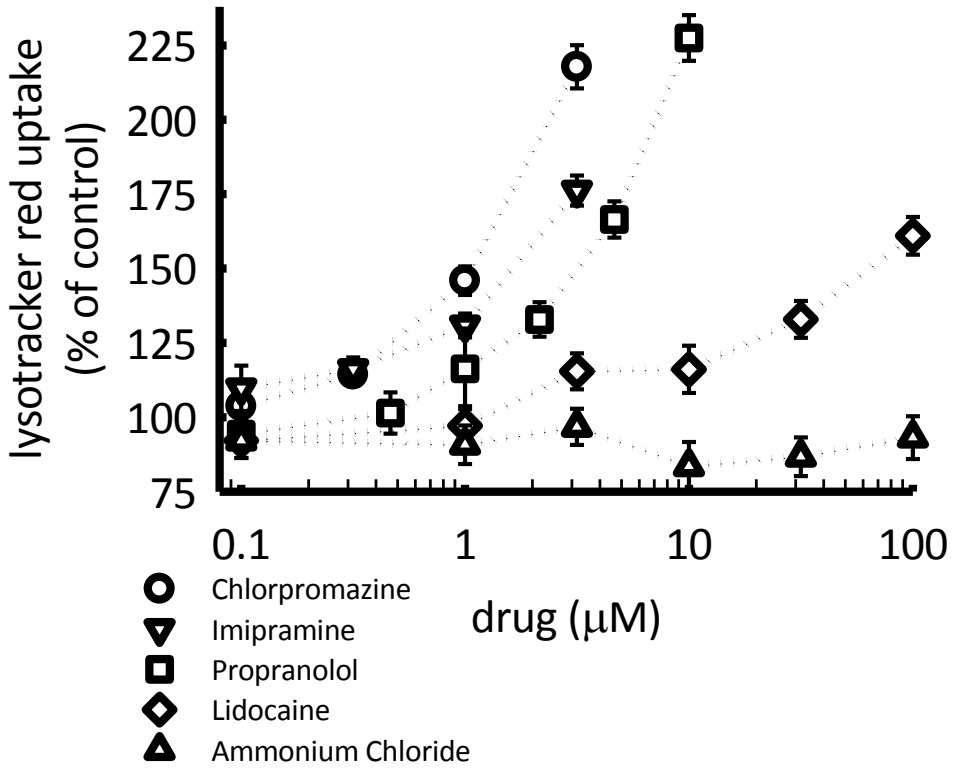

Figure 4.10 Concentration-dependent cellular accumulation of LTR (200 nM for 1 hour) in wild-type human fibroblasts with a 48-hour pretreatment of various lysosomotropic molecules. The reported values represent the average of approximately 500,000 cells. Cellular accumulation of LTR was measured in fluorescence units and then normalized to cellular protein. The normalized LTR uptake was then compared to the control condition (vehicle alone) and reported as a percentage of the control.

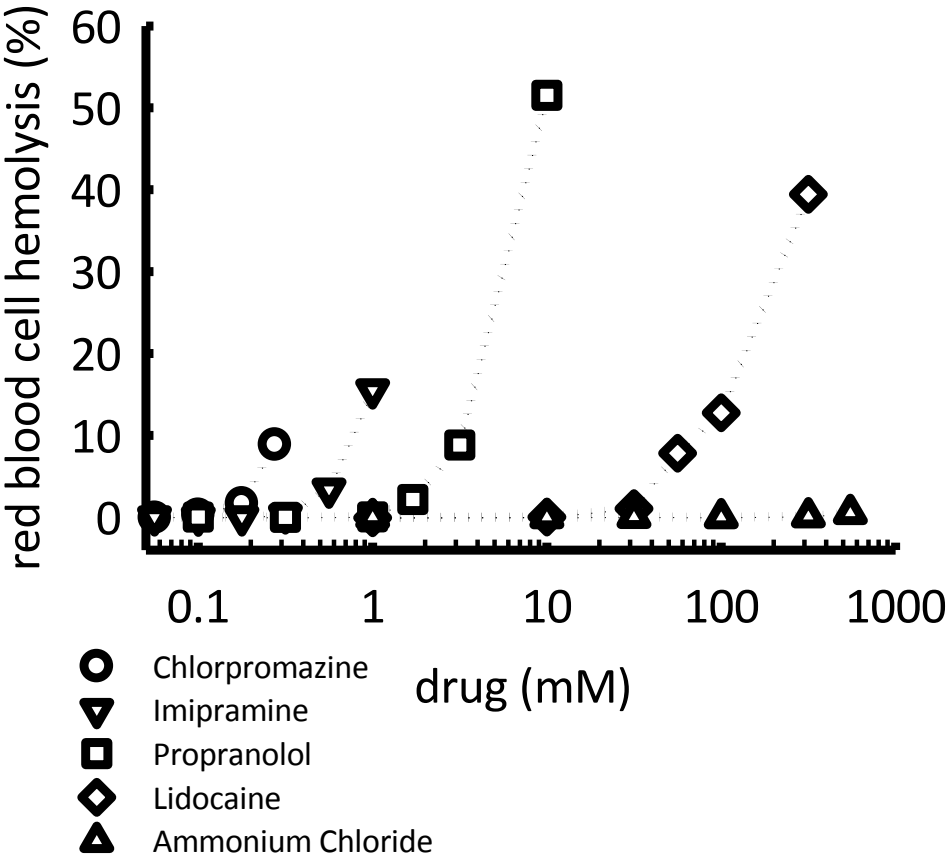

Figure 4.11 Concentration-dependent drug-induced hemolysis of human red blood cells (RBC). RBCs were isolated from whole blood and analyzed within 24hrs. RBCs were exposed to various concentrations of lysosomotropic drugs for 3hrs at 37°C. The extracellular release of hemoglobin was then analyzed by measuring the absorbance at 545nm. The reported values represent the percentage of RBCs in the sample that was hemolyzed due to drug exposure. The data illustrated in this graph was derived from an average of 3 to 4 independent experiments.

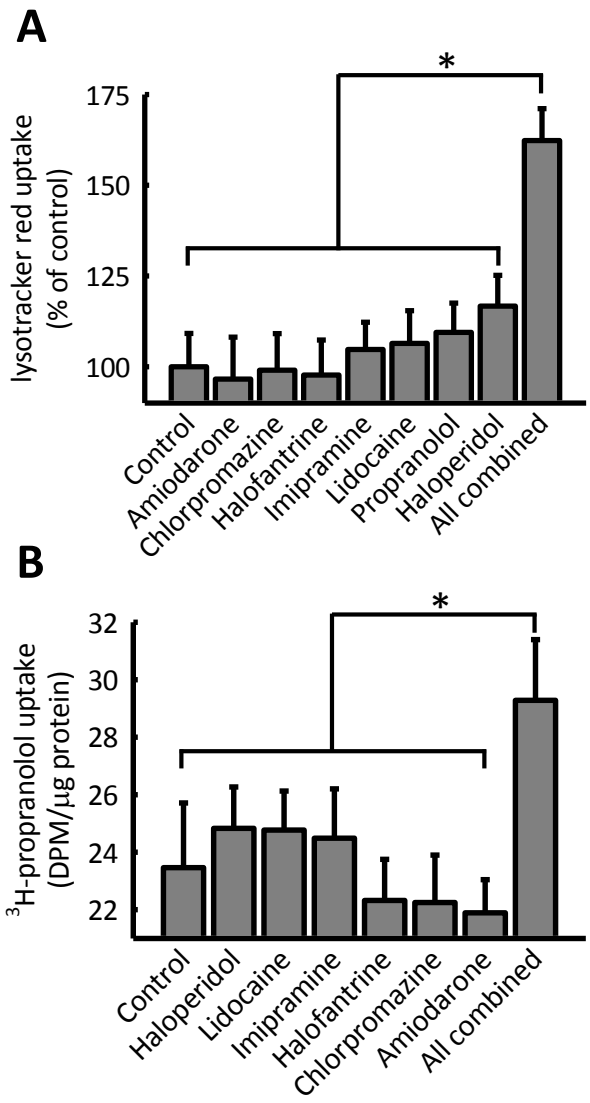

Figure 4.12 Lysosomotropic drugs affect lysosomes in an additive manner. Cells were exposed to the indicated drug or combination of drugs for 48 hours. After the 48hr drug treatment the cellular accumulation of (A) LTR or (B) tritium-labeled propranolol was measured. The following drug concentrations were used in both (A) and (B) individually or in combination: amiodarone 215nM, chlorpromazine 30nM, halofantrine 100nM, imipramine 30nM, lidocaine 800nM, propranolol 450nM, haloperidol 430nM.

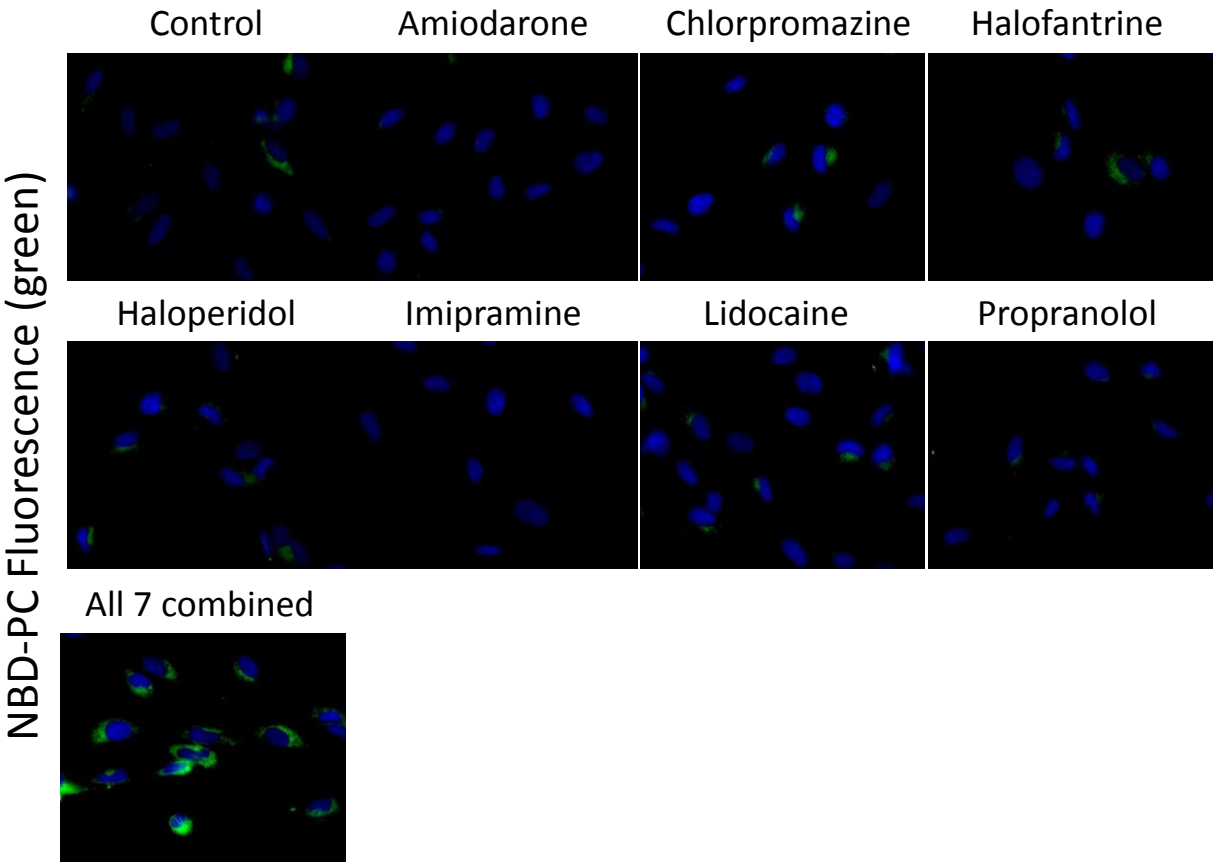

Figure 4.13 Lysosomotropic drugs affect lipid transport in an additive manner. Cells were exposed to the indicated drug or combination of drugs for 48 hours. 24hrs prior to cell imaging NBD-PC was spiked into the existing cell culture media to a concentration of 40µM. At the end of the 48hr drug exposure the cells were imaged using identical lamp power and exposure times. The green signal represents NBD-PC fluorescence while the blue signal (circular shapes) represent individual cell nuclei. Each image contains approximately 6 to 12 cells. The following drug concentrations were used in both (A) and (B) individually or in combination: amiodarone 215nM, chlorpromazine 30nM, halofantrine 100nM, imipramine 30nM, lidocaine 800nM, propranolol 450nM, haloperidol 430nM.

References

Anderson, N. and J. Borlak (2006). "Drug-induced phospholipidosis." FEBS Lett 580(23): 5533-5540.

Butler, J. D., J. Blanchette-Mackie, E. Goldin, R. R. O'Neill, G. Carstea, C. F. Roff, M. C. Patterson, S. Patel, M. E. Comly, A. Cooney and et al. (1992). "Progesterone blocks cholesterol translocation from lysosomes." J Biol Chem 267(33): 23797-23805.

Chatman, L. A., D. Morton, T. O. Johnson and S. D. Anway (2009). "A strategy for risk management of drug-induced phospholipidosis." Toxicol Pathol 37(7): 997-1005.

Fujiwara, T., N. Hirashima, S. Hasegawa, M. Nakanishi and T. Ohwada (2001). "Space-filling effects in membrane disruption by cationic amphiphiles." Bioorg Med Chem 9(4): 1013-1024.

Halliwell, W. H. (1997). "Cationic amphiphilic drug-induced phospholipidosis." Toxicol Pathol 25(1): 53-60.

Isomaa, B., H. Hagerstrand, G. Paatero and A. C. Engblom (1986). "Permeability alterations and antihaemolysis induced by amphiphiles in human erythrocytes." Biochim Biophys Acta 860(3): 510-524.

Kasahara, T., K. Tomita, H. Murano, T. Harada, K. Tsubakimoto, T. Ogihara, S. Ohnishi and C. Kakinuma (2006). "Establishment of an in vitro high-throughput screening assay for detecting phospholipidosis-inducing potential." Toxicol Sci 90(1): 133-141.

Kolzer, M., N. Werth and K. Sandhoff (2004). "Interactions of acid sphingomyelinase and lipid bilayers in the presence of the tricyclic antidepressant desipramine." FEBS Lett 559(1-3): 96-98.

Lowe, R., R. C. Glen and J. B. Mitchell (2010). "Predicting phospholipidosis using machine learning." Mol Pharm 7(5): 1708-1714.

Maruoka, N., T. Murata, N. Omata, Y. Takashima, H. Tanii, Y. Yonekura, Y. Fujibayashi and Y. Wada (2007). "Effects of chlorpromazine on plasma membrane permeability and fluidity in the rat brain: a dynamic positron autoradiography and fluorescence polarization study." Prog Neuropsychopharmacol Biol Psychiatry 31(1): 178-186.

Rampe, D. and A. M. Brown (2013). "A history of the role of the hERG channel in cardiac risk assessment." J Pharmacol Toxicol Methods 68(1): 13-22.

Rayan, A., M. Falah, J. Raiyn, B. Da'adoosh, S. Kadan, H. Zaid and A. Goldblum (2013). "Indexing molecules for their hERG liability." Eur J Med Chem 65: 304-314.

Reasor, M. J. (1991). "Influence of a pre-existing phospholipidosis on the accumulation of amiodarone and desethylamiodarone in rat alveolar macrophages." Research communications in chemical pathology and pharmacology 72(2): 169-181.

Reasor, M. J., K. L. Hastings and R. G. Ulrich (2006). "Drug-induced phospholipidosis: issues and future directions." Expert Opin Drug Saf 5(4): 567-583.

Reinhart, W. H. and S. Chien (1986). "Red cell rheology in stomatocyte-echinocyte transformation: roles of cell geometry and cell shape." Blood 67(4): 1110-1118.

Reinhart, W. H. and F. Rohner (1990). "Effect of amiodarone on erythrocyte shape and membrane properties." Clin Sci (Lond) 79(4): 387-391.

Spinedi, A., L. Pacini and P. Luly (1989). "A study of the mechanism by which some amphiphilic drugs affect human erythrocyte acetylcholinesterase activity." Biochem J 261(2): 569-573.

Suwalsky, M., F. Villena, C. P. Sotomayor, S. Bolognin and P. Zatta (2008). "Human cells and cell membrane molecular models are affected in vitro by chlorpromazine." Biophys Chem 135(1-3): 7-13.

Tang, W., J. Kang, X. Wu, D. Rampe, L. Wang, H. Shen, Z. Li, D. Dunnington and T. Garyantes (2001). "Development and evaluation of high throughput functional assay methods for HERG potassium channel." J Biomol Screen 6(5): 325-331.

te Vruchte, D., E. Lloyd-Evans, R. J. Veldman, D. C. Neville, R. A. Dwek, F. M. Platt, W. J. van Blitterswijk and D. J. Sillence (2004). "Accumulation of glycosphingolipids in Niemann-Pick C disease disrupts endosomal transport." J Biol Chem 279(25): 26167-26175.

Tengstrand, E. A., G. T. Miwa and F. Y. Hsieh (2010). "Bis(monoacylglycerol)phosphate as a non-invasive biomarker to monitor the onset and time-course of phospholipidosis with drug-induced toxicities." Expert Opin Drug Metab Toxicol 6(5): 555-570.

Tomizawa, K., K. Sugano, H. Yamada and I. Horii (2006). "Physicochemical and cell-based approach for early screening of phospholipidosis-inducing potential." J Toxicol Sci 31(4): 315-324.

Vandenberg, J. I., M. D. Perry, M. J. Perrin, S. A. Mann, Y. Ke and A. P. Hill (2012). "hERG K(+) channels: structure, function, and clinical significance." Physiol Rev 92(3): 1393-1478.

Vandenbroucke-Grauls, C. M., R. M. Thijssen, J. H. Marcelis, S. D. Sharma and J. Verhoef (1984). "Effects of lysosomotropic amines on human polymorphonuclear leucocyte function." Immunology 51(2): 319-326.

Yamamoto, A., S. Adachi, K. Ishikawa, T. Yokomura and T. Kitani (1971). "Studies on drug-induced lipidosis. 3. Lipid composition of the liver and some other tissues in clinical cases of "Niemann-Pick-like syndrome" induced by 4,4'-diethylaminoethoxyhexestrol." J Biochem 70(5): 775-784.

Zachowski, A. and P. Durand (1988). "Biphasic nature of the binding of cationic amphipaths with artificial and biological membranes." Biochim Biophys Acta 937(2): 411-416.

Zheng, N., X. Zhang and G. R. Rosania (2011). "Effect of phospholipidosis on the cellular pharmacokinetics of chloroquine." The Journal of pharmacology and experimental therapeutics 336(3): 661-671.

Chapter 5. Studies on the influence that amphiphilic phenols have on the steady-state volume of lysosomes

Introduction

Lysosomal storage diseases (LSD)s are a set of inheritable diseases that occur when an individual harbors a functional mutation in a lysosome associated protein that leads to impaired catabolic activity of lysosomes. This impaired catabolic activity can result in the buildup of metabolic substrates or undegraded material within the cells leading to additional downstream effects and toxicity (Kolter and Sandhoff 2010). Overall, these diseases present in the human population at a relatively high frequency at 1 in 8,000 live births (Jeyakumar, Dwek et al. 2005). Although there are approximately 40-50 known LSDs that are identified by mutations in unique proteins, these diseases can surprisingly share similar features including onset at a very early age and involvement of brain pathology. In the previous chapters we have primarily focused on the drug-induced expansion of lysosomal volume and the ensuing changes to cellular physiology seen after treating cultured cells with lysosomotropic drugs. Interestingly, LSDs can also present a similar biochemical and morphological phenotype to that seen in cells treated with lysosomotropic drugs. We and others have observed that LSDs also exhibit an expanded lysosomal volume phenotype (Figure 5.1) (Karageorgos, Isaac et al. 1997, Kolter and Sandhoff 2010, Xu, Liu et al. 2012), an impaired rate of vesicle-mediated lysosomal egress (Goldman, Funk et al. 2009), and the presentation of multilamellar bodies (lipid laden lysosomes) (Jeyakumar, Dwek et al. 2005). The similarity between LSDs, especially Niemann-Pick Type C Disease (NPC) (Matsuzawa, Yamamoto et al. 1977, Anderson and Borlak 2006), and drug-induced lysosomal dysfunction has also been recognized by the FDA and resulted in the formation of a special advisory board (*Phosphoplipidosis Working Group*) to more thoroughly explore this relationship (Reasor, Hastings et al. 2006, Tengstrand, Miwa et al. 2010).

Both LSDs and drug-induced changes to lysosomal function have been reported to cause severe toxic effects and even death (Honegger, Scuntaro et al. 1995, Futerman and van Meer 2004, Jeyakumar, Dwek et al. 2005). Unfortunately, there are currently no FDA approved treatments for the brain pathologies caused by LSDs (Jeyakumar, Dwek et al. 2005) or treatment strategies to mitigate drug-induced dysfunction of lysosomes. With this in mind we have focused the efforts of the current chapter on exploring treatment strategies that can help recover a normal lysosome phenotype in both the lysosomotropic drug-induced model and the LSD model. Although these two models both present complex and multi-component impairments, we reasoned that lysosome dysfunction ultimately manifests itself as an expansion in lysosomal volume. For this reason we have used lysosomal volume measurements (lysotracker red (LTR) uptake) as a surrogate marker for lysosome function.

Within the last few years many reports have detailed the promising results that vitamin E has shown in its capacity to improve lysosome function and mitigate the ensuing toxicities seen with lysosome dysfunction. For example, Arai and Coworkers have shown that the normal homeostatic balance of vitamin E plays an important role in reducing the severe cytotoxic effects of the lysosomotropic drug chloroquine in rat hepatoma cells (Shichiri, Kono et al. 2012). Wiesmann and Coworkers have also shown that cultured human cells treated with 50μM α-tocopherol, one of the eight isomeric molecules that are collectively referred to as vitamin E (Figure 5.2) (Wang and Quinn 1999), exhibit a remarkable recovery in amiodarone-induced lysosome dysfunction (Honegger, Scuntaro et al. 1995). Additionally, vitamin E has also been shown to improve lysosome-dysfunction in LSD models. Xu et. al. has very recently reported on the capacity of δ-tocopherol (another of the eight isoforms of vitamin E) to improve cholesterol transport, reduce the hyperaccumulation of lipids, and recover lysosomal volume in NPC diseased human fibroblasts (Xu, Liu et al. 2012).

Although vitamin E shows great promise in its potential to be used as a treatment strategy to mitigate lysosomotropic drug toxicity and ameliorate the ill effects of LSDs, vitamin E is recognized as a poor drug-like molecule. In addition to its very poor aqueous solubility, vitamin E has is also very prone to oxidation (Wang and Quinn 1999) and P450 enzyme metabolism by CYP4F2 (particularly δ-tocopherol) (Xu, Liu et al. 2012). With this in mind, we sought to answer two main questions. First, what changes are occurring to lysosomes after the administration of vitamin E. And secondly, what physicochemical property of vitamin E is responsible for its activity. We reasoned that if we could understand how vitamin E is influencing lysosomes and what structural feature of vitamin E is responsible for its activity then we could rationally design a drug that is capable of treating lysosome-dysfunction in either a drug-induced scenario or in LSDs.

Materials and Methods

Cell Lines and Reagents

Wild-type (WT) human fibroblasts (catalogue # CRL-2076), Niemann-Pick Type C1 (NPC1) diseased fibroblast, Niemann-Pick Type C2 (NPC2) diseased fibroblast, Niemann-Pick Type A (NPA) diseased fibroblast, and Sandhoff diseased fibroblast were all purchased from ATCC (Manassas, VA). All cells were cultured in glutamine-free DMEM supplemented with 10% FBS, 10mM HEPES, 1mM Sodium Pyruvate, and 2mM Glutamax and maintained at 37 degrees C and 5% CO 2. Cells were routinely subcultured to maintain 50% to 90% confluency. Experiments were carried out within 10 passages following removal from cryopreservation. Dulbecco's phosphate buffered saline (D-PBS), Dulbecco's modified Eagle's medium (DMEM), HEPES, sodium pyruvate, glutamax, Hoechst stain, and LysoTracker Red DND-99 (LTR) were purchased from Invitrogen (Carlsbad, CA). Fetal bovine serum (FBS) was purchased from Atlanta Biologicals (Lawrenceville, GA). Halofantrine, propranolol, verapamil, Laemmli buffer, and sodium deoxycholate were purchased from Sigma-Aldrich (St. Louis, MO). Pierce BCA

protein assay kit was ordered from ThermoScientific (Rockford, IL). Anti-p-glycoprotein primary antibody was a generous gift from Dr. Micheal Wang (Pharmaceutical Chemistry Department, University of Kansas, Lawrence, KS). Anti-beta actin antibody (catalogue #8H10D10) was purchased from Cell Signaling Technology (Danvers, MA). ^{3}[H]-halofantrine, and ^{3}[H]-propranolol were purchased from American Radiolabeled Chemicals, Inc. (St. Louis, MO).

LysoTracker Red accumulation assay

Various human fibroblast cell lines were grown in plastic 12-well culture plates (Corning Life Sciences) at a seeding density of approximately 75,000 cells per well. Following pretreatments with various drugs (concentrations and durations for each drug is stated in the figure legend), LysoTracker Red was spiked into the growth media to a concentration of 200nM and the cells were incubated for 1 hour. Cells were then rapidly washed twice with 4 degrees C D-PBS. Cells were lysed with lysis buffer (50 mM tris base, 150 mM NaCl, 1% NP40, pH 7.4). The quantity of LTR was determined by fluorescent signal in relative fluorescence units (RFU) using a Bio-Tek FL600 microplate fluorescence reader. Protein abundance was measured for each sample using the BCA method. Measured LTR signal (RFU) was then normalized to protein. These normalized values were then compared to the control condition (vehicle treated) and depicted as a percentage of the control.

Drug Accumulation Assays

WT human fibroblasts were seeded and grown in plastic 12-well culture plates (Corning Life Sciences). On the following day the extracellular media was replaced with test media as stated in each figure legend. The extracellular media was refreshed every 48hrs (sustaining the test condition) to maintain optimal growth conditions. To assess the total drug accumulation at the end of the experiments the cells were immediately washed twice with 4°C D-PBS. To assess the drug uptake by ion-trapping independent mechanisms, nigericin and monensin was spiked directly into the existing cell culture

media (final concentration of 10µM and 20µM, respectively) 2 hrs prior to reaching the desire drug exposure duration. Once the desire drug exposure time was achieved, the cells were then washed twice with 4°C D-PBS. The washed cells were then lysed using lysis buffer (50 mM tris base, 150 mM NaCl, 1% NP40, pH titrated to 7.4 with HCl) for 30mins at 37°C. The lysate was recovered from each well by aspiration using a standard pipette. The quantity of radio-labeled drug was measured in DPMs using a Beckman LS 60001C liquid scintillation counter. Background signal contributed from non-specific binding of drug to the plate surface was subtracted from each measurement. Dilutions of each radiolabeled drug stock were performed to attain a standard curve relating DPMs to nanomoles of drug. Measured DPMs in the cell samples were then converted to nanomoles of drug. Protein abundance was measured for each sample using the BCA method. The calculated nanomoles of drug present in each sample was then normalized to mg protein.

The ion-trapping dependent cellular accumulation of propranolol was determined mathematically by subtracting the ion-trapping independent cellular accumulation (nigericin/monensin treated samples) from the total cellular accumulation at each indicated time point. The activity used for all of the drug accumulation experiments were as follows: .06µCi/mL for ^{3}H-propranolol or .1µCi/mL ^{3}H-halofantrine.

Drug Release Assay

WT human fibroblasts were grown in plastic 12-well culture plates at a seeding density of 20,000 cells per well. The cells were exposed to either 5µM propranolol (consisting of 4.995µM unlabeled propranolol and 5nM of ^{3}H-propranolol at a final activity of .06µCi/mL) or 5µM halofantrine (consisting of 4.995µM unlabeled halofantrine and 5nM ^{3}H-halofantrine at a final activity of .1µCi/mL) for 4 days. The media was refreshed every 48hrs to maintain optimal growth conditions. At the end of this 4 day exposure nigericin and monensin were spiked into the extracellular media to a concentration of 10µM

and 20µM, respectively. At the indicated time points the cells were then rapidly washed twice with 4°C D-PBS. The cells were then lysed for 30 min at 37°C using lysis buffer and the lysate was capture by aspiration using a standard pipette. The quantity of tritium-labeled drug (propranolol or halofantrine) was measured in disintegrations per minute (DPM) using a Beckman LS 60001C liquid scintillation counter. Background signal contributed from non-specific binding of drug to the plate surface was subtracted from each measurement. Dilutions of each radiolabeled drug stock were performed to attain a standard curve relating DPMs to nanomoles of drug. Measured DPMs in the cell samples were then converted to nanomoles of drug. Protein abundance was measured for each sample using the BCA method. Measured DPMs were then converted to nanomoles of drug and normalized to protein.

Cell imaging

All cell imaging was performed on a Nikon Eclipse 80i epifluorescence microscope equipped with a 40× (1.40 NA) oil immersion SFLOR objective. All images were acquired on a Hamamatsu ORCA ER digital camera. Images were analyzed using Metamorph software version 7.0 (Universal Imaging) and ImageJ software (free online atrsbweb.nih.gov) software. Madin-Derby Canine Kidney (MDCK) cells were grown on glass coverslips under the stated growth conditions and durations of exposure. Following the end of the pre-treatment period the cells were cooled to 4°C for 10mins. The extracellular media was replaced with the test condition plus the addition of 25µM rhodamine 123 (R123) and incubated at 4°C for 1hr (R123 utake). The cells were then washed twice with 37°C D-PBS and the extracellular media was replaced with the test condition devoid of R123 and incubated for 30mins at 37°C (R123 efflux period). At the end of the efflux period the cells were washed twice in 4°C D-PBS. Fluorescent images were taken during each one of these steps as labeled in the figure. The live cells were mounting onto a glass slide and imaged using the appropriate filter sets for R123 fluorescence. Images were captured under identical instrument settings and scaled equally so that a direct comparison of fluorescence intensity

and localization could be performed. Hoechst stain was used as nuclear marker for cells 30mins prior to taking all images at 3µg/mL.

Western blot analysis

MDCK cells were grown in 12well culture plates at a seeding density of approximately 150,000 cells per dish. Following a 4 day exposure to the presence or absence of α-tocopherol the cells were washed twice with 4 degrees C D-PBS. Cells were then lysed with RIPA buffer (150mM sodium chloride, 1% TX-100, 0.5% sodium deoxycholate, 0.1% SDS, 50mM tris, pH 8.0, and the protease inhibitors APL & PMSF). The protein abundance was then determined by the BCA method. Protein samples were then mixed with Laemmli buffer. All protein samples (25 µg per lane) were subjected to 12% sodium dodecyl sulfate-polyacrylamide gel electrophoresis (SDS-PAGE) for 120 minutes. The proteins were then transferred to a 0.2 µm pore PVDF membrane (Millipore) using 300 V*hours. The PVDF membrane was then exposed to primary antibody (1:8000 anti-p-glycoprotein, 1:30,000 anti-ß-actin) for two hours, washed, and then exposed to secondary antibody (1:4000 goat anti-mouse HRP) for two hours. Detection of HRP-conjugated antibody was achieved by chemiluminescence using Western Lightning-ECL (PerkinElmer) on autoradiograph film.

Transmission Electron Microscopy

WT human fibroblasts were grown in 175cm^2 culture flasks for 6 days with vehicle alone or 5µM propranolol. Media was refreshed every 48 hrs in order to maintain optimal nutrient conditions. At the end of the 6 day time period the cells were removed and fixed using 0.25% glutaraldehyde for 2 hrs at room temperature. Cells were then washed once and stained with osmium tetroxide 2% w/v in D-PBS for 1 hour at room temperature. The cells were washed one time with D-PBS and stained with tannic acid 1% for one hour at room temperature. The cells were then washed with water and stained with

uranyl acetate 4% for 30mins at room temperature. Following one wash step with water the cells were washed in progressively higher concentrations of ethanol until the wash reached 100% ethanol. Following the ethanol washes the cells were stained with propylene oxide. Cells were then embedded in EPON resin. All images were taken on an FEI Tecnai F20 XT Field Emission Transmission Electron Microscope.

Sizing of the lysosomal structures was performed manually using the Image J software (freely available at http://rsbweb.nih.gov/ij/). The data obtained from the manual sizing was then normalized to the surface area of cytosol present within the analyzed cell slice and then reported as counts per mm^2. Lysosomes were divided into three distinct categories, primary, secondary, and lipid laden membrane whorls, using published descriptions of their structural features as a guide.(Fawcett 1981) Briefly, small dense granules with homogenous contents were considered to be primary lysosomes. Due to the excessive number of primary lysosomes present within each cell slice, the data present in Figure 5.7 B for primary lysosomes is representative of one cell slice (n=1) for each condition. Larger bodies with heterogeneous content including undigested material were considered to be secondary lysosomes. Larger densely stained bodies with multiple concentric membrane-like whorls were considered to be lipid-laden membrane whorls. Data presented in Figure 5.7 B for secondary lysosomes and membrane whorls are representative of ten cell slices (n=10) for each condition.

Results and Discussion

α-Tocopherol recovers the steady state volume of lysosomes in lysosomotropic drug-treated cells

Although many reports have detailed the positive effects that vitamin E can have on recovering lysosome dysfunction and reducing the toxicity of lysosomotropic drugs (Honegger, Scuntaro et al. 1995, Scuntaro, Kientsch et al. 1996, Shichiri, Kono et al. 2012), very few have focused specifically on how these positive effects ultimately influence the steady state volume of lysosomes. With this in mind, we

first sought to validate the notion that the steady state volume of lysosomes could be used as a surrogate marker for lysosomes function. Honeggar and Coworkers have previous shown that 50μM α-tocopherol is capable of reducing the lysosome dysfunction caused by propranolol and many other lysosomotropic drugs (Scuntaro, Kientsch et al. 1996). Using a similar vitamin E treatment protocol the lysosomal volume of cultured human fibroblasts was assessed in the presence or absence of α-tocopherol (Figure 5.3). These results indicated that α-tocopherol was capable of recovering the steady state volume of lysosomes in cells treated with propranolol or halofantrine in wild-type human fibroblasts.

α-Tocopherol reduces lysosomotropic drug uptake, reduces ion-trapping dependent mechanisms, and reduces the abundance of lipid-laden lysosomes

In order to more thoroughly explore how α-tocopherol might be reducing the toxic effects of lysosomotropic drugs we next sought to explore the effects that α-tocopherol had on the cellular accumulation of lysosomotropic drugs. Others have shown that α-tocopherol is capable of reducing the cellular accumulation of lysosomotropic drugs but a thorough analysis of how α-tocopherol was mediating this effect was not performed. Many groups have proposed that α-tocopherol reduces the hyper accumulation of lipids within drug-treated cells and by virtue of the decreased lipid content the cells accumulate less drug (Honegger, Scuntaro et al. 1995, Scuntaro, Kientsch et al. 1996, Agoston, Orsi et al. 2003). To more deeply explore this we first confirmed that α-tocopherol caused a reduction in the cellular accumulation of two lysosomotropic drugs propranolol and halofantrine (Figure 5.4). We then more closely examined the way in which α-tocopherol was reducing the cellular accumulation of these drugs. By using nigericin and monensin to dissipate the lysosomal pH gradient, we specifically measured the cellular accumulation of drug by ion trapping-dependent (aqueous volume of lysosomes) and ion trapping-independent (lipid binding) mechanisms. Interestingly, we found that the ion trapping-dependent drug accumulation mechanisms were most affected by α-tocopherol treatments (Figure 5.5).

The data in Figure 5.5 shows that the reduction in propranolol uptake is almost entirely due to reduced ion trapping-dependent drug accumulation mechanisms. Due to the slow kinetic release of halofantrine from the cells an accurate measurement of the ion trapping-dependent and -independent drug accumulation mechanisms was not attainable. Following the dissipation of the lysosomal pH gradient with nigericin and monensin the halofantrine that accumulated due to ion trapping-dependent mechanisms begins to partition out of the cells; however, prior to reaching equilibrium, the nigericin and monensin begins to cause visible signs of toxicity to the cells. Measurements of the ion trapping-dependent drug accumulation of halofantrine would therefore be lower than the actual value as all the halofantrine that accumulated by ion trapping-dependent mechanism has not left the cells. Propranolol on the other hand reaches equilibrium after only a few minutes in the presence of nigericin and monensin (Figure 5.6 A) compared to halofantrine which requires greater than 2 hours (Figure 5.6 B).

Once we had established that α-tocopherol was reducing the ion trapping-dependent drug accumulation mechanisms we next sought validate these findings using transmission electron microscopy (Figure 5.7). These results showed that α-tocopherol causes a significant reduction in the size of secondary lysosomes (Figure 5.7 A) while also substantially reducing the abundance of membrane whorls (lipid-laden lysosomes) (Figure 5.7 B).

In our consideration of α-tocopherol-mediated reduction in lysosomotropic drug uptake we had also envisaged the possibility that α-tocopherol could be modulating the activity or expression of p-glycoprotein (p-gp). P-gp has been well established as a promiscuous drug-transporter that is capable of capable of reducing the intracellular accumulation of many drugs (Ward, Szewczyk et al. 2013). Conditions that increase expression and/or increase activity of p-gp could conceivably reduce the total cellular accumulation of drugs. To test this possibility we examined the expression and activity of p-gp in two closely related Madin-Darby canine kidney cells, MDCK WT and MDCK MDR1 (Figure 5.8). MDCK

WT cells do not express p-gp; however, MDCK MDR1 cells have been stably transfected with the gene for p-gp and exhibit a detectable expression of this protein under normal growth conditions (Figure 5.8 A). The results shown in Figure 5.8 A show that α-tocopherol does not change the expression of p-gp in either MDCK WT or MDCK MDR1 cells. To test potential changes in the activity of p-gp we employed a rhodamine 123 (R123) efflux assay. R123 is a well-established substrate for p-gp and due to its fluorescent properties it is easy to analyze in fluorescence microscopy and quantitative microplate assays (Mittapalli, Manda et al. 2013). With this in mind we measured the efficiency of R123 efflux using fluorescence microscopy and a quantitative microplate assay using the cellular lysate from an ensemble of approximately 500,000 cells. Included in Figure 5.8 B & C is the known p-gp inhibitor verapamil (labeled as +pgp inhibited). If α-tocopherol inhibited p-gp activity we would expect the R123 signal to be similar to that of the verapamil treated (+pgp inhibited) cells. Conversely, if α-tocopherol enhanced the activity of p-gp then we would expect the α-tocopherol treated cells to have a lower R123 signal as compared to the untreated cells (labeled as WT or MDR1). Our results indicated that α-tocopherol did not alter the activity of p-gp-mediated efflux of R123 in either the multi-cell experiment (Figure 5.8 B) or in the fluorescence microscopy based experiment (Figure 5.8 C).

α-Tocopherol recovers the steady state volume of lysosomes in LSD cells

Similar to improving lysosomal-dysfunction in drug-treated cells, vitamin E has also been shown to ameliorate many of the functional impairments of lysosomes seen in LSDs (Xu, Liu et al. 2012). Although many of these functional impairments have been shown to improve (e.g., cholesterol transport, vesicle-mediated transport, and lysosomal catabolism) the effect of α-tocopherol on the steady state volume of lysosomes has not been thoroughly examined. We therefore sought to evaluate the steady state volume of lysosomes in LSD cells with or without α-tocopherol treatment. We have previous established that LSD cells possess a significantly greater lysosomal volume compared to wild type cells (Figure 5.1). Although there are many different LSD disease models to be evaluated, we narrowed our

evaluations to just NPC diseased cells due to its phenotypic similarity with the lysosomotropic drug-induced model (Matsuzawa, Yamamoto et al. 1977, Anderson and Borlak 2006). Our data showed that the steady state volume of lysosomes in NPC diseased cells showed a marked time-dependent and concentration-dependent reduction in lysosomal volume in the presence of α-tocopherol (Figure 5.9 A & B, respectively).

Structure activity analysis of vitamin E and its ability to recover lysosomal volume

In order to establish the key structural features of vitamin E that are primarily responsible for its ability to exert its positive effects on lysosomes we performed a targeted structure activity relationship. Many groups have postulated mechanisms by which vitamin E can elicit its beneficial effects. Common among these hypotheses is that vitamin E helps to protect cells from free radical lipid peroxidation by virtue of its strong antioxidant characteristics (van Acker, Koymans et al. 1993). The phenolic acid functional group present on the heterocyclic ring of vitamin E is responsible for its antioxidant properties allowing vitamin E to work as a "chain terminator" which stops the "propagation steps" of free radical damage (van Acker, Koymans et al. 1993, Wang and Quinn 1999). To test the importance of this phenolic acid-mediated antioxidant property we evaluated several different molecules, all of which possessed phenolic acid or poly-phenolic acid functional groups, for their capacity to recover the steady state volume of lysosomes in NPC diseased cells (Figure 5.10). We reasoned that if the antioxidant properties of vitamin E were the mechanism by which vitamin E helped to recover lysosomal function then we would expect to see a decrease in the steady state volume of lysosomes as measured by LTR uptake. The results illustrated in Figure 5.10 indicated that none of these phenolic acid-containing molecules reduced the bloated lysosomal volume seen in NPC diseased cells, i.e., they did not reduce the lysotracker red uptake below 100% which represents a cell with a full NPC-diseased lysosome. Due to the cytotoxic effects of some of these test compounds depicted in Figure 5.10 we were unable to evaluate a 50μM concentration as was done with vitamin E. However, the compounds there were not

toxic up to 100μM (albuterol and rutin) still showed no reduction in the steady state volume of lysosomes (data not shown).

After observing that the phenols and polyphenols were incapable of reducing the bloated lysosomal volume of NPC diseased cells, we next sought to assess how changes to the phenolic acid functional group on vitamin E itself would influence its ability to recover lysosomal volume (Figure 5.11). Our data indicated that vitamin E, specifically α-tocopherol (Figure 5.11 A) and δ-tocopherol (Figure 5.11 B), was capable of reducing the lysosomal volume in NPC diseased cells with or without a free (unconjugated) or intact phenolic acid on its heterocyclic ring. These intriguing results suggested that vitamin E does not mediate its beneficial effects to lysosomes by its antioxidant properties.

Conclusion

Both LSDs and drug-induced lysosome dysfunction have been observed to cause severe toxic effects (Honegger, Scuntaro et al. 1995, Futerman and van Meer 2004, Jeyakumar, Dwek et al. 2005). LSDs represent a category of diseases that present in the human population at a relatively high frequency at approximately 1 in 8000 live births. Unfortunately, many of these LSDs lead to progressive neurodegeneration and ultimately death. There are currently no FDA approved treatments for the brain pathologies caused by these diseases (Jeyakumar, Dwek et al. 2005). LSDs therefore represent a poorly served disease in regard to available pharmaceutical interventions. In addition to the inherited acquisition of lysosomal storage diseases, many lysosomotropic drugs have been shown to cause perturbations in lysosome function that ultimately give rise to a biochemical and morphological phenotype similar to that seen in LSD cells (Matsuzawa, Yamamoto et al. 1977, Anderson and Borlak 2006). Although the clinical ramifications of this drug-induced phenotype are currently not known, the FDA has considered this off-target drug effect to be highly dubious and has consequently formed a

special working group (*Phosphoplipidosis Working Group*) to examine drug-induced changes to lysosomes (Reasor, Hastings et al. 2006, Tengstrand, Miwa et al. 2010).

Very recently, vitamin E has shown great promise in its ability to help recover lysosome dysfunction in both LSDs and in cells treated with lysosomotropic drugs (Honegger, Scuntaro et al. 1995, Shichiri, Kono et al. 2012, Xu, Liu et al. 2012). In this chapter we have sought to explore how vitamin E helps to recover a normal lysosome phenotype in both LSDs and in cells treated with lysosomotropic drugs. In addition, we have also sought to develop a structure activity relationship to explore what structural features are important for vitamin E's ability to recover a normal lysosome phenotype.

We have shown that the steady state volume of lysosomes in LSDs (Figure 5.1) and in lysosomotropic drug-treated cells (Figure 1.2) both exhibit a substantially larger volume compared to their respective controls. We reasoned that the greater lysosomal volume seen in both of these conditions is the ultimate manifestation of an amalgam of several different lysosomal impairments and that lysosomal volume can therefore be used as a surrogate marker for determining proper lysosome function. Following this assumption we measured the steady state volume of lysosomes in the presence or absence of vitamin E (α-tocopherol) in both the LSD model, NPC diseased cells (Figure 5.9), and the lysosomotropic drug-induced model, propranolol or halofantrine treated cells (Figure 5.3). In both of these models we found that vitamin E was capable of reducing the steady state volume of lysosomes. We believe that this indicated that vitamin E was helping to recover proper lysosome function and thereby facilitated a recovery of a more normal steady state volume of lysosomes. Consistent with this idea previous reports have shown that this same vitamin E treatment regime, i.e., 50μM α-tocopherol in human fibroblasts, was capable of improving the lysosomal impairments caused by LSDs and lysosomotropic drug treatments (Honegger, Scuntaro et al. 1995, Shichiri, Kono et al. 2012, Xu, Liu et al. 2012).

Although the precise mechanism for vitamin E-mediated recovery of lysosome function is not currently understood, many groups have made an interesting observation in that α-tocopherol treatments tend to reduce the intracellular accumulation of lipids in both in vitro and in vivo models (Honegger, Scuntaro et al. 1995, Scuntaro, Kientsch et al. 1996, Agoston, Orsi et al. 2003). As a consequence of this reduced lipid content others have postulated that the total cellular accumulation of the offending lysosomotropic drug, and its toxic effects, are thereby reduced because of the lower abundance of lipid-binding sites (Xu, Liu et al. 2012).

In previous chapters we detailed that the accumulation of lysosomotropic drugs is due to both ion trapping-dependent (aqueous volume of lysosomes) and ion trapping-independent (intracellular protein binding, lipid binding, DNA binding etc) mechanisms. Decreases to either of these components should conceivably result in a decrease in the total accumulation of lysosomotropic drugs. In an effort to more thoroughly evaluate the way in which vitamin E (α-tocopherol) was reducing the accumulation of lysosomotropic drugs we assessed the changes occurring to both the ion trapping-dependent and ion trapping-independent drug accumulation mechanisms (Figure 5.5). To our knowledge this is the first evaluation of this nature. Interestingly, our results indicated that vitamin E (α-tocopherol) primarily reduces the ion trapping-dependent drug accumulation mechanisms for propranolol. The drug accumulation-capacity for the ion trapping-dependent mechanisms should primarily be influenced by changes in the total volume of the lysosomal system. We reasoned that the reduced ion trapping-dependent drug-accumulation of propranolol seen with the coadministration of α-tocopherol should be the result of a decrease in the total number of lysosomes and/or a decrease in the size of the lysosomes. To elucidate which one of these changes was occurring we performed a quantitative ultrastructure analysis of the lysosomes in wild type human cells receiving 5μM propranolol with or without vitamin E (α-tocopherol) (Figure 5.7). Our results indicated that the size distribution of secondary lysosomes was

significantly reduced (Figure 5.7 A) and the abundance of membrane whorls (lipid-laden lysosomes) was also substantially decreased (Figure 5.7 B).

Although vitamin E has shown great promise in resorting lysosome function in both LSD models and in the drug-induced model, vitamin E possesses very poor drug-like properties. Vitamin E has an extremely poor water solubility, is highly susceptible to oxidation (Wang and Quinn 1999), and is a substrate for liver P450 enzyme metabolism by CYP4F2 (particularly δ-tocopherol) (Xu, Liu et al. 2012). Vitamin E is therefore unlikely to ever become a viable treatment for either of these two conditions. With this in mind we have performed a targeted structure activity relationship of vitamin E (α-tocopherol and δ-tocopherol) in an attempt to identify the primary structural feature that is responsible for vitamin E's ability to restore lysosome function. Others have postulated that vitamin E elicits its positive effects primarily through its antioxidant properties that mitigate the cellular damage caused by lipid peroxidation (van Acker, Koymans et al. 1993). The antioxidant properties of vitamin E have been well characterized and have been attributed to the phenolic acid functional group present on its heterocyclic ring (van Acker, Koymans et al. 1993, Wang and Quinn 1999). With this in mind we tested a battery of many different phenol and polyphenol-containing molecules for their ability to restore a normal lysosome volume in NPC diseased cells (Figure 5.10). The results illustrated in Figure 5.10 indicated that the antioxidant properties of phenolic acids alone is not capable of restoring a normal lysosomal volume in NPC diseased cells.

From these results we had reasoned that intercalation into membrane was likely playing an important functional role in vitamin E's ability to restore lysosome function, and by extension reduce the bloated lysosomal volume of the diseased cells. Consistent with this idea others have postulated that vitamin E exerts its beneficial effects by influencing membrane dynamics such as membrane fluidity and order (Wang and Quinn 1999). To more thoroughly dissect the importance of the antioxidant properties

versus the influence on membrane dynamics, we analyzed a battery of vitamin E analogs that all contained various functional changes to the phenolic acid group (Figure 5.11). Interestingly, we found that the phenolic acid functional group was not responsible for these molecules ability to restore lysosomal volume in NPC diseased cells. Although a more thorough evaluation of membrane dynamics is in order, these results support the notion that vitamin E improves lysosome function primarily through its ability to influence membrane dynamics rather than its ability to function as an antioxidant.

In this chapter we have explored the effect that vitamin E has on the steady state volume of lysosomes in NPC diseased cells and in wild type cells treated with lysosomotropic drugs. We have shown that vitamin E reduces the bloated lysosomal volume seen in both of these conditions. In addition we have also provided the foundation for a structure activity relationship that highlights the importance of vitamin E's membrane interactions rather than its antioxidant properties. Although further studies are required to more thoroughly characterize how vitamin E is influencing lysosomal membrane dynamics, this chapter provides a proof of principle showing that it can be possible to rationally design drugs that could potentially be used to treat lysosomal storage disorders or the toxic effects of lysosomotropic drugs.

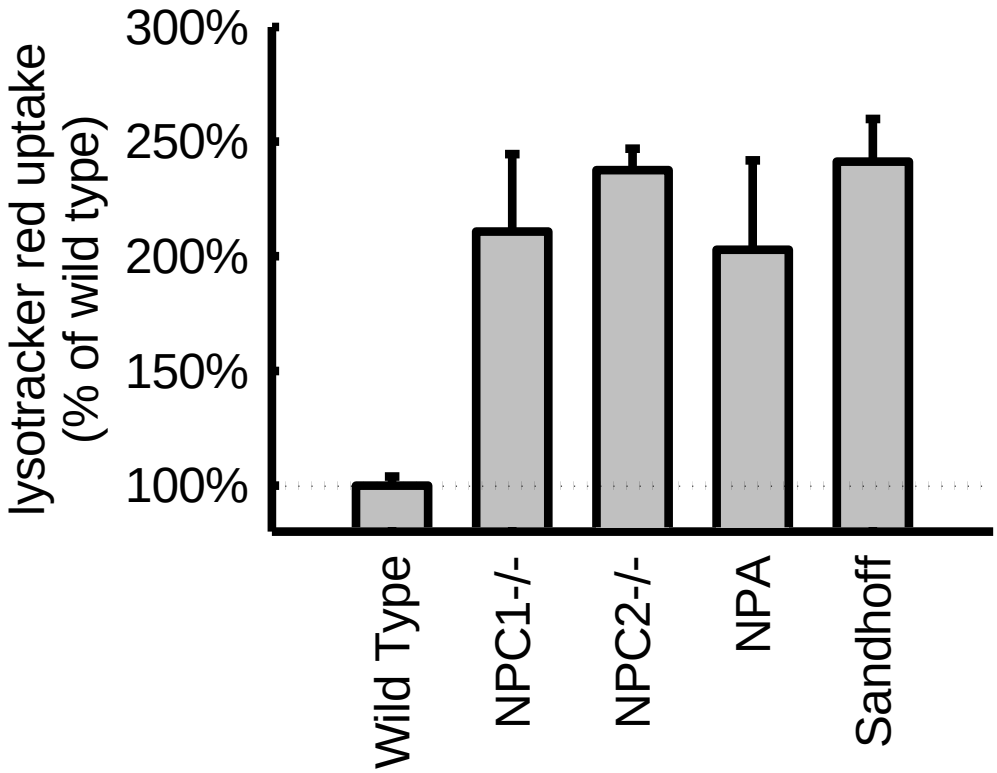

Figure 5.1 Assessments of the steady-state volume of lysosomes in multiple human fibroblast cell lines. Wild-type represents non-diseased cells while Niemann-Pick Type C1 (NPC1-/-), Niemann-Pick Type C2 (NPC2-/-), Niemann-Pick Type A (NPCA), and Sandhoff Diseased (Sandhoff) cells represent cell lines that all exhibit dysfunctional lysosomes. The reported values represent the average of approximately 500,000 cells measured by a minimum of three independent experiments. The cellular accumulation of lysotracker red (LTR) was measured in fluorescence units and then normalized to cellular protein. The normalized LTR uptake was then compared to the wild-type condition and reported as a percentage of the wild-type.

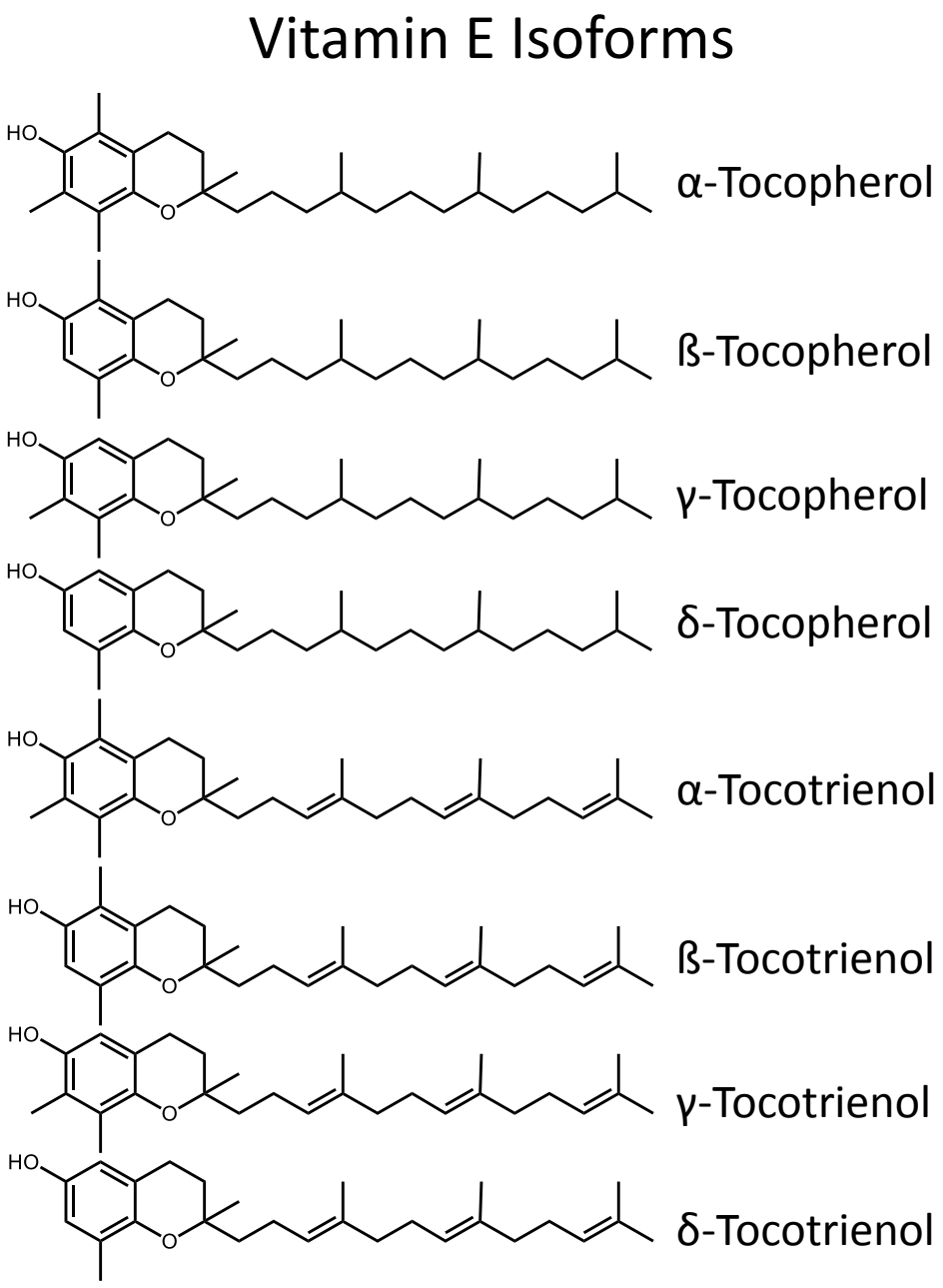

Figure 5.2 The molecular structures of the 8 isoforms of vitamin E.

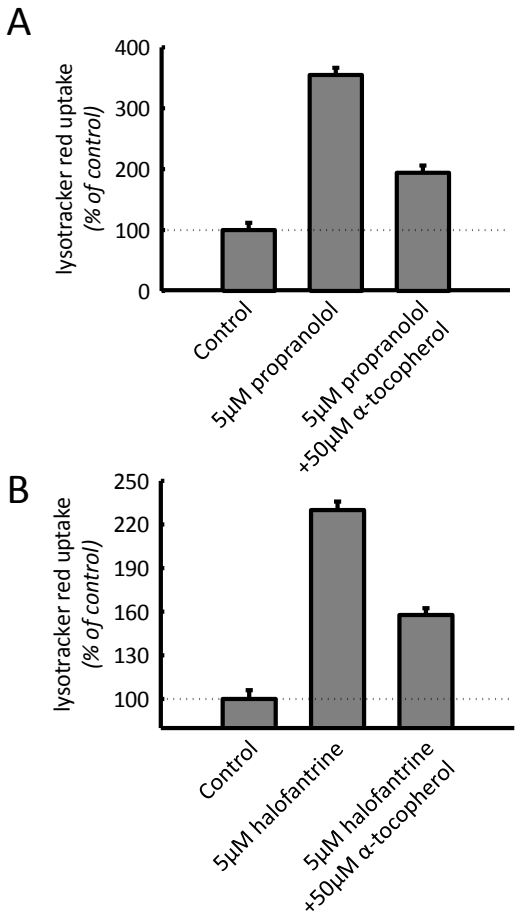

Figure 5.3 Assessments of the steady-state volume of lysosomes in wild-type human fibroblasts pre-treated for 48hrs under various conditions, as stated in the figure. The graph illustrates the cellular uptake of lysotracker red (LTR). The reported values represent the average of approximately 500,000 cells measured by a minimum of three independent experiments. The cellular accumulation of lysotracker red (LTR) was measured in fluorescence units and then normalized to cellular protein. The normalized LTR uptake was then compared to the vehicle-treated control and reported as a percentage of control.

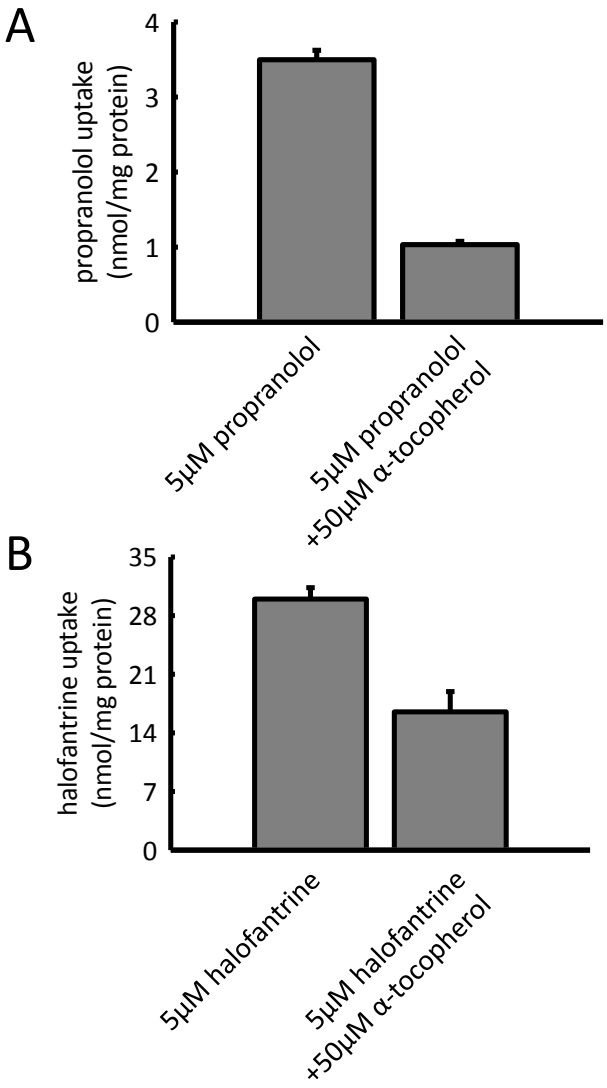

Figure 5.4 Total cellular accumulation of (A) propranolol or (B) halofantrine in the presence or absence of 50μM α-tocopherol (as indicated in the figure). Cells were exposed to the indicated condition over a 6 day period prior to analizing the cellular accumulation of the drug. The cellular accumulation of drug was measured using tritrium-labeled drugs at an activity of .06μCi/mL (propranolol) or .1μCi/mL (halofantrine) and then reported as nanomoles of drug. The nanomoles of drug were then normalized to the cellular protein present within the sample.

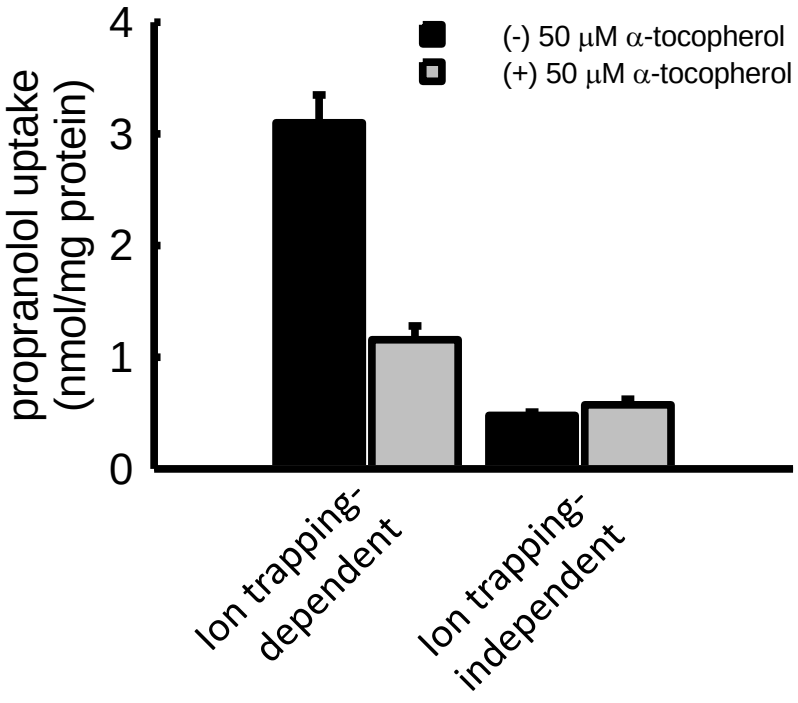

Figure 5.5 Cellular accumulation of propranolol by ion trapping-depenedent and ion trapping-indpendent drug accumulation mechanisms (as indicated in the figure) after a 6 day treatment with or without the coadministration of α-tocopherol. The ion trapping-independent values were obtained by measuring the cellular accumulation of propranolol in the absence of a lysosomal pH gradient (nigericin and monensin treated). The ion trapping-dependent values were obtained mathematically by subtracting the ion trapping-independent value from the total cellular accumulation of propranolol with an intact lysosomal pH gradient (normal growth conditions). The cellular accumulation of drug was measured using tritrium-labeled drugs at an activity of .06μCi/mL (propranolol) or .1μCi/mL (halofantrine) and then reported as nanomoles of drug. The nanomoles of drug were then normalized to the cellular protein present within the sample.

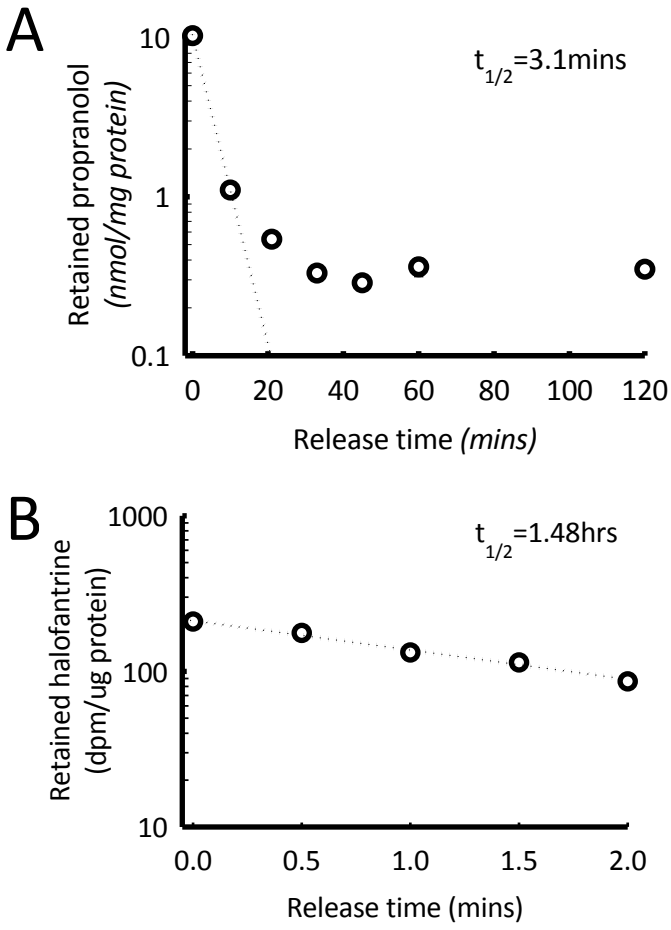

Figure 5.6 The washout kinetics of ion trapping-dependent drug (A) propranolol or (B) halofantrine from cells after a 4 day 5 micromolar drug-uptake period in wild-type human fibroblasts. Following the 4 day uptake period nigericin and monensin was spiked into the exsisting cell culture media and then incubated for the times indicated on the graph. The amount of drug remaining in the cells was then plotted as a function of time. The cellular accumulation of drug was measured using tritrium-labeled drugs at an activity of .06µCi/mL (propranolol) or .1µCi/mL (halofantrine) and then reported as either nanomoles of drug or decays per minute (dpm). The abundance of drug was then normalized to the cellular protein present within the sample.

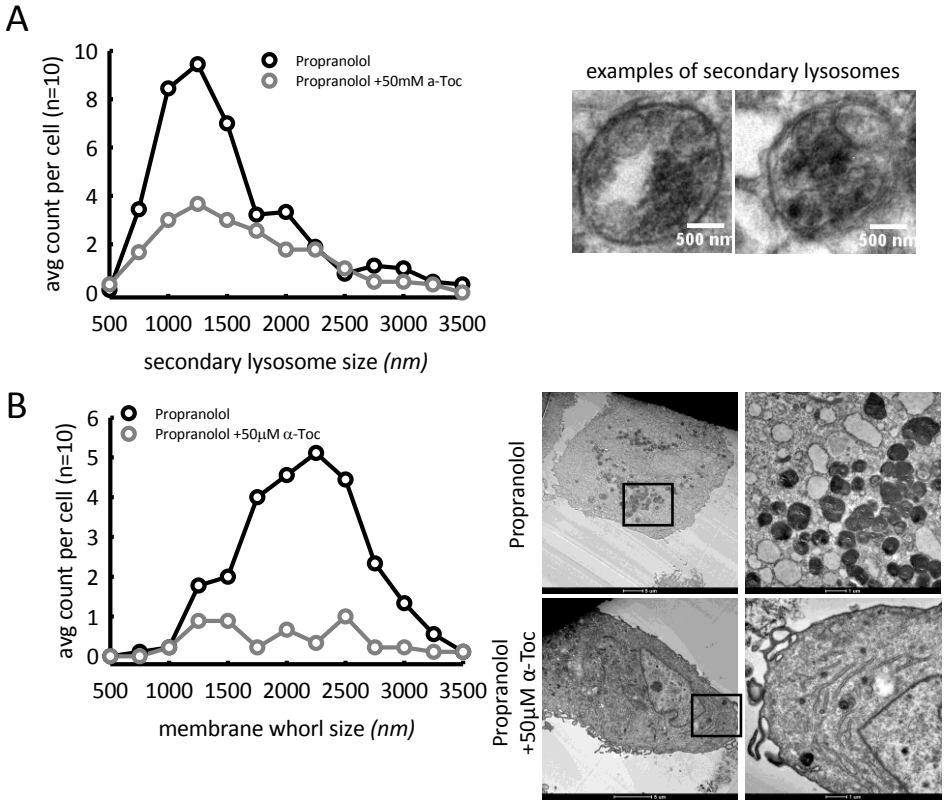

Figure 5.7 Quantitative ultrastructure analysis of lysosomes in wild-type human fibroblasts treated with 5µM propranolol with or without 50µM α-tocopherol for a 6 day period. Lysosomes were designated as either (A) secondary lysosomes or (B) membrane whorls and then manually sized using Image J (a software freely available at chemaxon.com). The size distribution and frequency of occurace (avg count per cell) was then depicted as a histogram. The values illustrated in the graphs are measurments from 10 independent cells.

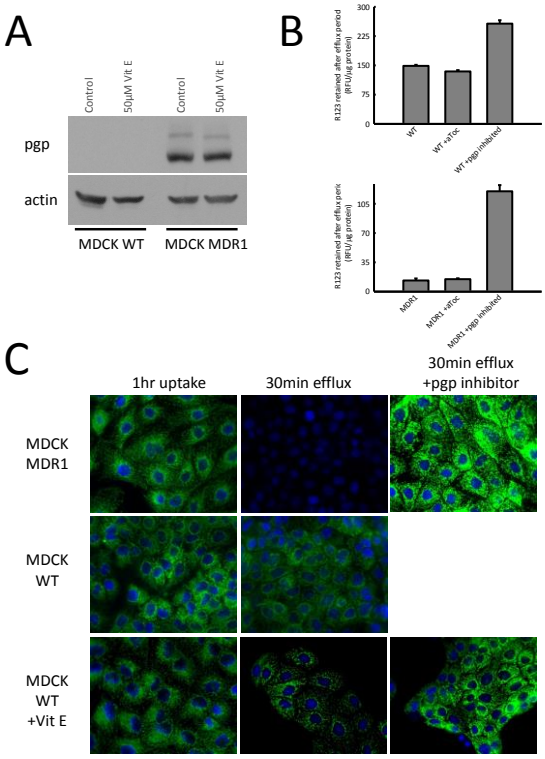

Figure 5.8 Cellular abundance and activity of of p-glycoprotein (p-gp) in Madin-Darby canine kidney (MDCK) cells. (A) Westernblot analysis of the cellular abundance of p-gp in MDCK wild-type (WT) that do not express p-gp and MDCK MDR1 that have been stabily transfected with the gene for p-gp. Both cell lines were exposed to vehicle (control) or 50μM α-tocopherol (50μM Vit E) for a 6 day period prior to westernblot analysis. The activity of p-gp was assessed by measuring the cellular accumulation of the p-gp substrate rhodamine 123 (R123) using a (B) quantitative microplate assay of approximately 750,000 cells or (C) fluorescence microscopy approximately 6-12 cells. In both (B) and (C) cells were grown in the presence or absence of 50μM α-tocopherol for 6 days. The cells were then exposed to R123 for a 1hr period followed by a 30minute R123 wash-out period. The remaining R123 that was present within the cells was measured in relative fluorescence units (RFU) and normalized to the abundance of cellular protein. As a positive control for altered p-gp activity the control condition was duplicated; however, during the R123 uptake and release period 100μM verapamil (a known p-gp inhibitor) was added to the exsisting cell culture media.

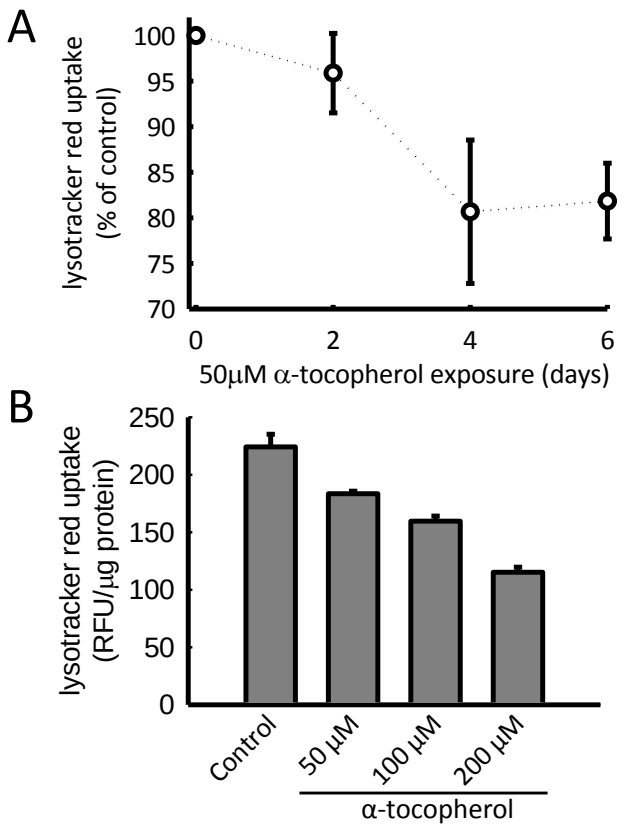

Figure 5.9 Assessments of the (A) time-dependent and (B) concentration-dependent affects that vitamin E (α-tocopherol) on the steady-state volume of lysosomes in Niemann-Pick Type C (NPC) diseased human fibroblasts. (A) NPC diseased cells were exposed to 50μM α-tocopherol for the indicated exposure time. The lysosomal volume was measured by lysotracker red (LTR) uptake in relative fluorescence units (RFUs) and then normalized the abundance of cellular protein. (B) NPC diseased cells were grown for 6 days in the absence (control) or presence of various concentrations of α-tocopherol. The lysosomal volume was measured by lysotracker red (LTR) uptake in relative fluorescence units (RFUs) and then normalized the abundance of cellular protein. In (A) the RFUs per μg protein were compared to the values for NPC diseased cells grown in α-tocopherol-free media (control) and then depicted as a percent of control. The data illustrated in (A) and (B) are representative of a minium of 3 independent experiments.

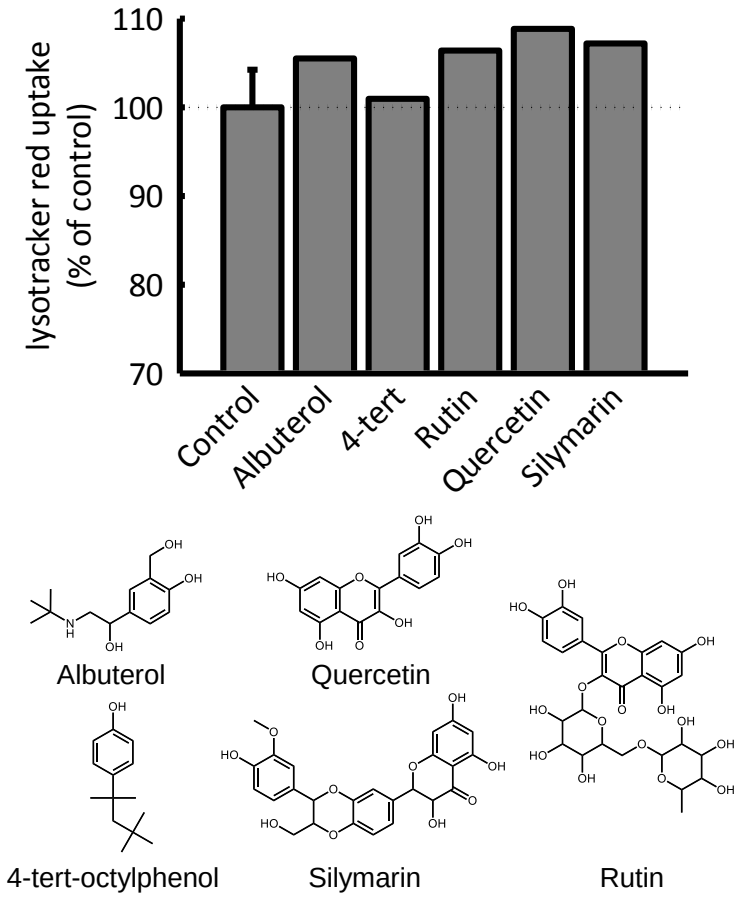

Figure 5.10 Assessments of the steady-state volume of lysosomes of Niemann-Pick Type C (NPC) diseased cells in the presence or absence of various phenol and poly-phenol containing molecules. NPC diseased cells were exposed to 10µM of each of the indicated compounds for a 4 day time period. At the end of the 4 day exposure to the test compounds the cellular uptake of lysotracker red (LTR) was measured in fluorescence units (RFUs) and then normalized to the abundance of cellular protein. These values were then compared to NPC diseased cells with no test compound (control) and depicted as a percent of control. The data illustrated in this figure are representative of a minium of 3 independent experiments.

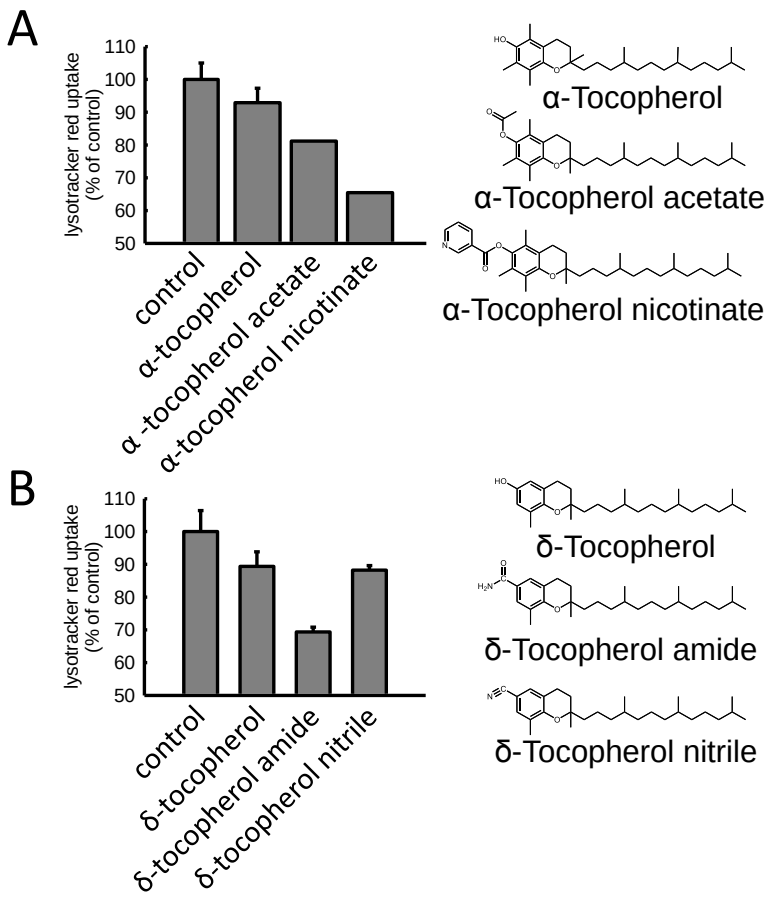

Figure 5.11 Assessments of the steady-state volume of lysosomes of Niemann-Pick Type C (NPC) diseased cells in the presence or absence of vitamin E and vitamin E derivatives. NPC diseased cells were exposed to 50µM of each of the indicated compounds for a 4 day time period. At the end of the 4 day exposure to the test compounds the cellular uptake of lysotracker red (LTR) was measured in fluorescence units (RFUs) and then normalized to the abundance of cellular protein. These values were then compared to NPC diseased cells with no test compound (control) and depicted as a percent of control. The data illustrated in (A) and (B) are representative of a minium of 3 independent experiments.

References

Agoston, M., F. Orsi, E. Feher, K. Hagymasi, Z. Orosz, A. Blazovics, J. Feher and A. Vereckei (2003). "Silymarin and vitamin E reduce amiodarone-induced lysosomal phospholipidosis in rats." Toxicology 190(3): 231-241.

Anderson, N. and J. Borlak (2006). "Drug-induced phospholipidosis." FEBS Lett 580(23): 5533-5540.

Futerman, A. H. and G. van Meer (2004). "The cell biology of lysosomal storage disorders." Nat Rev Mol Cell Biol 5(7): 554-565.

Goldman, S. D., R. S. Funk, R. A. Rajewski and J. P. Krise (2009). "Mechanisms of amine accumulation in, and egress from, lysosomes." Bioanalysis 1(8): 1445-1459.

Honegger, U. E., I. Scuntaro and U. N. Wiesmann (1995). "Vitamin E reduces accumulation of amiodarone and desethylamiodarone and inhibits phospholipidosis in cultured human cells." Biochem Pharmacol 49(12): 1741-1745.

Jeyakumar, M., R. A. Dwek, T. D. Butters and F. M. Platt (2005). "Storage solutions: treating lysosomal disorders of the brain." Nat Rev Neurosci 6(9): 713-725.

Karageorgos, L. E., E. L. Isaac, D. A. Brooks, E. M. Ravenscroft, R. Davey, J. J. Hopwood and P. J. Meikle (1997). "Lysosomal biogenesis in lysosomal storage disorders." Exp Cell Res 234(1): 85-97.

Kolter, T. and K. Sandhoff (2010). "Lysosomal degradation of membrane lipids." FEBS Lett 584(9): 1700-1712.

Matsuzawa, Y., A. Yamamoto, S. Adachi and M. Nishikawa (1977). "Studies on drug-induced lipidosis. VIII. Correlation between drug accumulation and acidic phospholipids." J Biochem 82(5): 1369-1377.

Reasor, M. J., K. L. Hastings and R. G. Ulrich (2006). "Drug-induced phospholipidosis: issues and future directions." Expert Opin Drug Saf 5(4): 567-583.

Scuntaro, I., U. Kientsch, U. N. Wiesmann and U. E. Honegger (1996). "Inhibition by vitamin E of drug accumulation and of phospholipidosis induced by desipramine and other cationic amphiphilic drugs in human cultured cells." Br J Pharmacol 119(5): 829-834.

Shichiri, M., N. Kono, Y. Shimanaka, M. Tanito, D. E. Rotzoll, Y. Yoshida, Y. Hagihara, H. Tamai and H. Arai (2012). "A novel role for alpha-tocopherol transfer protein (alpha-TTP) in protecting against chloroquine toxicity." J Biol Chem 287(4): 2926-2934.

Tengstrand, E. A., G. T. Miwa and F. Y. Hsieh (2010). "Bis(monoacylglycerol)phosphate as a non-invasive biomarker to monitor the onset and time-course of phospholipidosis with drug-induced toxicities." Expert Opin Drug Metab Toxicol 6(5): 555-570.

van Acker, S. A., L. M. Koymans and A. Bast (1993). "Molecular pharmacology of vitamin E: structural aspects of antioxidant activity." Free Radic Biol Med 15(3): 311-328.

Wang, X. and P. J. Quinn (1999). "Vitamin E and its function in membranes." Prog Lipid Res 38(4): 309-336.

Xu, M., K. Liu, M. Swaroop, F. D. Porter, R. Sidhu, S. Firnkes, D. S. Ory, J. J. Marugan, J. Xiao, N. Southall, W. J. Pavan, C. Davidson, S. U. Walkley, A. T. Remaley, U. Baxa, W. Sun, J. C. McKew, C. P. Austin and W. Zheng (2012). "delta-Tocopherol reduces lipid accumulation in Niemann-Pick type C1 and Wolman cholesterol storage disorders." J Biol Chem 287(47): 39349-39360.

Chapter 6. Conclusions

Summary and Conclusion

In this work we have detailed how lysosomotropic drugs can alter lysosome form and function and cause an expanded lysosomal volume phenotype (expanded LVP). This phenotype was characterized by an increase in the aqueous volume of lysosomes that consequently lead to the enhanced cellular accumulation of lysosomotropic drugs. Although lysosomotropic drugs have previously been shown to enhance the cellular accumulation of secondarily administered drugs, and thereby create a drug-drug interaction involving lysosomes, a mechanistic basis for this phenomenon has not been established. The purpose of this work was to fill the gap in knowledge regarding the details of the expanded LVP; specifically, the structure activity relationship for molecules and their ability to induce an expanded LVP, the mechanism underlying their effect on lysosomes, and what cellular processes are involved in its development.

In an effort to establish a structure activity relationship, we have evaluated a wide array of lysosomotropic molecules and examined the influence that specific physicochemical properties had on their ability to induce an expanded LVP. We found that lysosomotropic properties greatly enhanced a molecule's capacity to increase lysosomal volume. Our data further showed that the amphiphilic properties of lysosomotropic molecules, e.g., the size of the hydrophobic region and the distance separating it from the hydrophilic region, dramatically influenced their potency to induce an expanded LVP.

We then explored the mechanisms underlying how these structural properties might be leading to an expanded LVP. We had reasoned that the amphiphilic properties of these molecules were important because it was determined how they were interacting with the biological membranes. To test this this we quantitatively measured the membrane intercalation potential (drug-induced red blood cell

hemolysis) of several different lysosomotropic molecules. Interestingly, we found that the membrane intercalation potential of 5 different lysosomotropic drugs correlated strongly with their relative potency in causing an expanded LVP. To strengthen this hypothesis we further showed that low concentrations of lysosomotropic drugs could work in an additive manner to ultimately bring about an expanded LVP similar to that seen with a single drug at a higher concentration. We deemed these findings to be further evidence that these lysosomotropic drugs were interacting with the lysosomal membranes and that this interaction was causing a non-specific effect such as changing membrane fluidity and order.

Following the development of the structure activity relationship and implicating membrane intercalation as a likely mechanism underlying the initial effects of these drugs, we next sought to characterize the down-stream consequences of these interactions. We did not consider the membrane intercalation of lysosomotropic drugs to be the direct cause of the expanded LVP; rather, we envisaged that it was initiating some unidentified downstream cellular response. Due to the vast complexity of biological systems, we could not screen every cellular process for its potential involvement in this drug-induced phenomenon. Instead, we imaged a simplified model of the lysosomes where its steady state volume would be determined by the relative balance between pathways that bring membrane and material into the lysosomal systems compared to pathways that bring membrane and material away from the lysosomal system. We then evaluated the role that two well characterized input pathways, the autophagic pathway and the biosynthetic pathway, played in expanding lysosomal volume. Our results showed that cells exposed to lysosomotropic drugs exhibit increased levels of autophagy and biosynthesis of lysosomes (via transcription factor EB (TFEB) activation). We also evaluated the effect that lysosomotropic drugs had on vesicle-mediated trafficking away from lysosomes. We found that these in addition to enhancing the rate of input into the lysomal system these drugs were also decreasing the efficacy of vesicle-mediated trafficking out of the lysosomes. We concluded that these

two down-stream effects, i.e., increased rates of input into the lysosomal system and decreased rates of egress from the lysosomal system, ultimately lead to an increase in the steady state volume of lysosomes.

In continuation of the work by Funk and Krise, we next sought to evaluate the potential clinical ramifications of the expanded LVP by determining how this condition could impact the cellular accumulation of lysosomotropic drugs. We had reasoned that if these drugs were capable of altering the cellular accumulation of secondarily administered drugs then this phenomenon could ultimately instigate a drug-drug interaction involving lysosomes. Funk and Krise previously identified this drug-drug interaction pathway by reporting that the lysosomotropic drugs could enhance the cellular accumulation of lysotracker red (LTR). Because LTR is technically not a drug, we sought to re-evaluate this drug-drug interaction using more clinically relevant examples. In these assessments we addressed two important questions. First, can these lysosomotropic drugs increase their own cellular accumulation. And finally, can these lysosomotropic drugs cause an enhanced cellular accumulation of secondarily administered drugs.

Our results showed that the drug-induced expansion of lysosomal volume caused an increased cellular accumulation of the primary lysosomotropic drug, i.e., one lysosomotropic drug can increase its own cellular accumulation. We also found that the drug-induced expansion in lysosomal volume could also increase the cellular accumulation of secondarily administered drugs.

In the final chapter we explored potential treatment strategies for recovering lysosome function in lysosomal storage diseased (LSD) cells and in cells treated with lysosomotropic drugs. Inspired by previous reports showing the positive effects that vitamin E can have on improving lysosome-dysfunction we sought to further evaluate vitamin E and attempt to determine the important structural features of these molecules. By analyzing a battery of vitamin E analogs (α-tocopherol and δ-

tocopherol) and a group of compounds containing phenols and polyphenols we found that the antioxidant properties of vitamin E were not responsible for its ability to recover lysosome function in Niemann-Pick Type C (NPC) diseased cells. We concluded that the positive effects of vitamin E were likely due to beneficial membrane interactions that counteracted the impingement induced by lysosomotropic drugs or the build-up of undegraded substrates in LSDs cells. Although further studies are required to more thoroughly characterize how vitamin E is influencing lysosomal-membrane dynamics this chapter provides a proof of principle showing that it can be possible to rationally design drugs that could potentially be used to treat lysosomal storage diseases or the toxic effects of lysosomotropic drugs.

Future Work

The discovery process initially starts with a simple model and then expands to include increasingly more complex models. Throughout this work we have focused our studies on cells in culture. These studies represent only the beginning stage of discovery. We have used an in vitro model to develop our hypotheses on how many lysosomotropic drugs might be influencing and changing lysosomes. Based on these results we have made predictions on how these drug-induced changes could ultimately impact the pharmacokinetic properties of drugs in a clinical setting. Although we feel that our hypotheses and conclusions are well reasoned they are ultimately based on an in vitro model. The next stage in the discovery process is to apply what was learned in this work and expand it to an in vivo model.